Title
Polymer-Protein Nanoparticles for Systemic Detoxification, Anti-HIV and Biosensor Applications

Author
Zhao, Ming

Publication Date
2018

Peer reviewed|Thesis/dissertation

UNIVERSITY OF CALIFORNIA

Los Angeles

Polymer-Protein Nanoparticles for Systemic Detoxification, Anti-HIV and Biosensor Applications

A dissertation submitted in partial satisfaction of the

requirements for the degree Doctor of Philosophy

in Chemical Engineering

by

Ming Zhao

2018

ABSTRACT OF THE DISSERTATION

Polymer-Protein Nanoparticles for

Systemic Detoxification, Anti-HIV and Biosensor Applications

by

Ming Zhao

Doctor of Philosophy in Chemical Engineering

University of California, Los Angeles, 2018

Professor Yunfeng Lu, Chair

As the “engines of life”, proteins play the most dynamic and diverse roles among all macromolecules in the body. Owing to their high specificity and potency, more than 130 proteins or peptides therapeutics have been developed for clinical use, and many more are being developed. Despite their tremendous promises, effective delivery of protein therapeutics to achieve the maximum efficacy needs to overcome three major barriers, which are associated with the delivery of therapeutics to the target organs, entrance of the therapeutics to the tissues, and entrance of the therapeutics to the cells. The inability to overcome such barriers may result in rapid loss of the activity, fast clearance and undesirable tissue biodistribution of the therapeutic proteins. Engineering nanocarriers for escorting therapeutic proteins into their specified destination has thus generated considerable interests.

In this dissertation, a delivery strategy employing polymeric nanocapsules for efficient

extracellular and intracellular protein delivery is described. As an extension, zwitterionic polymer-based biosensors with effective protein immobilization and enhanced properties are also discussed. This dissertation work can be briefly outlined into three topics below:

1) Oxalate oxidase (OxO) was encapsulated within a thin layer of zwitterionic polymer shell via aqueous free-radical polymerization for the treatment of hyperoxaluria. As-synthesized OxO nanocapsules exhibited enhanced bioactivity, prolonged blood circulation half-life and reduced immunogenicity. This design enables systemic delivery of therapeutic enzymes for various applications.
2) The transcription activator-like effector nucleases (TALEN) were encapsulated. The shell properties were judiciously modulated to be cationic and acid-labile, which facilitates cellular uptake and subsequent cargo release. TALEN pairs recognizing the TAR region of HIV LTRs were delivered through this platform to induce robust excision of HIV-1 provirus in a variety of human cell lines, especially the primary T cell lines. This work provides useful suggestions for the research and development of anti-HIV therapies.
3) Zwitterionic polymers bearing amine groups were developed to facilitate the enzyme immobilization on chitosan-coated electrode for choline sensing. Such zwitterionic coating brought in sensors with improved enzyme loading, sensitivity and detection limit.

In summary, this research utilizes the nanocapsule platform to overcome different delivery barriers to realize specific delivery goals. The zwitterionic polymers can be used to prepare biosensors with enhanced properties.

The dissertation of Ming Zhao is approved.

Yi Tang

Samanvaya Srivastava

Yu Huang

Yunfeng Lu, Committee Chair

University of California, Los Angeles

2018

Table of Contents

List of Figures

List of Tables

Acknowledgement

The five-year Ph.D. journey of at UCLA was filled with challenges and rewards. Foremost, I would like to express my sincere appreciation to my advisor, Professor Yunfeng Lu, who has brought me into the fantastic frontiers in nanobiomedical research, which broadened my perspective and stimulated my research interest. During my entire Ph.D. pursuit, Prof. Lu provided me with every bit of guidance, support and expertise, without which, this dissertation would not have been possible.

I would also like to acknowledge Professor Yi Tang, Professor Yu Huang and Professor Samanvaya Srivastava for being my committee members and providing valuable comments, advice, and encouragements in regard to research and the dissertation. Besides, special gratitude is given to my former committee member Professor Tatiana Segura for her generous offer to access some of her lab instruments.

I would like to thank my former and current group members: Dr. Jie Li, Dr. Chaoyong Liu, Dr. Zaiyuan Le, Dr. Dong Chen, Dr. Xiaomin Qian, Di Wu, Duo Xu, Kang Peng, Jie Ren, Peng Gao, Xinru Li, Gurong Shen, Addis Fuhr and all other Lu lab members for their various kinds of help and support during my Ph.D. study.

I would like to extend my thanks to my collaborators: Prof. James W. Whittaker at Oregon Health and Science University, Prof. Jia Liu at Shanghaitech University, Professor Harold Monbouquette and his student Brenda Huang from CBE department at UCLA, and Dr. Jing Wen from MIMG department at UCLA. I wouldn't have made my research and dissertation this far if it hadn't been for their insightful advice and collaborative supports.

At last, my deepest gratitude goes to my parents, Tongjian Zhao and Xiuhua Zhang, for their unconditional love and support ever since I was born.

VITA

Education:

2006-2010 Department of Bioenigeering, Zhengzhou University, China

Bachelor of Science in Biology, July 2010

2010-2013 College of Life Sciences, Zhejiang University, China

Master of Science in Biochemistry, March 2013

Publications:

M. Zhao; J. Wen; Y. Lu. "Deactivation of Proviral HIV-1 DNA in Human Primary Cells with Cell Penetrating TALEN Nanocapsules," In preparation

M. Zhao; D. Xu; D. Wu; J. Whittaker; R. Terkeltaub; Y. Lu. "Nanocapsules of Oxalate Oxidase for Hyperoxaluria Treatment," ***Nano Res.*** (2017) (Accepted)

M. Zhao; P. Sun; L. Du; G. Wang; X. Jia; Y. Zhao. "Biodegradation of Methyl Red by Bacillus sp. Strain UN2: Decolorization Capacity, Metabolites Characterization and Enzyme Analysis," ***Environ. Sci. Pollut. Res.*** (2014) 21:6136-6145

M. Zhao; L. Du; G. Li; F. Xu; W. Chen ; Y. Zhao. "Biodegradation Exploration of Malachite Green by Micrococcus sp. Strain BD15: Biodegradation Pathway and Enzyme Analysis," ***Int. Biodeterior. Biodegradation*** (2013) 78:108-116.

Presentations:

"Poly(2-methacryloyloxyethyl phosphorylcholine) Encapsulated Oxalate Oxidase-A Potential Anti-Hyperoxaluria Drug with Prolonged Blood Residence and Mitigated Immunogenicity" Material Research Society Spring Meeting & Exhibit, Phoenix, AZ, Apr. 18, 2017.

Chapter 1. Introduction

1.1 Protein Therapeutics

As the "engines of life", proteins play the most dynamic and diverse roles among all the macromolecules in the body, such as catalyzing biochemical reactions, controlling cell fates, forming cellular structures, providing tissue scaffolds, and transporting molecules within a cell or from one organ to another.[1] On one hand, owing to this functional specificity, disease may result when any one of these proteins contains mutations or other abnormalities, or is present in abnormally high or low concentrations, which poses an enormous challenge to modern medicine. Viewed from the perspective of therapeutics, on the other hand, the highly specific action of proteins makes them less likely to interfere with normal biological processes, and their high number represents a tremendous opportunity in terms of harnessing protein therapeutics to alleviate disease.[2] In the early days, therapeutic proteins were isolated from natural biological sources and were not commonly used. For example, insulin was first purified from bovine pancreas in 1922 to treat diabetes,[3] and growth hormone and the follicle-stimulating hormone were isolated from human pituitary glands.[4,5] It was not until the early 1980s, with the advent of recombinant gene technologies that the number of therapeutic applications of proteins started to explode remarkably. In 1982, the first recombinant pharmaceutical-human insulin came onto the market from Genentech,[6] and hitherto more than 130 proteins or peptides have been approved for clinical use by the FDA, with over 70% being recombinant, and many more are being developed world wide.[2] Recombinant production offers distinct benefits: it provides drugs that could not have been made available by conventional methods; it manufactures proteins more efficiently and inexpensively, and in almost unlimited quantities; and it rules out certain possibilities of human pathogenic virus contamination.[7] Common heterologous proteins production systems

include microbial fermentation, plant, insect and mammalian cell cultures. *Escherichia coli* (*E. coli*) remains one of the most widely used hosts because of its easy and quick expression of proteins.[8] However, the bacterium is not the system of choice to express very large proteins or proteins that require post-translational modifications. In this case, yeast may be harnessed to produce eukaryotic heterologous proteins because they share similar subcellular post-translational protein modification machinery as eukaryotes.[9] Nevertheless, for the production of therapeutic glycoproteins, yeasts are still less useful since their glycoproteins are associated with high mannose oligosaccharides that are readily recognized and sequestrated by macrophages bearing large numbers of mannose receptors on their surface.[10] Mammalian cells have insofar become the dominant system for the production of recombinant versions of native proteins for clinical applications because of their capacity for proper protein folding, assembly and post-translational modification.[11]

1.2 Protein Engineering

Although recombinant proteins produced by mammalian cells are more biocompatible than those produced by other hosts, the full realization of their biomedical application is still largely restricted by poor catalytic activity, short shelf life and vulnerability to protease digestion. These drawbacks can be addressed with protein engineering to increase their clinical potential. Rational protein design and directed evolution are two general approaches of protein engineering.[12] The rational protein design, which requires detailed knowledge of the structure and function of proteins, employs site-directed mutagenesis methods to make desired changes to proteins, yet sometimes the detailed structural knowledge is unavailable or incomplete. In sharp contrast, directed evolution relies on random mutagenesis followed by high-throughput screening to select

variants having desired traits. The approach, however, entails immense screening efforts that even protein libraries with millions of members still sample a small fraction of possible sequence space for a protein.[13] As a more recent approach, semi-rational methodologies combining the benefits of directed evolution and rational design are being used to significantly increase the efficiency of biocatalyst tailoring.[12,13] As a result, a variety of improved enzyme properties have been attained, such as increased catalytic activity and stability,[14-16] higher stereospecificity and stereoselectivity,[14,17,18] altered pH profile,[19,20] reduced immunogenicity,[21,22] and enhanced inhibitor resistance. [23]

Instead of just evolving proteins with altered properties, DNA shuffling and related methods are powerful tools in protein engineering to devise chimeric proteins with novel structures and properties. In particular, chimeric protein methodologies could contribute to unearthing potential novel roles of specific protein domains, [24] preventing protein aggregation by altering net charge for a variety of applications,[25,26] regenerating enzymatic cofactors simply and inexpensively,[27,28] and facilitating protein purification.[29] More importantly, the careful analysis of chimeric proteins promotes deeper understanding of protein structures, functions and key amino acid substitutions, which in return, could direct the rational protein redesign.

In addition, impressive results of therapeutic proteins generated by other engineering approaches have also been reported, as evidenced by employing glycoengineering strategy to humanize yeast's heterogeneous high mannose-type glycosylation to mammalian-type glycosylation to acquire pharmacokinetic stability and efficacy,[30,31] and by utilizing the cell surface display and ribosome display approaches to engineer a variety of proteins for improved affinity, specificity, expression, stability and catalytic activity.[32]

Despite the fact that it is a powerful tool, protein engineering has overcome some of the limitations of biocatalysts and it is still flawed in many ways when it comes to biomedical applications. First, as a trial and error methodology, it may still take considerable time to implement.[13] Moreover, multiple functional domains of chimeric proteins may tangle together due to disadvantageous folding, leading to reduced activity and/or stability.[33] Lastly, in protein engineering, protein intrinsic structure change was limited in order to maintain catalytic activity and stability, due to which alterations and improvements of major properties in terms of size, surface properties and hydrophobicity are largely restricted.

To sum up, the past three decades have seen a drastic upsurge of engineered protein products on the market owing to the notable technical advances in recombinant DNA technology, high throughput genome sequencing, and protein engineering, providing a potential for a vast scope of biomedical study and applications. In the field of precision medicine these recombinant biologic agents nonetheless, are still at their primitive forms that require further decorations to accomplish the goal of a sustained and controlled release *in vivo*. Therefore, under these circumstances, major properties such as size, charge, surface shape and surface hydrophobicity of these biologics need to be revisited and redressed.

Table 1-1. List of FDA-approved protein conjugates by Year 2016

Name	Drug description	Diseases	Year approved
ADYNOVATE	PEGylated factor VIII	Hemophilia	2015
Plegridy®	PEGylated IFN beta-lα	Multiple Sclerosis	2014
Kaystexxa®	PEGylated porcine-like uricase	Chronic gout	2010
Cimzia®	PEGylated antibody fragment	Crohn's disease	2008

Micera®	Chemically synthesized ESA (erythropoiesis-stimulating)	Anemia associated with chronic kidney disease	2007
Abraxane®	Albumin-bound paclitaxel nanopaticles	Breast cancer	2005
Macugen®	PEGylated anti-VEGF aptamer	Macular degeneration, neovacular age-related	2004
Somavert®	PEGylated HGH receptor antagonist	Acromegaly	2003
Neulasta®	PEGylated GCSF protein	Neutrophenia, Chemotherapy induced	2002
Pegasys®	PEGylated IFN alpha-2b protein	Hepatitis B; Hepatitis C	2002
Peglntron®	PEGylated IFN alpha-2b protein	Hepatitis C	2001
Curosurf®	Liposome-proteins SP-B and SP-C	Pulmonary surfactant for Respiratory Distress Syndrome	1999
Ontak®	Engineered protein combining IL-2 and diphtheria toxin	Cutaneous T-Cell lymphoma	1999
Oncaspar®	PEGylated L-asparaginase	Acute lymophoblastic leukemia	1994
Adagen®1990	PEGylated adenosine deaminase enzyme	Severe combined immunodeficiency disease (SCID)	1990

1.3 Systemic Protein Delivery

Nanotechnology, in its rough definition, refers to structures that span up to several hundred nanometers in size and that are developed by top-down or bottom-up engineering of individual components.[34] Spurred by recent development in nanotechnology and drug delivery, protein delivery has been actively pursued to treat a broad range of diseases including metabolic disorders,[35,36] cancers[37] and tissue damage.[38,39] Systemic protein delivery, in particular, refers to delivering protein cargos to extracellular sites of action. Under these circumstances, lots of studies have been focusing on improving drug-loading capacity, targeting specificity,

pharmaceutical efficacy and co-delivery issues, while many others have sought to modulate drug delivery vehicles to achieve sustained drug release and stealth properties.

It is worth noticing that the mononuclear phagocyte system (MPS) composed of dendritic cells, blood monocytes and tissue-resident macrophages is the primary phagocytosing system in the body strategically placed in many tissues. The cells are able to recognize and clear a multitude of invading foreign substances including particulates, cell debris, and microorganisms tagged with opsonin corona. As a result, evading MPS recognition and engulfment are crucial for exotic therapeutics to acquire prolonged *in vivo* half-life for systemic protein delivery purposes.[40] In effect, there have been intensive studies showing that the biophysicochemical properties of a vehicle, such as size, charge, surface chemistry, and the nature and density of the ligands on their surface, have significant impacts on their clearance behavior and biodistribution.[34] Typically, large-sized nanoparticles (>100 nm) tend to be more efficiently coated with opsonizing complement proteins leading to fast accumulation into the reticuloendothelial systems (RES),[41,42] whereas small nanoparticles with a final hydrodynamic diameter < 5.5 nm undergo rapid urinary extraction and elimination from the body.[43] Ideally, nanoparticles in the 10-100 nm size range can slow the renal clearance, splenic filtration and surface opsonization process.[44] With respect to surface chemistry, charge and curvature, their combination could modulate the extent and type of opsonin binding in their coronas,[45,46] which dictate subsequent cell uptake, gene expression, and toxicity.[42,47] For example, positively charged nanoparticles are cleared more quickly from the blood due to spontaneous labeling with negatively charged serum components.[42] Neutral nanoparticles –instead display highest blood half-life compared with charged ones.[44] Hydrophobic particles have been shown to associate with blood serum opsonins more quickly than hydrophilic particles.[40] Although many hurdles still exist for the development of nano-sized

systemic protein therapeutics with truly exceptional blood circulation half-life, therapeutic efficiency, and none-toxicity and immune response, their potential advantages should drive their successful development and translation into a new class of clinical therapies. Towards this goal, several strides have been made at camouflaging or masking nanoparticles to temporarily bypass recognition by the MPS to increase blood or tissue resident time.

1.3.1 Poly (ethylene glycol) (PEG) –enzyme conjugates

Attaching polyethylene glycol (PEG) to proteins, known as PEGylation, remains thus far the gold standard and most established approach of stealth coating. As of today, 12 PEGylated proteins have been brought to market, including PEG-asparaginase (Oncaspar®), PEG-adenosine deaminase (Adagen®) and PEG-Intron®.[48] In the beginning, random PEGylation methods were adopted through reacting the ε-amino group of lysine residues, yet the resultant isomer mixtures were of high heterogeneity that complicated the subsequent purification steps.[49] To circumvent this limitation, site-specific amino PEGylation approaches were developed to selectively react the N-terminal α-amino groups, the carboxyl groups or the cysteines residues to yield more defined conjugating structures.[50,51]

The antifouling feature of PEGylated proteins is still not fully understood yet is considered to arise from the efficacious hydrated layers created by PEG chains, which extensively bond with surrounding water molecules through hydrogen bonding in aqueous solution. Such hydrated layer sterically shields blood serum proteins from approaching, endowing the underlying protein with improved bioavailability, pK behavior, and MPS-avoidance features.[52,53] It is important to note that the characteristics of this hydration layer such as thickness, surface density, and conformation play a dominant role for effective blocking or

repulsion of opsonins.[40] Specifically, low PEG coverage or surface density may leave unprotected patches in the PEG hydrated layer where opsonin proteins can freely bind with surface epitopes;[54] Also, long chain or branched PEG polymer decorated nanoparticles manifest longer blood circulation half-lives than short chain or linear PEG polymer does;[55] With respect to final biodistribution, PEGylated nanoparticles preferentially concentrated in the spleen compared to both the liver and spleen by uncovered nanoparticles.[56]

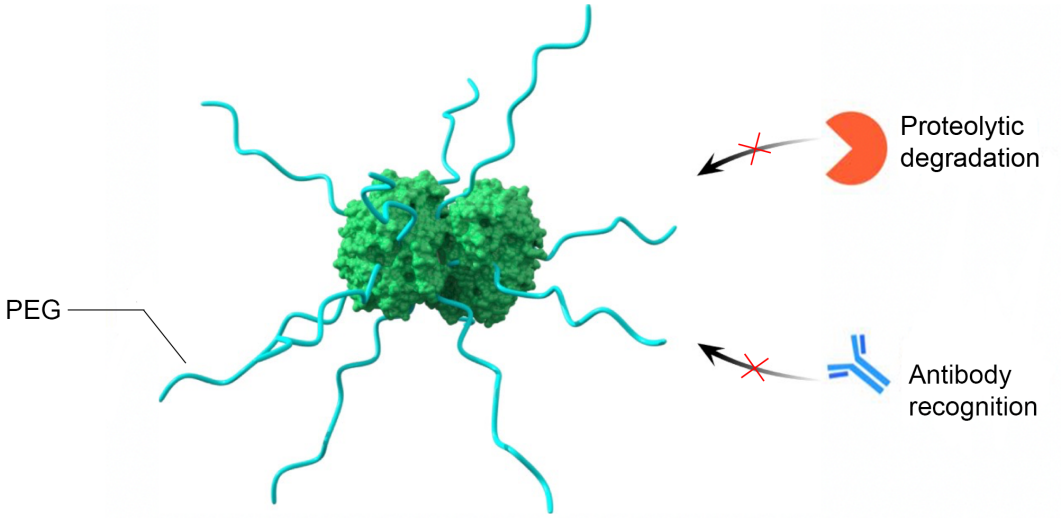

Figure 1-1 A schematic illustration of a PEGylated protein. The PEG chains are conjugated on an enzyme, which could protect the protein from proteolysis and help to evade the immune system. Reprinted with permission from ref. [57]

Unfortunately, the attachment of PEG to a protein is not without its own limitations. Although basic designing guidelines can be followed to make PEGylated products, there are still a large number of conflicting results reported, implying the lack of a comprehensive study of the antifouling mechanism and impact factors.[58] Moreover, the desire to make longer chain length and higher density of PEG polymers to increase body-residence time of nanoparticles is frequently compromised with decreased protein activity, and the inadequate PEG anchoring may, in turn, amplify the immunogenicity of conjugated polymers.[36] Besides, several studies have

discovered undesirable anti-PEG antibodies in patients after treatment with PEGylated therapies.[59,60] Given these facts, developing substitute stealth coatings that can further evade the immune system is urgently needed but still challenging.

1.3.2 Liposome–functionalized protein therapeutics for systemic delivery

Since its earliest reported synthesis in the 1973,[61] liposomes have become the mainstay components broadly used in drug delivery spectra over decades. Inherently, they are a class of lipid-based vesicles modulated to have specified sizes and permeability properties. According to their varied functionality, liposomes can be classified into long-circulating liposomes, stimuli-responsive liposomes, nebulized liposomes, elastic liposomes and covalent-lipid drug complexes.[62] Nonetheless, prior to the emergence of these novel liposomes, conventional "first-generation" liposomes are simply composed of native phospholipids and cholesterol, and are cleared from the circulation fairly rapidly.[63]

To circumvent this hurdle, long-circulating liposomes were invented aiming at evading blood opsonization and RES uptake, which make systemic detoxification,[64] cancer therapy[65] and transdermal drug delivery with liposomal nanovesicles possible.[66,67] Initial attempts of constructing stealth liposomes were based on naturally occurring glycolipids or phosphatidylinositol,[68] but the most successful and widely recognized stealth formulations are associated with PEG-coated liposomes,[69] where PEG is either directly anchored onto the liposome surface or forms PEG-conjugated lipids building blocks capable of self-assembly.[57] Since the first liposomal system was introduced for clinical use in 1995, the number has exploded to around a dozen as of 2015 and their compositions are either fully liposomal or PEGylated.[62]

Studies have demonstrated that stealth performance and biodistribution of PEGylated liposomes are largely influenced by their physical characteristics including particle size, bilayer fluidity, and surface charge. The upper size limit was considered to be around 275 nm, beyond which the stealth property of PEG-liposomes is largely undermined, and its biodistribution is characterized by high MPS accumulation.[70] Recent investigations with smaller sized PEG-liposomes have boosted their utility on tumor treatment as researchers discovered that <50 nm sized PEGylated liposomes possess greater tissue penetration and enhanced tumor inhibition characteristics, largely due to the extended circulation time that creates higher opportunity for tumor accumulation and retention via EPR (Enhanced permeability and retention) effect.[65,71]

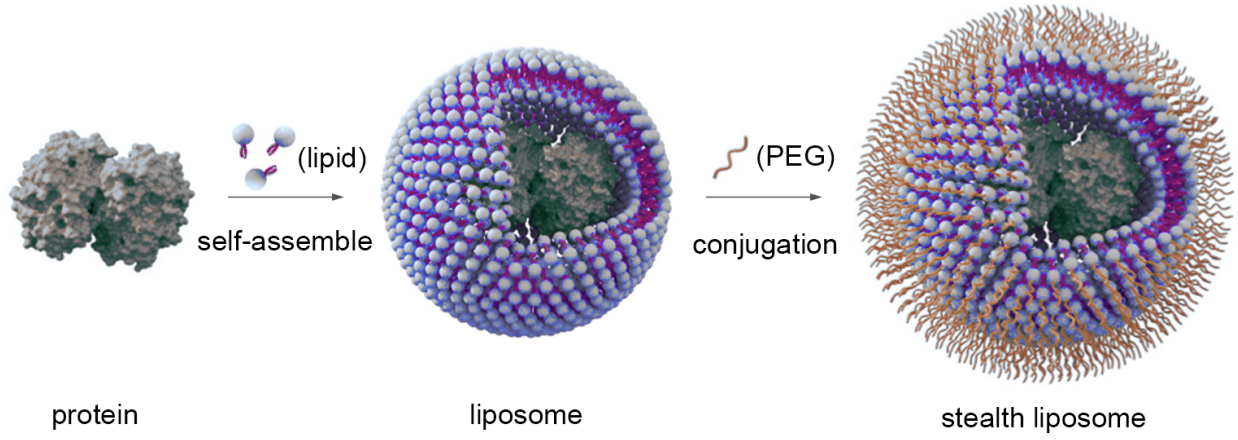

Figure 1-2 A schematic illustration of preparing liposomes through self-assembly of lipids. Stealth liposomes could be prepared by conjugating PEG chains onto the liposome surface.

Not only do liposomes appear primed for cancer therapy, but they have also been exploited as circulating depot for systemic toxins management and other systemic delivery purposes. Notable examples illustrating this include administration of artificial sphingomyelin liposomes containing high cholesterol as decoy targets *in vivo* to exhaust bacterial toxins that would otherwise bind and kill host cells,[72] and employing cell membranes coated polymeric

nanoparticles as nanosponge to absorb and cleanse various virulence factors.[64] Additionally, as an extension, the cell membranes coating technique was leveraged to fabricate anticancer vaccine that delivers autologous cancer cell membrane antigens and immunostimulatory adjuvant in a concerted fashion, showing efficacious antigen presentation and downstream immune activation.[73] Consistently, neutrophils carrying liposomes were validated to successfully penetrate the blood-brain barrier and suppress postoperative glioma recurrence.[74] In the light of the evidence above, liposomal systems for systemic delivery are still in their prime, and with ongoing technological advancement they will continuously diversify their functionality and utility against a broader spectrum of diseases.

1.3.3 Poly(zwitterion)–functionalized protein therapeutics

Bioinspired poly(zwitterions), such as poly(phosphobetaine), poly(carboxybetaine) (pCB) and poly(sulfobetaine) (pSB), have recently emerged as an important class of stealth biomaterials in the drug delivery domain owing to their superhydrophilicity and ultra-low fouling property in complex media.[75,35,76] They are structurally well-ordered polyelectrolytes simultaneously bearing a pair of oppositely charged ions on the same monomer residue. Unlike PEG or other hydrophilic biomaterials that build their hydration through hydrogen bonding, zwitterionic-based polymers bind water molecules more firmly through electrostatically induced hydration,[77,78] affording the protected underlying biomolecules with better antifouling properties than PEG conjugates. Another key feature where zwitterionic polymers outperform PEG is related to the binding affinity. While extensive studies have agreed that, low fouling property was achieved at the expense of losing some binding affinity in PEG-protein conjugates, polyzwitterions functionalized products instead are able to maintain or even enhance the binding affinity, due to

the uniformly distributed zwitterionic groups according to the Hofmeister effect.[79] As a result, without worrying about binding affinity loss, coatings with a higher surface packing density of polyzwitterions may be fabricated. Moreover, some zwitterionic polymers such as pCB and polyphosphorylcholine are biomimetic polymers whose headgroups can be found in cell plasma and the outside layer of cell membranes, exhibiting greater biocompatibility.

Another unique aspect that directs people's attention towards zwitterionic polymers is their structural and functional tunability. For instance, pCB has plenty of carboxylate functional groups interspersed among the polymer backbone, providing an easy-to-implement chemistry to attach amine-containing molecules.[80] Under some conditions, the antifouling functional groups on pCB could be temporally blocked to make a pCB ester that carries substantial positive charges for intracellular protein/gene delivery or antimicrobial applications;, upon being triggered, pCB ester is switchable back to pCB to regain the nonfouling feature, leaving no toxicity.[81] In addition, despite the fact that phosphobetaines intrinsically contain no functionalizable groups, various methods have been successfully employed to introduce functional groups into the polymers chains.[82,83]

The prospect of zwitterionic coatings as novel drug delivery vehicles has been assessed in several metabolic disorder disease animal models. Take uricase as an example, PEGylated uricase was approved by FDA to treat hyperuricemia in clinical practice in 2010 but still poses a risk because of the anti-PEG antibody issue.[84] Aiming at developing safer PEG substitutes able to nullify the immune response, Jiang et al. prepared a polycarboxybetaine-uricase conjugate that was dosed into rats intravenously.[85] It was expected to find that uricase-specific lgM and lgG titers were 8 × and 3 × less than that evoked by PEGylated uricase. Likewise, the elimination half-life of zwitterionic conjugate underwent 6 × increase than that of the PEG conjugate after

the first administration, and remained constant throughout following repeated injections. However, in spite of an overall improved performance over PEG, enzyme-specific antibody response was still clearly detectable, implying possibly a higher surface packing density of the zwitterionic moieties around the protein surface in demand. In effect, achieving higher packing density isn't easy with the conjugation approach because the number of available conjugation sites on protein surface is restricted. To overcome these obstacles, Jiang et al. synthesized a cross-linked hydrogel "mesh" to encapsulate uricase via *in situ* free radical polymerization, which as expected remarkably mitigated the generation of the anti-uricase/anti-polymer lgG and lgM to an undetectable level.[36]

Using polyphosphorylcholine (PMPC) encapsulated uricase, Lu et al. made complements to Jiang's study with evaluation of the therapeutic outcomes in a hyperuricemia mouse model.[86] It is observed that injection of PMPC encapsulated uricase nanogels steadily reduced uric acid to a much lower level during the entire study period of 120 h. In contrast, injection of bare unicase showed a mild decrease of uric acid concentration, but it rebounded slightly by 96 h. The nanocapsule platform was further generalized for systemic delivery of other proteins to treat diseases such as organophosphate poisoning[76] and hyperoxaluria,[35] which, analogous to the uricase nanogel, displayed noteworthy long-circulating bioscavenger behavior and low immunogenicity. Therefore, this approach may open up a new avenue for research and novel clinical strategies against a myriad of metabolic disorders diseases and systemic intoxications.

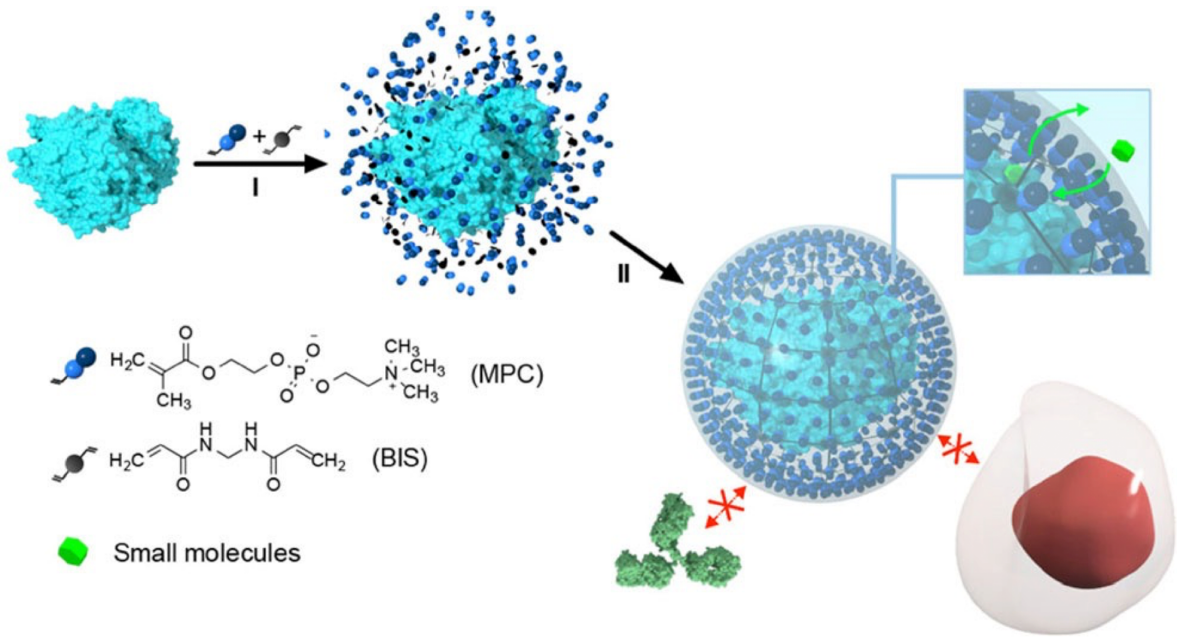

Figure 1-3 Design and synthesis of stealth protein nanocapsules. Schematic illustration of the synthesis of stealth protein nanocapsules by (I) enriching MPC (monomer) and BIS (crosslinker) around a protein molecule, and (II) in situ polymerization of the monomer and crosslinker forming a thin shell of PMPC around a protein molecule. PMPC shells are permeable to small-sized substrates, which enables enzymatic reactions to occur within the protein core. Zwitterionic shells also resist the adsorption of proteins and phagocytosis, endowing nanocapsules with stealth capabilities. Reprinted with permission from ref.[86]

1.3.4 Polysaccharides

Polysaccharides, either linear or branched, are polymeric carbohydrates composed of long chains of monosaccharide subunits bonded together through glycosidic linkages. Among them, dextran is a naturally occurring highly soluble glucose polymer comprised mainly of a linear α-1,6-glucosidic linkage with some degree of branching via 1,3-linkage. It is widely utilized as a drug surface modifying agent since 1978.[87] For instance, dextran has been used as a plasma expander in the clinic and attempted as a PEG substitute to resolve the activity loss issue associated with

PEG conjugation.[88] So far, due to possessing a similar steric hindrance effect as PEG molecules[88,89], dextran has been covalently attached to various proteins to protect them against renal filtration, proteolytic degradation and immunological response. Furthermore, dextran and its derivatives were also explored as antitumor dextran-drug conjugates which manifested superior antitumor activity compared to free drugs.[90,91] However, the use of dextran polysaccharide isn't without any problem. Studies suggest that intravenous administration of dextran with high molecular weight have a tendency to cause anaphylaxis.[92] As well, in certain studies, dextran coating on nanoparticles increased complement activation.[93]

Another polysaccharide, heparin is an endogenous anticoagulant made of variably sulfated repeating disaccharide units. It was used as a coating material to improve blood-compatibility and inhibit the complement activation process in several investigations.[94] As one example, the dextran and heparin coating on poly(methyl methacrylate) nanoparticles dramatically extended the *in vivo* circulation time of the nanoparticles compared to unmodified ones. However, heparin also exhibited undesirable side effects including hemorrhagic complications and thrombocytopenia when administered non-intravenously.[95]

1.3.5 Other polymers for systemic protein delivery

Since the first polymer-protein conjugates entered the market in the early 1990s, the field of polymer therapeutics is undergoing marked expansion. In addition to abovementioned classical drug delivery systems, there are still a number of other polymers that have been suggested. Poly(vinylpyrrolidone) (PVP) is an FDA approved synthetic polymer with highly attractive biocompatibility and immunocompatibility.[96] Its broad utility ranges from plasma volume expander to drug carrying vehicles and wound dressings.[96-98] Several surface modification

strategies of synthesizing a PVP layer around protein therapeutics have been described. In a most recent exploration, uricase was encapsulated within a thin PVP shell via *in situ* polymerization. Empowered by the PVP coating, the resulting uricase nanocapsule demonstrated evidently reduced immunogenicity, extended half-life and improved therapeutic efficacy in animal models.[97] Besides, the conventional conjugation approach was also adopted to modify several protein drugs for systemic detoxification or antitumor applications.[99,100] Take tumor necrosis factor-α (TNF-α) as an example. PVP conjugated TNF-α exhibited over 2-fold higher antitumor activity and 3-fold longer plasma half-life than that of PEG-TNF-α. More attractively, the conjugate displayed no side effects such as tissue inflammation and piloerection that are commonly induced by native TNF-α.[99]

Acrylamide derivative polymers were studied for their possible use in drug formulations since the early days of polymer therapeutics. Among those, poly[*N*-(2-hydroxypropyl) methacrylamide] (PHEMA) copolymers represent a group of most frequently studied hydrophilic polymers utilizable as a plasma expander and drug delivery system. In effect, the first synthetic polymer-based drug conjugate that entered clinical trial were made of PHEMA copolymers.[101] Morgen *et al*. covalently coupled insulin to PHEMA and observed a dramatically enhanced stability of insulin during incubation with luminal enzymes. What's more, the conjugate was capable of transferring insulin into the serosal fluid and sacs.[102] Liu et al. developed a biomimetic enzyme nanocomplex where enzymes with synergistic functions were enwrapped within a single polyacrylamide (pAAM) nanocapsule. Since the toxic intermediates generated were eliminated spontaneously, the nanocomplex showed minimized toxicity and enhanced antidotal efficiency in alcohol-intoxicated mice.[103]

Another commonly used blood plasma substitute is poly(*N*-acryloylmorpholine) (PAcM). Similar to PVP and PHEMA, PAcM was also explored to form polymer-derivatized proteins. For example, *N*-acryloylmorpholine (AcM) was copolymerized with *N*-acryloxysuccinimide) (NAS) to acquire water solubility, biocompatibility, and reactivity towards protein amino groups. Two model proteins, catalase, and ribonuclease, were then grafted with the copolymer, resulting in no activity loss.[104] In another scenario, PAcM-uricase conjugate displayed significantly subdued immunogenicity and antigenicity.[105]

Furthermore, amphiphilic PEG-containing block copolymers are another class of polymer used as a drug delivery system. At an aqueous interface, the amphiphilic property causes the formation of micelles where insoluble blocks are segregated into the core surrounded by the hydrophilic PEG surface. PEG/polylactide (PLA) block copolymers are typical representatives of this class. Especially, the hydrophobic PLAs segments are biodegradable and nontoxic, and the outer PEG-brushed layer carries a great advantage against blood protein absorption and cell adhesion. In a transmucosal drug delivery study, Tobio et al. encapsulated a model protein antigen, tetanus toxoid (TT), within the PEG/PLA block copolymers and observed that, in contrast to the PLA nanoparticles, PLA-PEG micelles led to a much greater penetration of TT into the blood circulation and longer persistence in the blood compartment over 48 h.[106] In addition, other hydrophobic block segments such as poly(propylene oxide) (PPO) and poly(propylene sulfide) (PPS) were also investigated. For example, PEG/PPO triblock copolymers were conjugated with organophosphate hydrolase (OPH), which could self-assemble into micelles in an aqueous milieu with stabilized OPH on the surface. Likewise, superoxide dismutase (SOD) was displayed on the surface of PEG-PPS micelles through a similar fashion.

More interestingly, the PPS within the micelle cores can synergistically scavenge the toxic hydrogen peroxide produced by SOD.

Taken together, due to limited space available in this chapter, it is impossible to elaborate all nanovehicles that have been explored for systemic protein delivery. Instead, special attention has been paid to these key illustrative examples that underline the future potential and direction of this critical research field.

1.4 Intracellular Protein Delivery

Intracellular protein delivery mainly refers to the transportation of protein cargo to specific cellular compartments or organelles aiming to repair the mechanisms underlying disease initiation and progression. The typical repairing events may involve gene editing, regulation of gene expression and function, modulation of metabolic pathways and probing the intracellular environment.[107] Despite its high potential in biomedical research and clinical applications, direct intracellular delivery of protein cargo is impractical due to the inherent cell membrane barrier, which effectively restricts the successful entry and accumulation of negatively charged and hydrophilic proteins at diseased sites of action.[108] To overcome this hurdle, various physical and biochemical approaches have been invented over the past several decades to permeabilize cells, which include membrane disruption, chemical transfection, and viral and non-viral vectors mediated transmembrane delivery.[107,109] The membrane disruption and chemical transfection approaches, nonetheless, are less amenable to *in vivo* translation and have the propensity to cause cytoplasmic content leakage, internal membrane breakdown, and protein denaturation.[110] Besides, the viral systems are limited to nucleic acid delivery only and can trigger adverse immune response.[111]

Recent breakthroughs in biological sciences and nanotechnology are providing an unparalleled opportunity to adapt non-viral carriers to realize many delivery goals that were once deemed impractical. The purpose of synthetic carriers is basically threefold: (1) to pack up the cargo and protect it against degradation, (2) to traverse the membrane to the targeted intracellular compartment, and (3) to unpack the payload in an appropriate spatiotemporal manner.[107] Despite the enormous promise, there still remain long-standing challenges such as relatively low delivery efficiency, payload capacity limit, and immunogenicity. In this review section, a brief overview of several prevalent intracellular delivery approaches is highlighted, but specific emphasis will be dedicated to the review of advanced carriers for gene-editing nucleases delivery that correlates closely with my research goal.

1.4.1 CPP-mediated intracellular protein delivery

Cell-penetrating peptides (CPPs), either naturally occurring or entirely synthetic, are a large group of very heterogeneous peptides that have become broadly applied to power cellular uptake of large biomolecules.[112] They are found ubiquitously within living organisms and typically comprised of <30 amino acids.[113] Despite that the first discovered CPPs, Tat peptide, and penetratin, are featured with cationic clusters of arginine or lysine residues,[114,115] many negatively-charged and amphipathic CPPs have also been exploited and successfully used.[116] It is well documented that CPPs can be installed on the protein cargo through chemical conjugation, non-covalent interaction or CPP protein fusion methodologies depending on the nature of protein cargo and CPPs involved. For example, transcription activator-like effector nucleases (TALENs) were covalently coupled with the distal cysteine residue of artificial Cys (Npys)-(D-Arg)$_9$ due to the presence of abundant cysteine moieties on TALENs surface.[117] In comparison, the

amphiphilic feature of Pep-1 allows the facile package of protein cargo through non-covalent electrostatic and hydrophobic interaction.[116]

Despite the variety of CPP design approaches currently available, the precise CPP translocation pathways at the molecular level remain elusive. It is generally accepted that CPP mediated cell penetration is non-disruptive, which first takes place through electrostatic interactions with proteoglycans and then is driven by several parameters including the secondary structure of the CPP, the type and concentration of the cargo and the host cell type.[118] Futaki and co-workers discovered that arginine-rich peptides could be internalized either by macropinocytosis or direct translocation through the plasma membrane, with the former being dominant.[119] Instead, Tat enters T cells essentially via clathrin-mediated endocytosis.[120] While new generations of CPPs and new applications continue to be developed, their therapeutic use is still hampered by the fundamental issues that these peptides have no cell-specific entry, and endosomal escape remains a rate-limiting step of CPP-mediated drug delivery.[112,121]

Table 1-2. Representative CPPs: origins and sequences (adapted from ref.[118])

Peptides	Origin	Sequences
Peptides deriving from protein transduction domains		
Tat	HIV-Tat protein	PGRKKRRQRRPPQ
Penetratin	Homeodomain	RQIKIWFQNRRMKWKK
Transportan	Galanin-mastoparan	GWTLNSAGYLLGKINLKALAALAKKIL
VP-22	HSV-1 structural protein	DAATATRGRSAASRPTERPRAPAR-SASRPRRPVD
Amphipathic peptides		
MPG	HIV Gp41-SV40 NLS	GALFLGAAGSTMGAWSQPKKKRKV
Pep-1	Trp-rich motif-SV40 NLS	KETWWETWWTEWSQPKKKRKV
MAP	Chimeric	KALAKALAKALA
SAP	Proline-rich motif	VRLPPPVRLPPPVRLPPP
PPTG1	Chimeric	GLFRALLRLLRSLWRLLLRA
Other cell-penetrating peptides: cationic peptides		

Oligoarginine	Chimeric	Agr8 or Arg9
hCT(9-32)	Human calcitonin	LGTYTQDFNKTFPQTAIGVGAP
SynB	Protegrin	RGGRLSYSRRRFSTSTGR
Pvec	Murine VE-cadherin	LLIILRRRIRKQAHAHSK

1.4.2 Liposome-mediated intracellular protein delivery

As discussed in the prior section, conventional liposome carriers are characterized by their rapid systemic clearance *in vivo*,[63] and PEGylated liposomes, though exhibiting improved pharmacokinetics, suffer from low target selectivity and transmembrane permeability. As a result, several engineering approaches have been introduced to enhance the *in vivo* performance of liposomes. These approaches include the attachment of site-directed surface ligands, the inclusion of stimuli-responsive constituents and the modulation of surface charge.[122]

Antibody fragments, folate, transferrin, and peptides are common biological ligands utilized to conjugate liposomes to enhance their targeting specificity towards designated cell types. In practice, multi-functional liposomes with more than one targeting ligand or functional constituents are usually constructed. For instance, PEGylation is normally performed to increase the circulation time of liposomes, which leads to more efficient accumulation at the target site. The site-directed ligands installed on liposome surface further enhance the selective targeting and cellular uptake of liposomes. After internalization, the stimuli-response components are crucial to promoting liposomal payload release into the designated spot upon stimulation.[123] Bungener and coworkers designed a virosome, essentially a liposome bearing tailored cell binding and fusion moieties derived from native viral envelopes, to deliver protein antigen ovalbumin into dendritic cells for MHC class I and II presentation. It was observed that once the virosome entered the cell through receptor-mediated endocytosis, low pH in endosomes triggered membrane fusion and release of the encapsulated antigen into the cell cytosol effectively.[124]

Apart from ligand-mediated liposome targeting, cationic lipid formulations have also been investigated and manifested notable utility in topical delivery. For example, Zuris et al. demonstrated in his work that cationic lipid-mediated *in vivo* delivery of Cas9:sgRNA complexes into the mouse inner ear successfully resulted in Cas9-mediated genome editing rates of up to 20% of hair cells, which is almost tenfold more specific genome editing than traditional plasmid transfection approach.[26]

1.4.3 Polymer-mediated intracellular protein delivery

As nanotechnology continues to develop, there is a concomitantly increased quest for intracellular protein delivery using polymeric nanocarriers, likely because their key properties such as size, surface charge, and display ligands can be tailored and customized with higher flexibility than that of other delivery vehicles.[125] Current strategies for assembling protein cargo with polymeric nanocarriers include direct attachment, physical adsorption and interaction, encapsulation, and polymer micelles.[126]

Attaching polyethylene-imine (PEI) to the surface of various proteins through covalent conjugation or electrostatic interaction has been broadly examined for intracellular protein transduction. Up to date, a diverse array of proteins such as Cas9:sgRNA complexes, lgG, and P53 have been successfully delivered into the cellular targets of murine and human cells without obvious protein function loss.[127,128] Aside from conjugation and physical adsorption, Yan et al. reported an intracellular delivery approach based on protein nanocapsules weaved by free radical copolymerization of acrylamide, 2-dimethylaminoethyl methacrylate, and acid-degradable glycerol dimethacrylate.[129] Cellular internalization results indicated that nanocapsules entered the cells through a clathrin/caveolae-mediated endocytosis pathway, which is more efficient than

TAT-induced cellular uptake. Following the same synthetic route but with varied monomers and extra targeting ligands LHRH (luteinizing hormone releasing hormone), p53 protein was selectively delivered into targeted cancer cells where p53-mediated apoptosis was potently activated.[130]

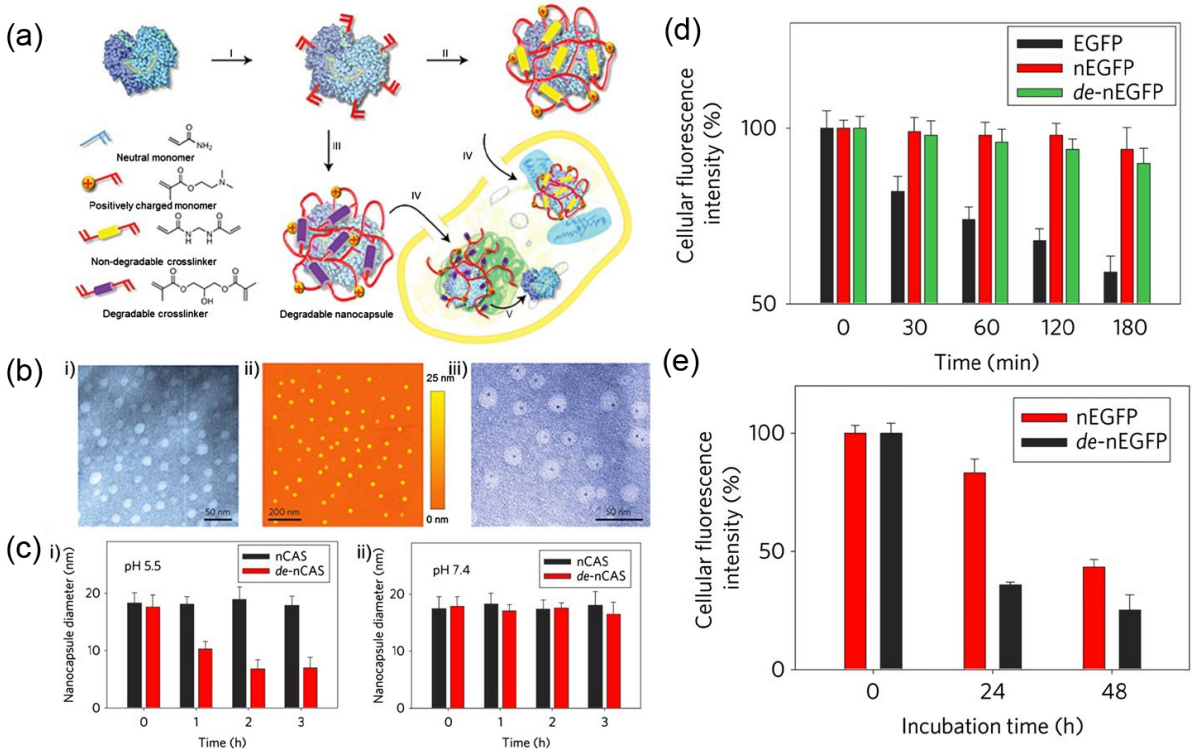

Figure 1-4 (a) Schematic illustration of the synthesis and cellular uptake of cationic single-protein nanocapsules with degradable and nondegradable polymeric shells. (b) (i)(ii) TEM (i) and AFM (ii) images of the HRP nanocapsules; (iii) TEM image of nanocapsules with a gold-quantum-dot-labeled HRP core for demonstration of nanocapsule architecture. (c) Particle sizes of degradable and non-degradable nanocapsules at pH 5.5 (i) and pH 7.4 (ii). (d) Fluorescence intensity of native EGFP, non-degradable EGFP nanocapsules (nEGFP) and degradable EGFP nanocapsules (de-nEGFP) after exposure to 1 mg·L^{-1} trypsin and α-chymostrypsin in buffer (pH 7.4, 50 °C). (e) Fluorescence intensity of Hela cells incubated with nEGFP or de-nEGFP for 3 h followed by incubation in fresh media. Reprinted with permission from ref. [1,129]

Analogous to protein nanocapsules, protein drugs can be encapsulated within polymeric micelles by self-assembly of block copolymers, as evidenced by Kim et al.'s study in which micelles were formed in aqueous phase when a positively charged di-block copolymer conjugate of poly(L-lysine)-poly(ethylene glycol)-folate (PLL-PEG-FOL) was complexed with bovine serum albumin (BSA). The extent of cellular uptake was dramatically enhanced against a folate receptor over-expression cell line compared to a folate receptor-deficient cell line.[131] Additionally, not only chemically synthetic but also naturally occurring polymers can be harnessed as cross-membrane drug carriers. For example, Su et al. prepared hollow polyelectrolyte nanocapsules composed of cysteamine conjugated chitosan and dextran sulfate and demonstrated that the formulation is able to decrease payload protein loss in acidic environments and retain a sustained cargo release in the cytosol responsive to glutathione level.[132]

1.4.4 Intracellular delivery of gene-editing nucleases

The advent of gene-editing technology is unprecedentedly transforming many aspects of human therapeutics, industrial biotechnology, and agriculture.[133] With customizable genetic scissors such as zinc-finger nucleases (ZFNs), transcription activator-like effector nucleases (TALEN), and clustered regularly interspaced short palindromic repeat (CRISPR)/Cas9 system, site-specific genomic tailoring of essentially any desired genomic sequence has become achievable and easy. Normally, the editing event starts with double strand breaks (DSB) induced by programmable nucleases into a pre-defined genomic site, followed by immediately stimulated repair either through non-homologous end joining (NHEJ) or homology-directed repair (HDR).[134] The NHEJ is an efficient but error-prone repair mechanism that usually results in gene disruption through

inducing indel mutations. In comparison, HDR is an accurate repair pathway that uses a homologous donor DNA template to correct DNA abnormalities. In this regard, HDR appears to hold a tremendous potential to revolutionize treatment options for genetic disorder diseases. However, gene correction or integration via HDR pathway is of low efficiency intrinsically. Besides, it is challenging in practice to deliver both site-specific nucleases and donor DNA simultaneously *in vivo*.[135,136]

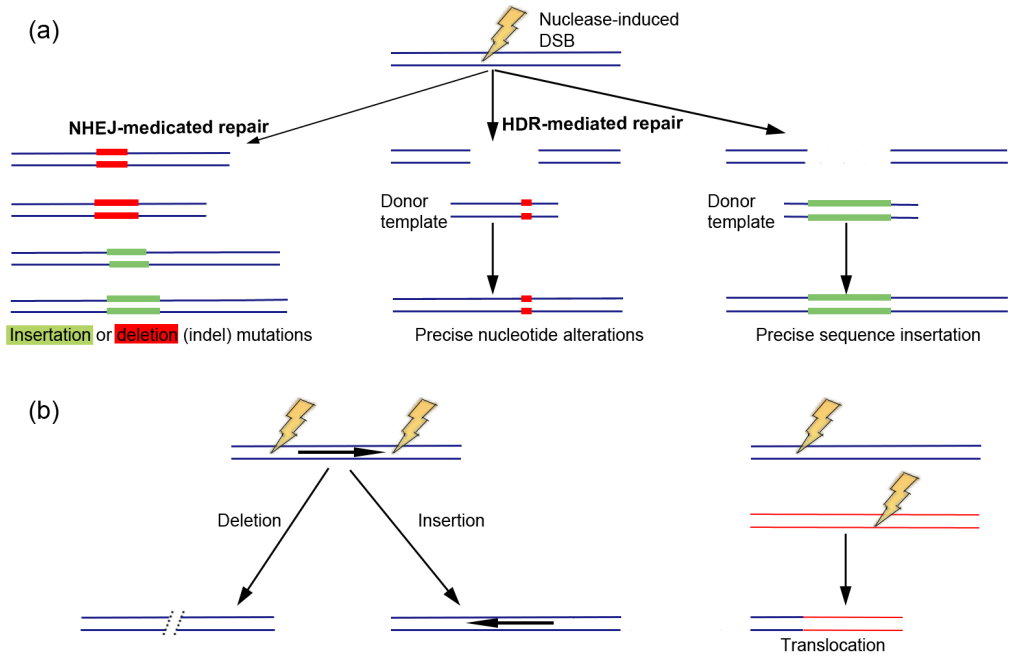

Figure 1-5 Nuclease-induced genome editing. (a) Single nuclease-induced double-strand breaks (DSBs) in a gene locus can be repaired by either non-homologous end-joining (NHEJ; thin black arrow) or homology-directed repair (HDR; thick black arrows). NHEJ-mediated repair leads to the introduction of variable length insertion or deletion (indel) mutations. HDR with double-stranded DNA donor templates can lead to the introduction of precise nucleotide substitutions or insertions. (b) Introduction of two nuclease-induced DSBs in *cis* on the same chromosome can lead to the deletion or inversion of the intervening sequence (left panel). The introduction of two nuclease-induced DSBs on two different chromosomes can lead to the creation of a translocation (right panel). Reprinted with permission from ref.[137]

In terms of molecular structure, ZFNs and TALENs are engineered fusion proteins comprised of a FokI nuclease combined with a customizable DNA-binding domain. Individual zinc finger domain typically contains a tandem array of Cys2-His2 fingers, each recognizing three-base pairs of DNA.[138] Distinctively, the TALE domain encompasses a series of approximately 34-amino-acid repeats that each uniquely binds a single nucleotide subsite. Besides, these TALE repeats are near identical except that two amino acids situated in position 12 and 13 in each repeat, termed the repeat variable di-residues (RVDs), are hypervariable and dictate the DNA binding specificity.[137] It is also worth noting that both ZFNs and TALENs function as dimeric proteins because FokI nuclease must dimerize to cleave DNA. Moreover, the two adjacent and independent DNA binding events required for dimer formation further enlarge the recognition region and increase targeting specificity.[134]

In order for gene-editing nucleases to modify targeted DNA sequences, they must be escorted into the nucleus of host cells to realize their full potential. In general, nuclease can be delivered with non-viral and viral vectors, the latter of which commonly includes adenovirus, lentivirus and, adeno-associated virus. Nonetheless, virus-based gene therapy that relies on delivering nuclease-encoding DNA sequences is fundamentally limited owing to the sustained nuclease expression and possible insertional mutagenesis, which poses a high risk of carcinogenesis, immunogenicity, and off-target genome damage.[139] Given these safety concerns, non-viral vehicles together with nonreplicable nuclease proteins that function in a transient fashion, emerge as a promising candidate to endow editing outcomes with improved specificity, increased safety, and broader applicability.[134] Therefore, in view of the above argument and in accordance with the topic of this section, the following review will principally center on recent

advances in gene therapy utilizing non-viral delivery systems, especially those by virtue of nanotechnology.

ZFNs have been reported to intrinsically possess cell-penetrating capabilities and were successfully adapted to disrupt endogenous genes in several cell lines without any delivery vectors,[140] nevertheless, their effective concentration is at micromolar levels—higher than the desired dose. Regarding TALEN protein delivery, Liu et al. validated that TALEN conjugated to poly-Arg peptides (R9) was able to penetrate through the membrane barrier of HeLa cells and induce CCR5 gene disruption at a frequency three-fold higher than that by TALEN-expressing plasmid.[117] Researchers also claimed that no overt cellular toxicity was observed and peptide/TALEN ratio was essential to attaining positive editing results. However, similar to ZFNs, the working concentration was at a rather high level. In another study, TALEN protein analog TALE-PV64, where the FokI nuclease was substituted with a VP64 transcription activation domain, was fused with negatively supercharged GFP to gain a net negative charge, which facilitated successive electrostatic-driven complexation with cationic lipofectamine. Remarkably, the resultant nanoparticle was able to activate tenfold increase in NTF3 gene expression level 4 h after treatment with a total protein concentration as low as 25 nM.[26]

Unlike ZFNs and TALENs that generate sequence recognition specificity via protein-DNA interactions, CRISPR/Cas9, essentially an RNA-guided endonuclease, relies on a customizable single guide RNA (sgRNA) to identify target DNA through Watson-Crick pairing.[141] On top of that, CRISPR can be applied for multiplex gene editing with high efficiency, but it is difficult for ZFNs and TALENs due to potential mismatched dimer formation.[134,142] Given its simplicity, convenience, and flexibility, this epochal CRISPR technology has turned into a standard tool for targeted gene modification with astonishing rapidity and popularity.

There have been several polymeric nanoparticles used to deliver Cas9-sgRNA complex *in vivo*. Sun and coworkers generated a self-assembled DNA nanoparticle called "nanoclew" where a Cas9-sgRNA complex was loaded through partial base pairing between sgRNA and single-stranded DNA of the nanoparticle. Prior to delivery, cationic polymer polyethylenimine (PEI) was coated as the outer layer to enhance endosomal escape. The delivery potency was assessed in a U2OS cell line where the target EGFP disruption ratio was 28% induced by the nanoclew compared to 9.7% by a CPP based vector. Consistent results were observed in a U2OS.EGFP xenograft tumor model, in which 25% of the cells manifested EGFP gene disruption near the intratumoral injection site ten days after Cas9/sgRNA nanoparticle administration.[127] Through the same local administration approach, another investigation employed cationic lipid to guide the transmembrane delivery of Cas9:sgRNA complexes into the inner ear of a mouse, which gave rise to a robust target gene silence in 13% of outer hair cells near the injection site with no obvious toxicity effect.[26]

Delivery of the Cas9 ribonucleoprotein (RNP) to induce HDR represents tremendous promise for clinical translation. However, development of HDR based therapeutics can be challenging because it requires simultaneous *in vivo* delivery of Cas9 RNP and donor DNA.[136] In a recent proof-of-concept study, a potent nanovehicle, named CRIPSR-Gold, was created to overcome these hurdles and provide useful insights into future development work. To be specific, gold nanoparticles (GNPs) were pre-coated with a densely packed DNA layer that was then hybridized with single-stranded donor DNA, after which Cas9 RNP was introduced via Watson-Crick interaction, and finally a cationic polymer poly(N-(N-(2-aminoethyl)-2-aminoethyl) aspartamide) (PAsp(DET) with endosomal disruption properties was complexed to direct endosomal release of Cas9 RNP and donor DNA. The ability of CRISPR-Gold to induce HDR

was first examined in HEK cells, which led to 11.3% of the BFP-HEK cells to express GFP via HDR. Similar results were observed with a wide range of other cells. More surprisingly, CRISPR-Gold was able to correct 5.4% of the dystrophin gene mutation *in vivo* in *mdx* mice following an intramuscular injection with minimal off-DNA damage and toxicity.[135]

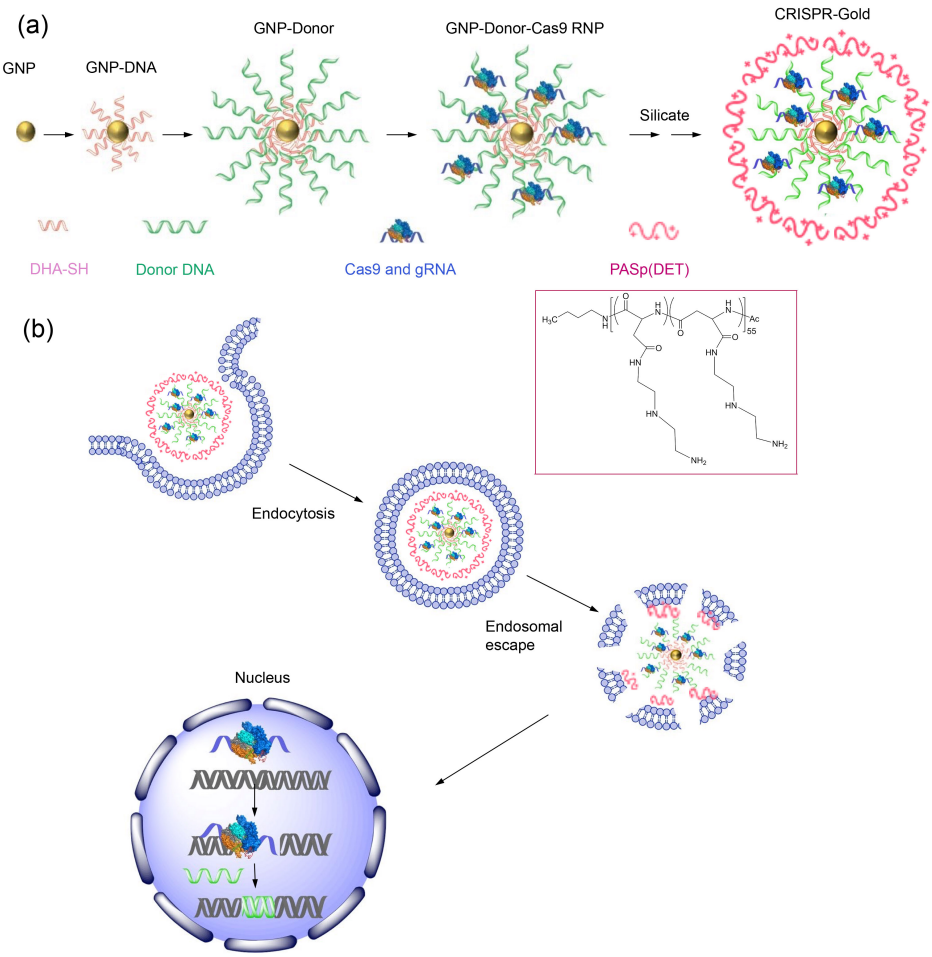

Figure 1-6 (a) Synthesis of CRISPR-Gold. GNPs 15 nm in diameter were conjugated with a 5' thiol modified single-stranded DNA (DNA-SH) and hybridized with single stranded donor DNA. Cas9 and gRNA were loaded and then a silicate and the PAsp(DET) polymer coating were added. The 'DET' stands for diethylenetriamine. (b) CRISPR-Gold is internalized by cells in vitro and in vivo via endocytosis. This triggers endosomal disruption and releases Cas9 RNP and donor DNA into the cytoplasm. Nuclear delivery results in HDR. Reprinted with permission from ref.[135]

1.5 Protein Immobilization by Polymers for Biosensors Construction

Not only have recombinant proteins been extensively harnessed as therapeutics, but they have also been broadly explored to fabricate biosensors. In general, a biosensor is a device having a biological recognition element connected to or integrated within a transducer that continuously converts recognition events into measurable signals in biological media. The unprecedented interest in biosensor development is mostly attributed to its unparalleled sensitivity, selectivity and ability for real-time analysis.[143] The biological recognition element normally comprises a catalytic enzyme which is prone to deactivation in its free form or when applied *in vivo*, therefore, enzyme immobilization emerges as a common stabilization procedure in many biosensor fabrications. It is widely acknowledged that the supporting materials for enzyme immobilization impact sensor performance to a large extent. A key criterion of selecting supporting materials is that they could provide a biocompatible and inert environment without interfering with the conformation and activity of the enzyme.[144] As a result, there has been an increasing appreciation of utilizing polymeric materials as immobilization matrices over the past decade owing to their good mechanical, easily tunable and biocompatible properties.[145]

Basically, enzyme immobilization for biosensors can be roughly divided into physical and chemical approaches. The physical method contains physical adsorption, enzyme entrapment, microencapsulation, etc., whereas the chemical immobilization method encompasses covalent binding, crosslinking, electrochemical polymerization and micelle.[146] In terms of types of biosensors: calorimetric biosensors, optical biosensors, potentiometric biosensors and electrochemical biosensors are the four most common categories, among which, electrochemical biosensors, are the oldest and most widely available group in the solid-state sensor field.[145]

Taken together, a brief overview of recent contributions of incorporating major functional polymers into biosensor construction is summarized in the following section.

Polystyrene (PS) film is a promising matrix for enzyme immobilization because of its extraordinary characteristics such as chemical inertness, low molecule permeability, biocompatibility, strong adsorption ability, etc.[147] However, functional moieties for crosslinking must be introduced into the polymer chain before enzyme immobilization and subsequent coating on the electrode surface can be carried out; in this scenario, polymaleimidestyrene (PMS) was invented with two polymerizable vinylene groups.[148] The vinyl group located in the maleimide ring, in particular, possesses strong reactivity towards SH groups, leading to the efficient and extensive covalent bonding between enzymes and PMS, and enzyme micelles formation in certain reaction conditions. As an example, Wang et al. employed PMS to construct a glucose biosensor where glucose oxidase micelles were immobilized covalently onto a carbon electrode. The resultant biosensor exhibited steady sensitivity and activity over a study phase of one month. Nonetheless, the immobilization process that involved dispersion of PMS bonded-enzyme in hydrophobic PS solution was detrimental to enzyme activity to a certain degree.[147]

The biofouling and interferents are two primary issues frequently affecting the performance of a biosensor. The problem may become aggravated if the interferents happen to be electroactive and the electrochemical measurements are implemented *in vivo*.[145] The cellulose acetate layer behaves as an ideal immobilization matrix on the electrode surface, which allows only small molecules such as hydrogen peroxide to permeate to the electrode whereas a number of electrochemically-active species are largely restricted.[149] Nafion is another chemically inert polymer frequently used as an electrode coating material as well. The as-formed membrane harbors outstanding thermal stability, antifouling properties and mechanical strength. Moreover,

its anionic nature showed significant exclusion of anionic interferents such as ascorbic acid in the body.[150] Likewise, polypyrrole is a cationic coating film that finds its special utility in filtering out positively charged dopamine from the brain tissue.

Chitosan and chitin are naturally occurring biopolymer carrying a unique set of properties: physiological inertness, high affinity to proteins, mechanical stability, biocompatibility and biodegradability.[151] The demands for exploiting natural biomaterials from renewable sources and in view of plentiful chemically convertible moieties in their backbone, Chitosan and chitin have been put under the spotlight. As of today, there are numerous chitosan-based biosensors being described. Taking a glucose biosensor as an example, where a glucose oxidase (GOD)-graphene-chitosan nanocomposite film was generated, affording the immobilized enzyme good stability and retained bioactivity. Furthermore, this film lent the biosensor a wider linearity range and much higher sensitivity as compared with other nanostructured supports.[152]

Conductive polymers (CPs) like polypyrrole (PPy), polyaniline (PANI), polythiophene (PT) are a class of macromolecules with high electrical conductivity, electron affinity, stability and biocompatibility, because of which, application of CPs as suitable matrices for biomolecules in biosensor assembling has aroused a lot of interest. Similarly, sol-gel and hydrogel materials have also been broadly investigated as immobilization support of enzymes, and the sol-gel and hydrogel-based biosensors essentially exhibited high sensitivities and improved diffusivity.

In conclusion, the above short overview only encompasses some most common polymers being used in biosensor fabrication given the rapid development pace of novel polymers. Further, the integration of these novel polymeric materials with nanotechnology should drive the quicker emergence of biosensors with more sensitive and faster assays. More attentively, smart polymers

with facile tunability, multi-functionality and multi-responsiveness for novel enzyme-based bioelectronics synthesis are becoming a new intense focus.

1.6 Summary

Overall, my search mainly concentrated on overcoming these challenges discussed above within the context of protein delivery and enzymatic biosensors. In more detail, my research endeavored to address four common issues regularly encountered in systemic protein delivery, intracellular protein delivery and enzymatic biosensor fabrication through the introduction of polymeric protein nanoparticles based on the protein nanocapsule and protein immobilization platforms respectively. In this thesis, research pertaining to the following topics are intensively investigated.

- Design and synthesis of poly(phosphorylcholine) encapsulated oxalate oxidase-nanocapsules as a potential anti-hyperoxaluria drug with prolonged plasma half-life and mitigated immunogenicity. (Chapter 2)
- Intracellular delivery of TALEN nucleases with cationic nanocapsules for efficient excision of integrated HIV-1 from primary cells. (Chapter 3)
- Design and fabrication of a novel choline biosensor that exhibits enhanced sensitivity and stability using poly(zwitterionic) polymer immobilized choline oxidase. (Chapter 4)

Chapter 2. Nanocapsules of Oxalate Oxidase for Hyperoxaluria Treatment

2.1 Introduction

Ever since recombinant human insulin was introduced to regulate diabetes, protein therapeutics has emerged as a powerful tool for the treatment of various systemic disorders such as hyperuricemia, phenylketonuria, and adenosine deaminase deficiency. This strategy may be extended to other metabolic disorders such as hyperoxaluria or systemic oxalosis, a disease caused by excessive accumulation of oxalate. Given that oxalate cannot be metabolized by humans and is primarily eliminated through the kidney, oxalate from endogenous biosynthesis or dietary sources may accumulate, causing organ disorders such as urolithiasis and nephrocalcinosis.[153-155] Although clinical treatment with vitamin B6 or thiazide diuretics can temporarily relieve the symptoms, long-term management of the systemic oxalate level is expected to provide better therapeutic outcomes.[156,157]

To effectively treat hyperoxaluria, oxalate accumulation needs to be reversed, potentially by the systemic clearance of oxalate. In this context, oxalate oxidase (EC 1.2.3.4, denoted as OxO), which breaks down oxalate into carbon dioxide (CO_2) and hydrogen peroxide (H_2O_2), is a highly promising therapeutic protein for the systematic clearance of oxalate.[158] However, the OxO overexpressed in *Pichia pastoris* often contains non-human glycans,[159,160] which may be subject to rapid clearance, and may induce high immunogenicity.[57,161,162] Liposomes containing OxO have been administered intraperitoneally to rats with hyperoxaluria, resulting in reduced oxalate concentration in the urine. However, essential information regarding the stability, biodistribution, pharmacokinetics, and immunogenicity of the OxO liposomes was not

reported.[163,164] Developing delivery vectors for OxO with prolonged circulation time and reduced immunogenicity is of great importance for the treatment of hyperoxaluria. Therefore, we herein report the generation of OxO nanocapsules for the effective treatment of hyperoxaluria.

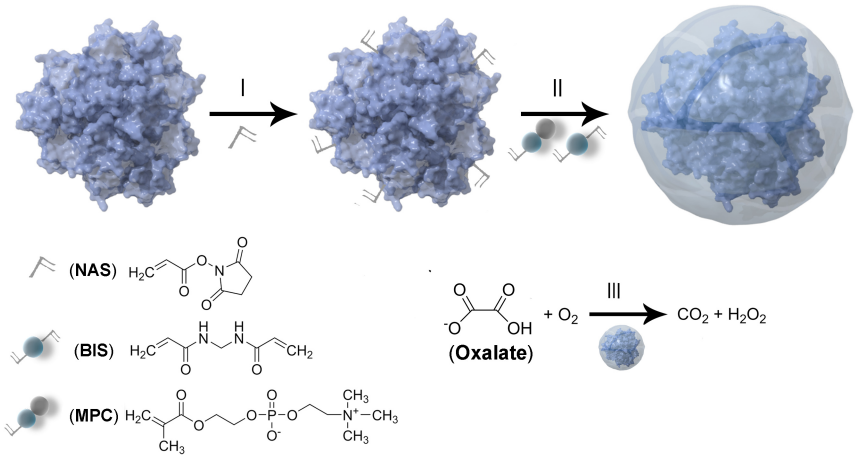

Figure 2-1 Synthesis of oxalate oxidase (OxO) nanocapsules (nOxO). (I) Conjugation of acryloyl groups with the native OxO molecule. (II) *In situ* polymerization of 2-methacryloyloxyethyl phosphorylcholine (MPC, the monomer) and N,N-methylenebisacrylamide (BIS, the crosslinker) to form a thin layer of zwitterionic polymer around an OxO molecule. (III) oxalate degradation catalyzed by nOxO.

Figure 2-1 illustrates the synthesis of OxO nanocapsules. First, OxO is conjugated with acryloyl groups by reacting it with *N*-acryloxysuccinimide (NAS) (Step I). Subsequently, *in situ* polymerization is performed using 2-methacryloyloxyethyl phosphorylcholine (MPC) as the monomer and *N,N′*-methylenebisacrylamide (BIS) as the crosslinker (Step II). Driven by noncovalent interactions, the monomers and crosslinkers are enriched around the OxO molecules, and the polymerization process leads to the formation of OxO nanocapsules (denoted as nOxO) that contain an OxO core and a crosslinked polymer shell. Such shells are thin enough to allow

the rapid transport of oxalate to the core OxO, ensuring effective breakdown of the oxalate. Also, the shells comprised of a zwitterionic polymer are able to prolong the circulation time of the nanocapsules.[36,86,165]

2.2 Methods, Experiment, and Characterizations

2.2.1 Materials and instruments

All chemicals were purchased from Sigma-Aldrich unless otherwise noted, and were used as received. *N*-(3-Aminopropyl) methacrylamide was acquired from Polymer Science, Inc. J774.1 and 3T3 cells were purchased from American Type Culture Collection (ATCC). The Dulbecco's modified eagle medium (DMEM) and penicillin/streptomycin were purchased from Invitrogen (Carlsbad, CA). Fetal bovine serum (FBS) was purchased from Lonza Walkersville Inc. (Walkersville, MD). Resazurin was obtained from Acros Organics (Pittsburgh, PA). Goat anti-mouse lgG (H+L) secondary antibody, HRP conjugate was purchased from Thermo Scientific (Rockford, IL). BALB/C (6-8 weeks) were ordered from Jackson Laboratory (Bar Harbor, ME). Barley OxO and its nonglycosylated variant (S49A-OxO) overexpressed in *Pichia pastoris* were kind gifts of Professor James W. Whittaker (Oregon Health and Sciences University).

UV/Vis adsorption was acquired with a Beckman Coulter DU®730 UV/Vis spectrophotometer. TEM images were obtained on a Philips EM-120 TEM instrument. Particle size and zeta potential were measured with Zetasizer Nano-ZS (Malvern Instruments Ltd., UK). Fluorescence intensity was measured with a Tecan infinite M200PRO microplate reader. Cells were observed with a Leica DMi8 inverted fluorescence microscope. Flow cytometry analysis was monitored on a Becton Dickinson Fortessa flow cytometer. NIR fluorescent images were acquired using an IVIS Lumina II imaging system (Xenogen, Toronto, ON, Canada).

2.2.2 Acryloxylation of OxO

To start with, oxalate oxidase (2 mg/mL) was dialyzed against sodium borate buffer (20 mM, pH 8.5), after which, *N*-Acryloxysuccinimide (NAS, 10% in DMSO, m/v) was added at 20:1 molar ratio (NAS to protein) to perform the conjugation. The reaction was kept at 4 °C for 1 h. Residual NAS was removed through dialysis against phosphate buffer (20 mM, pH 7.0).

As NAS conjugation consumes lysine groups on OxO surface, the average amount of acryloyl groups attached can be determined by quantifying the residual (unreacted) lysines on the protein with a fluorescamine assay. A typical procedure for the conjugation is described as follow; fluorescamine was dissolved in anhydrous DMSO to make a 3 mg/mL stock solution. OxO and its acryloylated counterpart were initially prepared as 1 mg/mL with phosphate buffer (0.1 M, pH 7.0), and then underwent a series of dilutions into 0.00781, 0.01563, 0.03125, 0.0625, 0.125, 0.25, 0.5 and 1 mg/mL separately; pipette 100 μL of each dilution into an opaque 96-well, followed by adding 30 μL of the fluorescamine solution. The plate was incubated at room temperature (25 °C) for 1 hr. After the incubation, the fluorescence intensity (Ex = 360 nm, Em = 465 nm) was read with a microplate reader. The number of residual lysines was estimated and the result was shown in Table 2-1.

Table 2-1. The conjugation of acryloyl groups

NAS/OxO Ratio	Total Lys groups	Unreacted Lys (%)	Average No. of acryloyl groups conjugated
20	48.0	75.4%	12.0

2.2.3 Synthesis of n(OxO)

1 mL of acryloxylated OxO (1 mg/mL), 134 μL 2-methacryloyloxyethyl phosphorylcholine (MPC, 25%, w/v) and 26.4 μL *N,N′*-methylenebisacrylamide (BIS, 10%, w/v)

were added and thoroughly mixed in phosphate buffer (50 mM, pH 7.0). Free radical polymerization was initiated by adding 16.3 μL of ammonium persulfate (APS, 10%, w/v) and 4.2 μL of *N,N,N′,N′*- tetramethylethylenediamine (TEMED). The reaction was allowed to proceed for 2 hr at room temperature (25 °C). After the polymerization, the solution was extensively dialyzed against 1×PBS buffer to remove unreacted small molecules. To remove unencapsulated OxO, n(OxO) was purified by passing through a hydrophobic interaction column (Phenyl-Sepharose CL-4B) with 2.0 M ammonium sulfate as the elution buffer. This procedure was applied to OxO variant (S49A) nanocapsule fabrication as well.

2.2.4 TEM and DLS measurement

10 μL TEM samples were dropped on a copper grid. After 2 min, excess amount of samples was removed. The grid was then stained with 1% phosphotungstic acid (PTA) solution for 5 min. After that, the grid was rinsed three times with deionized-water and allowed to dry for TEM observation. DLS measurements were taken at 173° scattering angle using a Zetasizer nano instrument equipped with a 10-mW helium-neon laser (λ=632.8 nm) and a thermoelectric temperature controller.

2.2.5 Agarose gel electrophoresis and SDS-PAGE

0.7% (w/v) agarose gel was prepared in TAE buffer (pH 8.3). Protein sample with a concentration of 0.2-1 mg/mL was pre-mixed with 20% glycerol at a volume ratio of 9:1 before being loaded. Electrophoresis was conducted with an Edvoket M12 electrophoresis cell under a constant voltage of 110 V for 15 min. SDS-PAGE was carried out in a 10% (w/v) polyacrylamide resolving gel. In brief, 10 μL of 1 mg/mL protein sample was re-suspended in 2× loading buffer. Without boiling, the samples were loaded and the electrophoresis was performed at 120 V and 40 mA for 60 min. The gel was stained by the Coomassie Brilliant Blue.

2.2.6 Characterization of OxO content

OxO concentration was determined by optical absorption measurements, using the reported extinction coefficient (ε = 50,400 $M^{-1} \cdot cm^{-1}$ at 278 nm). The OxO content in nanocapsules was determined by the bicinchoninic acid (BCA) colorimetric protein assay. Briefly, a tartrate buffer (pH 11.25) containing 25 mM BCA, 3.2 mM CuSO4, and an appropriately diluted OxO sample was incubated at 37 °C for 30 min. Absorbance at 562 nm were determined with a UV/Vis spectrophotometer. OxO solutions with known concentration were used as standards.

2.2.7 Characterization of OxO content

OxO activity assay was performed in sodium acetate buffer (50 mM, pH 5.3) at room temperature. The reaction mixture (0.5 mL) contained 5 units horseradish peroxidase, 2 mM oxalate solution, 1.6 μM *N, N*-dimethylaniline and 1.6 μM 4-amino-antipyrine. The reaction was initiated by adding 5 μL OxO (1 mg/mL) and the absorbance at 555 nm was monitored continuously with a UV/Vis spectrophotometer. OxO activity was also examined in phosphate buffer (50 mM, pH 7.0) at 37 °C. Identical reagents as above were prepared in the reaction mixture (0.5 mL). The reaction was initiated by pipetting 40 μL OxO (1 mg/mL) into the mixture and incubated for 2 hr. The absorbance variation at 555 nm was recorded and analyzed. One unit of OxO activity was defined as the amount of enzyme required to generate 1 μM H_2O_2 in 1 min.

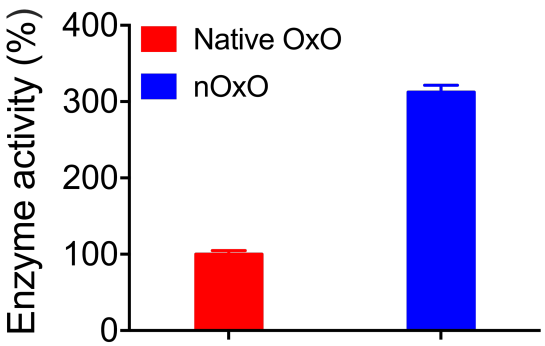

Figure 2-2 The activity of the native OxO and nOxO at acidic pH (pH=5.3)

2.2.8 OXO stability assay

The long-term storage stability experiment was made by incubating the native OxO, nOxO and their nonglycosylated counterparts S49A-OxO and nS49A-OxO (all 1 mg/mL) in 1 × PBS at 4 °C for up to 6 months. Aliquots of samples were taken out at specified time intervals and their OxO activities were examined and normalized.

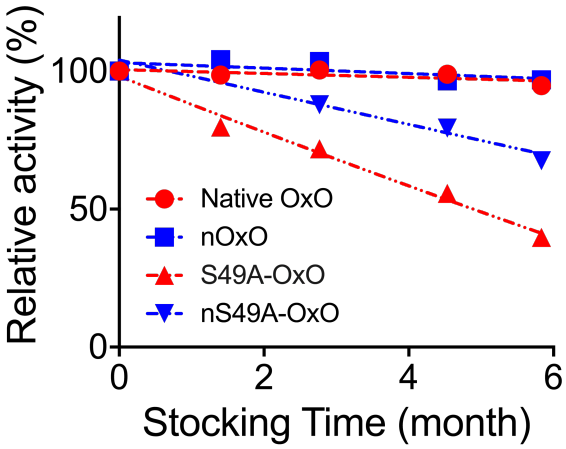

Figure 2-3 Long-term stability of native OxO, nOxO, nonglycosylated S49A-OxO and nS49A at 4 °C for 6 months. Residual activity was normalized to the original activity.

2.2.9 Antifouling property determination of nOxO

The antifouling property was evaluated in terms of OxO associated on surfaces pre-coated with mouse serum. To start with, mouse serum was diluted into 10 μg/mL protein in sodium carbonate buffer (0.1 M, pH 9.6). To each well of a 96-well plate, 100 μL of the diluted mouse serum was added and incubated at 4 °C overnight. Afterwards, the plate was washed twice with 1 × PBS to remove uncoated serum proteins. 30 μL of native OxO and nOxO (20 μg/mL) samples were then added into the as-coated wells and incubated at 37 °C for 2 hr. After that the plate was washed with 1 × PBS to remove unbound proteins. In the end, 100 μL of OXO substrate reagent 3,3′,5,5′-tetramethylbenzidine (TMB, 0.15 mg/mL, pH 4.0) was added and the reaction rate was monitored at 655 nm as ΔA655/min with a microplate reader. Standard curve was created by mixing 2 μL of above samples of known OxO content with 100 μL TMB reagent in each well and the reaction rate ΔA655/min was expressed as a function of OxO concentration.

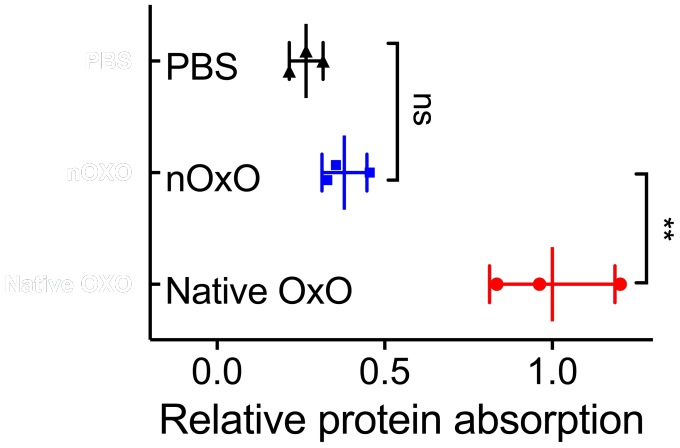

Figure 2-4 Quantitative measurements of the amount of the native OxO or nOxO absorbed onto the surfaces that were pre-treated with mouse serum.

2.2.10 Phagocytosis studies

Phagocytosis studies were assessed via fluorescence microscopy and fluorescence-activated cell sorting (FACS). Mouse macrophages J774A.1 cells were cultured in Dulbecco's Modified Eagle's Media (DMEM) supplemented with 10% fetal bovine serum (FBS) and 1% penicillin/streptomycin at 37 °C with 98% humidity and 5% CO_2. One day prior to the assay, cells were seeded into a 96-well plate at a density of 5,000 cells/well. 4 hr ahead of the inspection, 10 μL of 1 mg/mL native OxO and nOxO were added into each well. After incubation at 37 °C, the cells were stained with DAPI for 20 min and washed three times with 1×PBS before being visualized with a fluorescence microscope. Likewise in FACS experiment, cells (50,000 cells/well, 24-well plate) were seeded one day before. 100 μL of 1 mg/mL Rhodamine B-labeled native OxO and nOxO were added respectively and incubated for 4 h. Then the cells were washed three times with 1×PBS and analyzed via FACS.

2.2.11 Cell proliferation assay

The toxicity of nOxO was assessed by a resazurin assay. NIH/3T3 cells were seeded at a density of 10000 cells /well in a 96-well plate the day before the experiment. Native OxO and nOxO via gradient dilutions were then added into the cell medium and incubated for 24 hr. After incubation, culture medium was replaced with fresh one. Next, resazurin was added to a final concentration of 0.01 mg/mL and incubated for 3 hr. The cell viability was examined by measuring the fluorescence of each well (Ex = 535 nm, Em = 595 nm) with a microplate reader. Untreated cells and fresh medium were used as the 100% and 0% cell proliferation control.

2.2.12 Pharmacokinetics and biodistribution study

All animal experiments were performed in compliance with the Guidelines for the Care and Use of Research Animals established by the University of California, Los Angeles

Chancellor's Animal Research Committee (ARC). BALB/c mice (8–10 weeks old) were selected as the animal model during the entire animal studies. For PK study, 200 μL of native OxO and nOxO (3.5 mg/mL) were intravenously administered. At pre-determined time intervals (0.3, 12, 24, 36 and 48 h), blood samples (20 μL) were collected and centrifuged at 2,500 ×g for 15 min to remove the blood cells. Plasma OxO activity was then analyzed by mixing 4 μL of plasma with 100 μL of assay solution and monitoring the absorbance change at 655 nm. The assay solution was composed of 0.005 mg/ml HRP, 0.15 mg/ml TMB and 2 mM oxalate in succinate buffer (0.1 M, pH 4.0). For biodistribution investigation, the mice were intravenously injected with Cy5.5-labeled native OxO and Cy5.5-labeled nOxO with Cy5.5 dose of 0.75 nmol. Images of mice were taken on IVIS Lumina Imaging system II (Xenogen, Toronto, ON, Cananda) at 2, 18, 36 and 50 h time points after the injection. Meanwhile, the mice in another group were sacrificed and major organs (heart, liver, spleen, lung and kidney) were harvested and subjected for *ex vivo* imaging at 12, 24 and 48 h postinjection. The fluorescence intensity of region-of-interests (ROI) was inspected by Living Image software. Each sample has triplicates to generate statistical significance.

2.2.13 ELISA of anti-OxO antibodies

Sera collected at day 14 after initial injections were tested for anti-OxO antibodies using an indirect ELISA. Basically, 50 μL of pre-diluted native OxO solution (10 μg/mL in 50 mM carbonate/bicarbonate buffer, pH 9.6) was used to coat each well of a 96-well plate. After incubation at 4 °C overnight, the wells were washed four times by 1 × PBS. Then, a serial dilutions of mouse sera in blocking buffer (1 × PBS comprising 1% BSA and 0.05% tween 20) were added (50 μL/well) and incubated at room temperature for 2 h. Again, the wells were washed four times with 1×PBS, followed by loading each well with 50 μL of diluted anti mouse

lgG-HRP conjugate. After another 2 h incubation and four times wash with 1 × PBS. HRP substrate TMB was added (50 μL/well) and the plate was shaken for 15 min and 50 μL stop solution (1 M sulfuric acid) was added to each well. Absorbance at 450 nm was recorded by a microplate reader and prebleeding sera were used as negative control.

2.3 Results and discussions

Prior to encapsulation, OxO was reacted with NAS to conjugate the acryloyl groups with the OxO molecules. The extent of NAS modification was determined by fluorescamine assay, which indicated that approximately 12 acryloyl groups were attached to each OxO molecule (Table 2-1). The successful encapsulation of OxO was verified by various characterization techniques. The size and morphology of nOxO were first characterized by transmission electron microscopy (TEM), which revealed that the nOxO were spherical and had an average diameter of approximately 30 nm (Fig. 2-5(a)). The size of the nOxO was further evaluated by dynamic light scattering (DLS). As shown in Fig. 2-5(b), the hydrodynamic size of the nOxO increased to approximately 27 nm, compared with that of the native OxO, which had an average size of 6.5 nm. Furthermore, the zeta potential of the nOxO shifted to approximately 0 mV from −12 mV for the native OxO, indicating the successful encapsulation of OxO (Fig. 2-5(c)). The result was corroborated by agarose gel electrophoresis, in which the native OxO migrated to the positive electrode, whereas the nOxO did not move (Fig. 2-5(d)). Similarly, sodium dodecyl sulfate-polyacrylamide gel electrophoresis (SDS-PAGE) revealed different migration patterns for native OxO and nOxO. Unlike native OxO, the large size and neutral charge of nOxO prevented it from migrating into the separating gel (Fig. 2-5(e)).

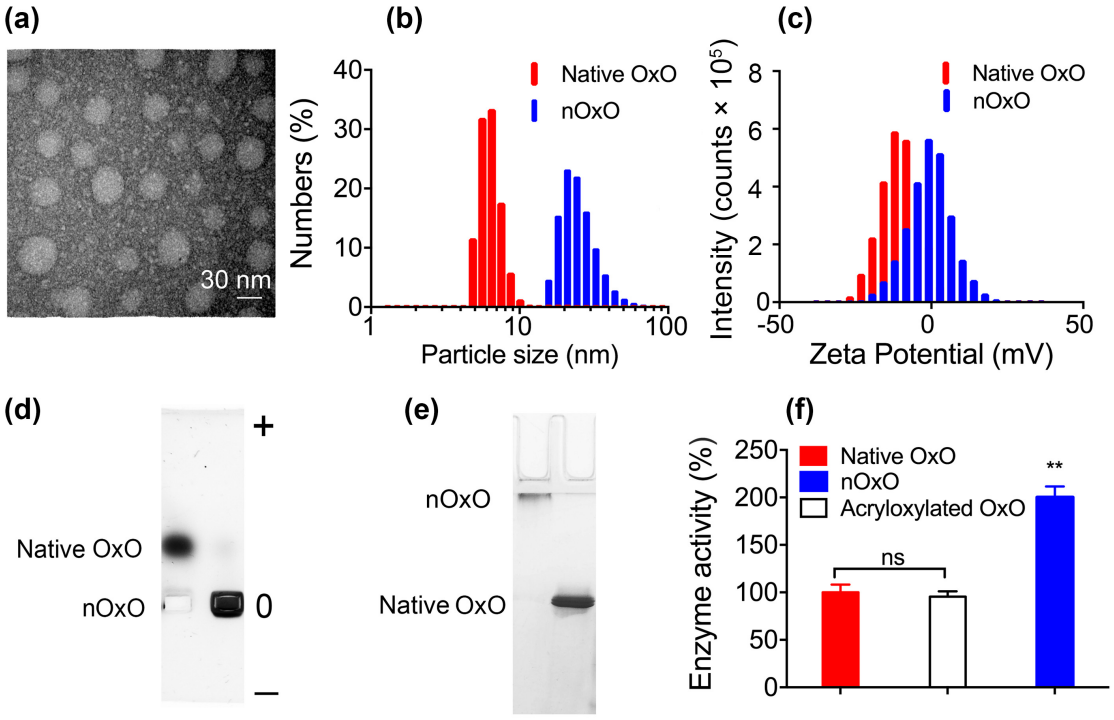

Figure 2-5 Charaterization of oxalate oxidase nanocapsules n(OxO). (a) A representative TEM image of nOxO. (b) Size distribution and (c) zeta potentials of the native OxO and nOxO, measured by DLS. (d) Agarose gel electrophoresis of the native OxO and nOxO. (e) SDS-PAGE of the native OxO and nOxO. (f) Relative activity of the native OxO, acryloxylated OxO, and nOxO at neutral pH. Data are presented as mean ± SEM in (f) (*n*=3). ** *P*<0.05.

The activity of OxO was largely retained during encapsulation. The native OxO retained almost 100% activity after conjugation with acryloyl groups (Fig. 2-5(f)). After encapsulation, the activity of the nOxO increased by twofold, compared with that of the native OxO. The increase in activity was even more pronounced in acidic conditions; the nOxO exhibited an approximately threefold increase in activity compared with that of the native OxO (Fig. 2-2). We speculate that the dramatically increased OxO activity can be attributed to the extraordinary permeability of the substrate and the interspersed zwitterions of the polymer shell, which promote the specific interaction between the substrate and the binding site.[166-168] Moreover, both

the native OxO and the nOxO retained approximately 100% of their activity for at least six months (Fig. 2-3).

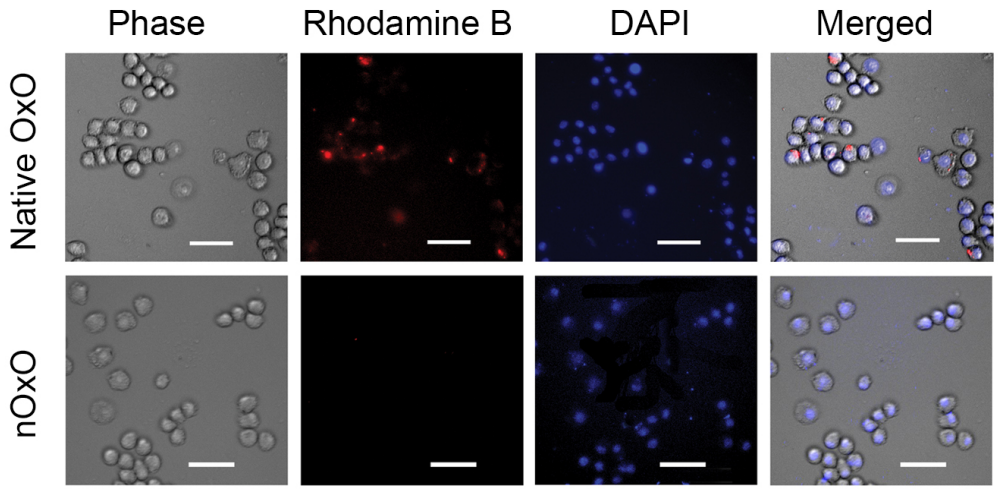

Figure 2-6 Phagocytosis of the native OxO and nOxO. Fluorescence images of mouse macrophages (J774A.1) after incubation with the native OxO and nOxO for 4 h. The native OxO and nOxO were labeled with rhodamine B, and the nuclei were stained with DAPI.

The introduction of exogenous enzymes to the blood circulation often results in rapid clearance by the reticuloendothelial system (RES), in which macrophages are the primary phagocytic cells.[169] Cellular uptake and flow cytometry experiments were conducted to determine whether zwitterionic shells mitigate the uptake of nOxO by macrophages. Native OxO and nOxO were first incubated with mouse macrophages (J774A.1) for 4 h, and intracellular fluorescence was then monitored. As shown in Fig. 2-6, the native OxO treated macrophages produced high-intensity fluorescence, indicating effective cellular uptake. In contrast, the incubation of nOxO with macrophages resulted in an insignificant fluorescent signal. More quantitative analysis by FACS revealed that the uptake of native OXO was 1.6-fold higher than that of nOxO (Figs. 2-7(a) and 2-7(b)). The substantial difference in cellular uptake was probably due to the nonhuman glycans on the native OxO. The zwitterionic polymer shells are able to

conceal the nonhuman glycans and shield the nOxO from the macrophages.[47] This observation is consistent with the reduced serum protein absorption on the nOxO (Fig. 2-4).

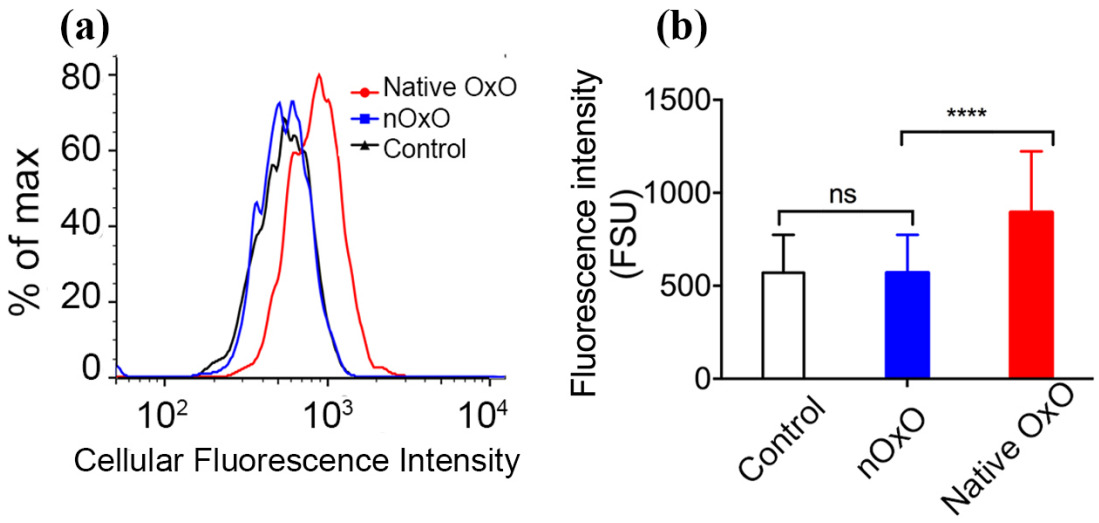

Figure 2-7 Phagocytosis of the native OxO and nOxO. (a) Quantification of the cellular uptake of the native OxO and nOxO using FACS. (b) Quantification of the FACS results. The data are presented as the the mean ± % robust CV from FACS data in (b).

The biocompatibilities of the native OxO and nOxO were also investigated. The native OxO and nOxO were incubated with NIH/3T3 cells for 24 h, and cell viability was assessed. Given a wide range of concen- trations (0–1,200 nM) for both native OxO and nOxO, cell viability was maintained at approximately 100% (Fig. 2-8).

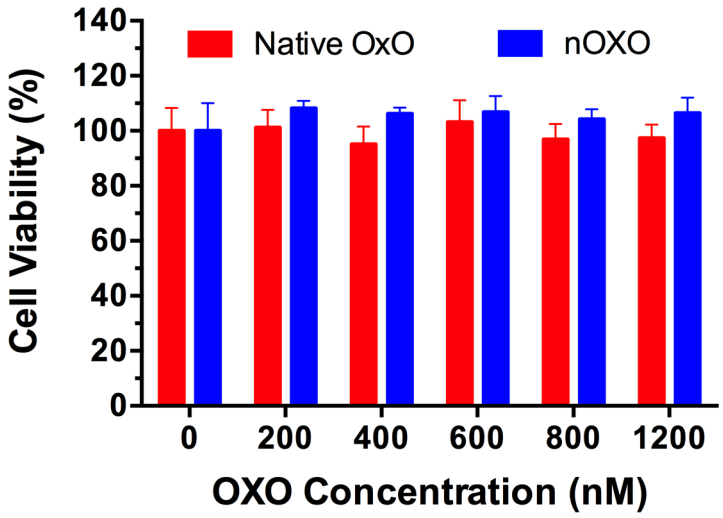

Figure 2-8 The viability of NIH/3T3 cells after incubation with native OxO and nOxO for 24 h. The data are presented as the mean ± SEM from six independent experiments

The reduced phagocytosis and protein adsorption observed for nOxO were also associated with the biodistribution profile. Near-infrared fluorescence imaging was used to qualitatively and quantitatively compare the biodistributions of native OxO and nOxO. Two groups of healthy BALB/c mice were intravenously injected with the same amount of Cy5.5-labeled OxO and nOxO. There was intense fluorescence around the liver region in the group injected with native OxO, whereas in the mice injected with nOxO, the highest fluorescence intensity was mainly observed around the heart region (Fig. 2-9(a)). Further quantitative results were obtained from the *ex vivo* organ distribution. There was considerable accumulation of native OxO in the organs of the reticuloendothelial system (the liver and spleen), and there was insignificantly lower accumulation of nOxO in these organs during the entire course of imaging (50 h) (Figs. 2-9(b), Fig. 2–10(a)(b)).

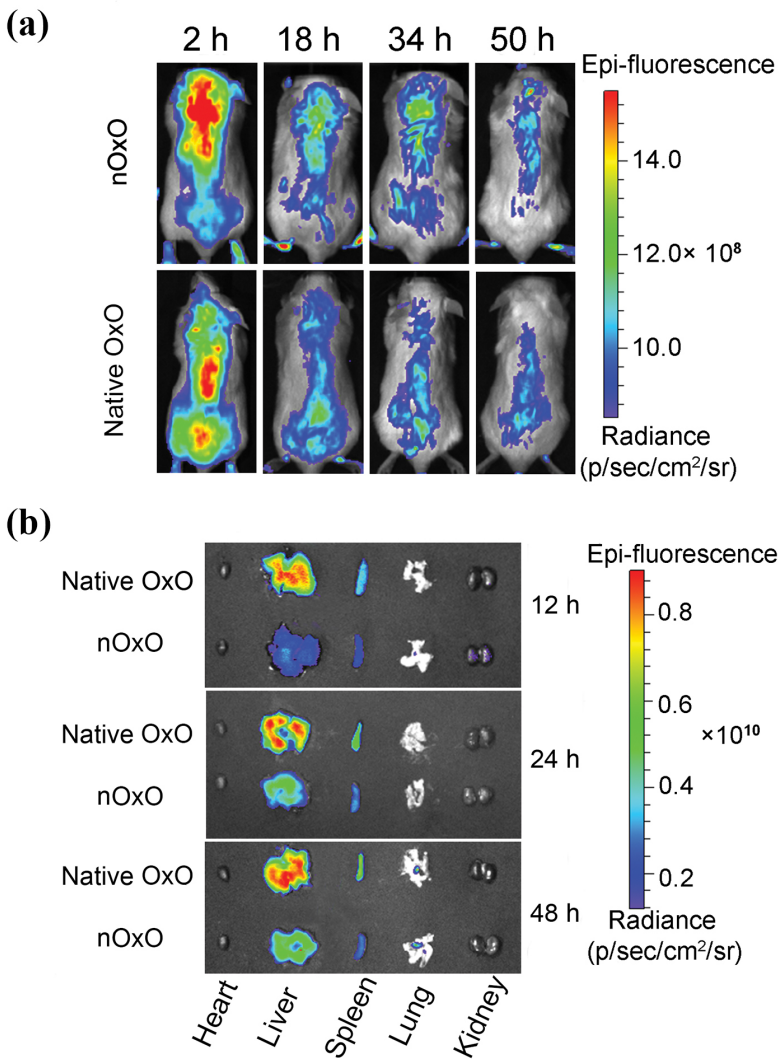

Figure 2-9 Biodistribution of native OxO and nOxO. (a) Fluorescence imaging of the mice 50 h after intravenous injection of Cy5.5-labeled native OxO and nOxO. (b) Organ distribution of the native OxO and nOxO via *ex vivo* fluorescence imaging.

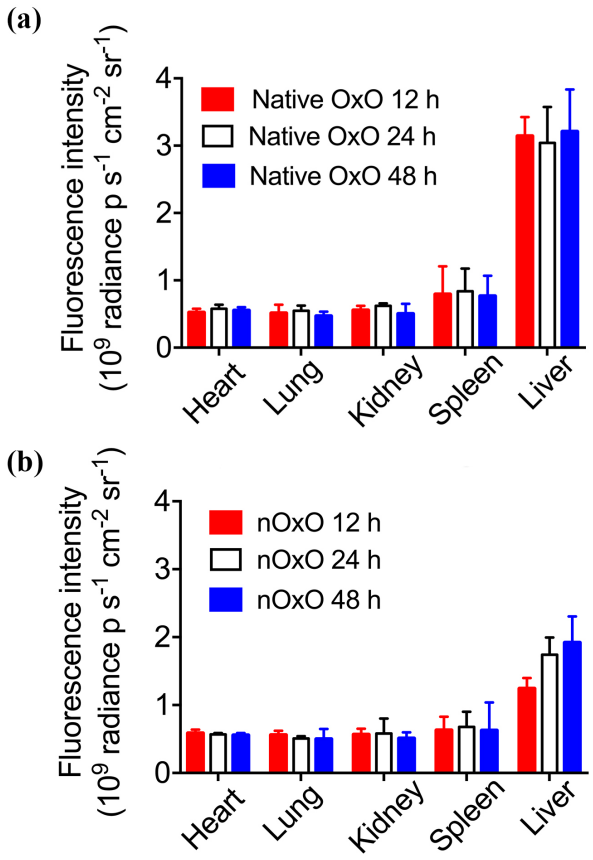

Figure 2-10 Quantitative analysis of the accumulation of native OxO (a) and nOxO (b) in each organ.

A pharmacokinetics study was conducted by intravenously injecting native OxO and nOxO. The residual OxO activity in the plasma was then measured at various time-intervals. Similar to the biodistribution profile, nOxO exhibited a much longer *in vivo* half-life than native OxO (Fig. 2-11(a)). More specifically, an approximately 13-fold increase in half-life was observed for nOxO (19.20 h) compared with that for native OxO (1.38 h) (Table 2-2). Moreover, the nOxO also exhibited a dramatic increase in the area under the curve (AUC) and the mean residence time (MRT), as well as a decreased clearance (CL), which are consistent with greater bioavailability.

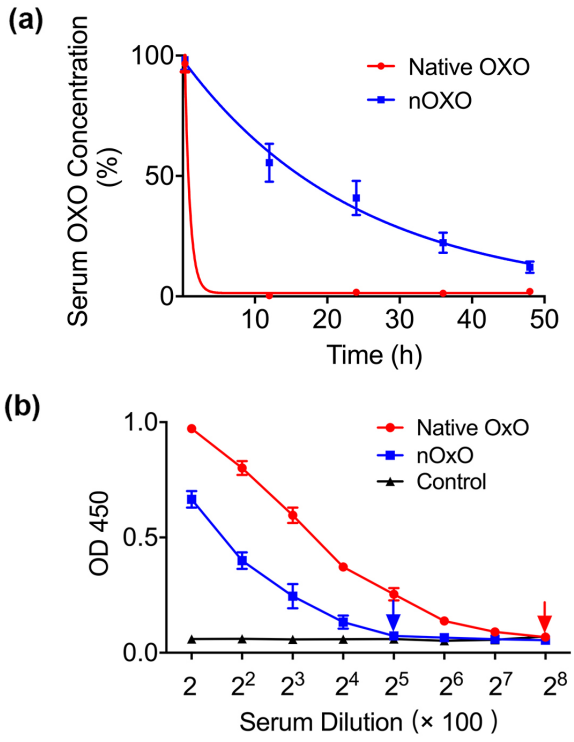

Figure 2-11 Pharmacokinetics and immunogenicity of native OxO and nOxO. (a) Residual OxO concentration in the serum within 50 h of the intravenous injection of the native OxO and nOxO. (b) Titers of the serum lgG after the administration of native OxO or nOxO to mice. Data represent means ± SEM from *n* independent experiments (*n* = 6 for (a) and (b))

Table 2-2. Pharmacokinetics parameters of native OXO and nOXO

Parameters	Native OXO	nOXO
$t_{1/2}$ (h^{-1})	1.38	19.20
AUC_{∞} (μg/mL × h)	120.54	1663.72
CL (mL/h)	5.81	0.42
MRT (h)	1.41	24.14

The immunogenicity elicited by administering native OxO or nOxO to mice was evaluated; subsequently, the IgG level in the serum was continuously monitored. The administration of native OxO elicited a high IgG titer in the serum (1:25,600), which was consistent with its high protein adsorption and macrophage clearance (Fig. 2-11(b)). In contrast, nOxO elicited an eightfold lower IgG serum titer (1:3,200), implying significantly reduced

immunogenicity. Note that IgG plays a critical role in antibody-based immune response and opsonization in the adaptive immune system.[170] Therefore, a noticeable decrease in IgG induction by nOxO can promote a more durable, and potentially safer therapeutic window.

2.4 Conclusions

In summary, we have developed a novel OxO therapeutic by encapsulating OxO in a thin layer of zwitterionic polymer. This encapsulation stabilizes the OxO, enhances its enzymic activity, and reduces phagocytosis, leading to a prolonged circulation half-life and reduced immunogenicity. This design provides an effective route for the systemic delivery of OxO for the treatment of hyperoxaluria and related diseases.

Chapter 3. Efficient Excision of Proviral HIV-1 genome in Human Primary Cells with Cell Penetrating TALEN Nanocapsules

3.1 Introduction

Infection with human immunodeficiency virus (HIV) unavoidably leads to acquired immune deficiency syndrome (AIDS), a chronic and eventually fatal disease in humans.[171] A critical step in the viral life cycle occurs when the complementary genome DNA is integrated into the host genome. This so-called "HIV provirus" becomes transcriptionally silent and sustains as a latent viral reservoir that can escalate a new infection upon self-reactivation.[172] At present, progression to AIDS has been largely curbed through the use of anti-retroviral therapies, which effectively suppresses active virus replication.[173] However, the latent HIV-1 reservoirs remain intractable and thus a tremendous risk to infected individuals.[171,174] Numerous studies have committed to developing HIV-1 reservoir activators, and some have achieved an effect on HIV-1 reservoir reactivation in clinical trials.[175,176] Despite these successes and utilities, there is recent evidence that HIV-1 can disseminate even under treatment with antiretroviral drugs through cell-cell interaction, making curing HIV-1 disease almost impossible.[177] Moreover, the clearance of cells producing activated HIV-1 is invasive and dependent on induced cell death.[178,179] Taken together, a noninvasive strategy that could abrogate proviral DNA without killing infected cells is highly desirable but extremely challenging.

Genome-editing technologies whereby cellular genomic information is readapted have become increasingly utilized recently.[134] The advantage over small molecule drugs is that the HIV-1 provirus or genes necessary for HIV-1 expression and/or infection can be directly knocked down or knocked out without the need to kill the infected cells. The approach most advanced in preclinical and clinical studies is knockdown of the HIV-1 co-receptor, CCR5, via

gene-modification of hematopoietic stem/progenitor cells (HSPC) or T-cells and rendering the cells resistant to HIV-1 infection.[180] Targets for gene modification, including the HIV-1 genome itself, have been considered as a therapy for the HIV-1 disease. Efficient gene-modification activity has been achieved by a number of systems including ZNFs, TALENs and CRISPR/Cas9.[137,138,141,180] The biggest advantage of CRISPR/Cas9 endonuclease is simplicity- a small guide RNA (gRNA) with homology to the target and a nuclease, Cas9, are all that is required to cleave specific target sequences.[142] Recently this system has been applied to knock out the HIV-1 provirus[181] and mutate the CCR5 co-receptor.[182] However, several research groups have expressed their concerns about off-target cleavage of the CRISPR/Cas9 system,[183,184] whereas TALENs possess significant accuracy for the targeted sequence.[185] Additionally, the new Platinum Gate TALEN construction system allows straightforward design and rapid construction of TALENs with robust nuclease activity.[186]

In theory, TALEN-encoding DNA may be packed and delivered by viral vectors to gain satisfactory transfection efficiency. Nevertheless, regardless of the risks of sustained nuclease expression and possible insertional mutagenesis,[139] the highly repetitive array of TALEN gene suffers from rearrangements in the nucleus,[187] and the large size of TALEN DNA is incompatible with space-constrained viral delivery vehicles.[117] Therefore, it is advisable to deliver TALEN protein or mRNA species that function in a transient fashion. Up to date, TALEN protein was validated to induce CCR5 gene disruption in Hela cells mediated by CPP, albeit the working concentration was excessively high.[117] Likewise, transfection of TALEN mRNA abolishes HIV proviral function drastically in T cell lines, which, however, is ineffective in excising proviral DNA in primary T cells, owing to the low level of TALEN protein synthesis in these primary cell lines.[188]

Our lab originated and adapted a nanotechnology platform whereby individual macromolecules, protein, siRNA or miRNA are encapsulated and protected within a thin polymer shell by *in situ* polymerizations of monomers and stabilized by environmentally responsive crosslinkers. Binding, entry, and release of the cargo into cells occur efficiently.[38,129] Herein, we provide a proof-of-concept study that this platform can be applied to TALEN protein delivery to target CCR5 gene and HIV-1 long terminal repeats (LTRs), such that infected cells are converted back to normal and resistant to HIV-1 further infection. Furthermore, special efforts will be dedicated to estimating editing outcomes in primary T cells and primary macrophages where anti-retroviral therapy and TALEN mRNA delivery hasn't been successful. We anticipate that this novel class of TALEN nanocapsule may provide a useful suggestion for developing anti-HIV drugs, particularly against integrated HIV genome in primary cells.

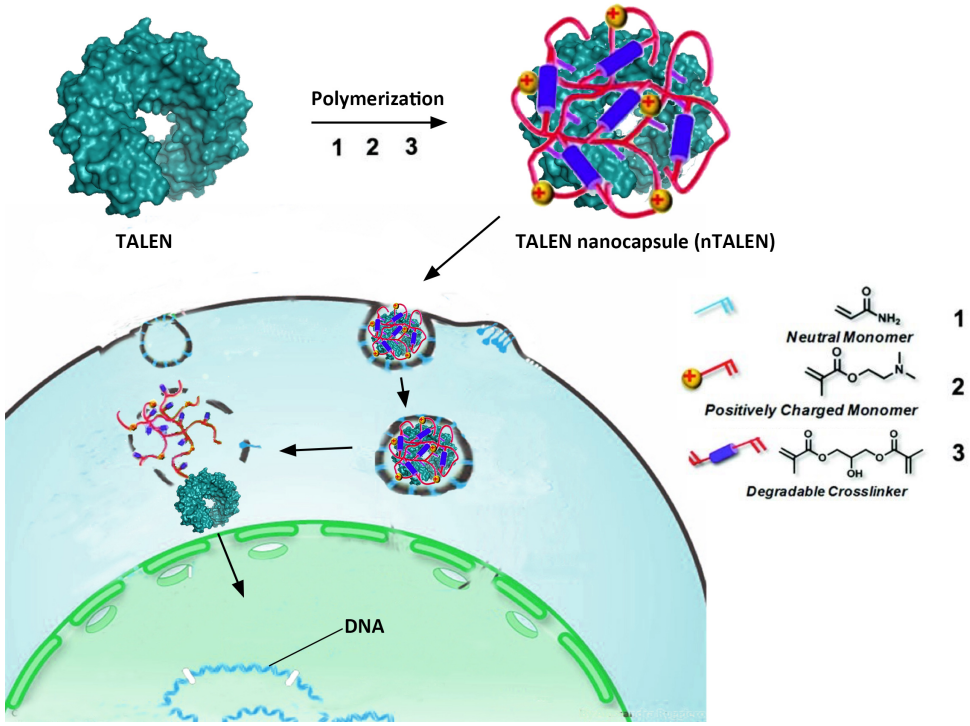

Figure 3-1 Schematic showing the synthesis and cellular uptake of cationic TALEN nanocapsules with acid-sensitive crosslinkers prepared by *in situ* polymerization

3.2 Methods, Experiment, and Characterizations

3.2.1 Materials and instruments

All chemicals were purchased from Sigma-Aldrich unless otherwise specified and were used as received. *N*-(3-Aminopropyl) methacrylamide was acquired from Polymer Science, Inc. HEK 293T and Raji cells were purchased from American Type Culture Collection (ATCC). Human embryonic kidney (HEK) Flp-In^{TM} 293 Cell line was obtained from Invitrogen. CEM T clone cell lines were provided by Calimmune, Inc. Bicinchoninic acid disodium salt hydrate (BCA) assay kit was purchased from Pierce. The Dulbecco's modified eagle medium (DMEM) and Opti-MEM^{TM} I Medium were purchased from Gibco. The RPMI 1640 medium was acquired from Life Technologies. Penicillin/streptomycin was acquired from Invitrogen. Fetal bovine serum (FBS) was purchased from Lonza Walkersville Inc. Cell Counting Kit-8 for cell proliferation assay and cytotoxicity assay was obtained from Dojindo Molecular Technologies, Inc. Lipofectamine 3000 kit for mammalian cell transfection was purchased from Invitrogen. PCR reagents (KOD-Plus-Neo) were purchased from Toyobo Co., LTD. Nuclear and Cytoplasmic Extraction Reagents were obtained from Beyotime Biotechnology, China, QuickExtract^{TM} DNA Extraction Solution was acquired from Epicentre, Ni-NTA resin was purchased from Qiagen, 4% paraformaldehyde was obtained from Beyotime, TAR TALEN overexpressed in *Escherichia coli* BL21(DE3) pLysS were kind gifts of Professor Yoshio Koyanagi (Kyoto University).

Protein concentration was measured by a Thermo Scientific NanoDrop 2000C Spectrophotometer. TEM images were obtained on a Philips EM-120 TEM instrument. Particle size and zeta potential were determined with Malvern Zetasizer Nano-ZS. Polymerase chain reaction was performed using a ProFlex PCR system (Life Technologies). Fluorescence intensity

was measured with a PerkinElmer EnSpire multimode plate reader. Fluorescence images of HEK Flp-In-293 cells were obtained with a Zeiss LSM710 confocal microscope. Flow cytometry analysis was monitored on a Beckman Coulter Cytoflex S flow cytometer. Agarose gels were imaged using a Bio-Rad molecular imager (FX Pro).

3.2.2 Protein expression and purification

The plasmid pET21a-TNsk-CCR5 for expression of the CCR5 TALEN was a generous gift from Dr. Jia Liu (ShanghaiTech University). *Escherichia coli* BL21(DE3) cells were transformed with plasmid pET21a-TNsk-CCR5R (right arm) and grown at 37 °C overnight on LB agar plate supplemented with 100 μg/mL ampicillin. A single colony was then picked, inoculated into 40 mL LB media (200 mM NaCl, 0.2% Glucose, 100 μg/mL ampicillin) and cultured at 37 °C under shaking (200 rpm). Overnight cultures were diluted in 2 L of LB media (200 mM NaCl, 0.2% Glucose, 100 μg/mL ampicillin) and incubated at 37 °C until the OD_{600} reached 0.8. Isopropyl *β*-D-1-thiogalactopyranoside (IPTG) was added to induce protein expression at a final concentration of 0.2 mM. After incubation at 25 °C for 4 h, the *E. coli* cells were harvested by centrifugation (8,000 g, 4 °C, 5 min), resuspended in 60 mL ice-cold lysis buffer (50 mM Na_2HPO_4, pH 8.0, 500 mM NaCl, 1 mM $MgCl_2$, 1 mM beta-mercaptoethanol, 1× Roche protease inhibitor cocktail) and lysed by sonication. Cell debris was removed by centrifugation (25,000g, 4 °C, 30 min), followed by the addition of 1 mL Ni-NTA resin (Qiagen) into the supernatant. The protein-bound slurry was slightly stirred at 4 °C for 30 min and then loaded onto a gravity-flow column. The column was washed twice with washing buffer (50 mM Na_2HPO_4, pH 8.0, 500 mM NaCl, 1 mM $MgCl_2$) containing 10 mM and 30 mM imidazole respectively. CCR5 TALEN-R was then eluted in elution buffer (50 mM Na_2HPO_4, pH 8.0, 500 mM NaCl, 1 mM $MgCl_2$, 250 mM imidazole). The fractions were collected and dialyzed

extensively against storage buffer (50 mM Na_2HPO_4, pH 8.0, 500 mM NaCl, 1 mM MgCl2, 10% glycerol) and frozen at -80 °C until further use. The purified protein was analyzed by SDS-PAGE and quantified by a NanoDrop 2000C UV-vis spectrophotometer and BCA assay kit. Left-arm CCR5 TALEN (CCR5 TALEN-L) was purified following the procedures exactly described above.

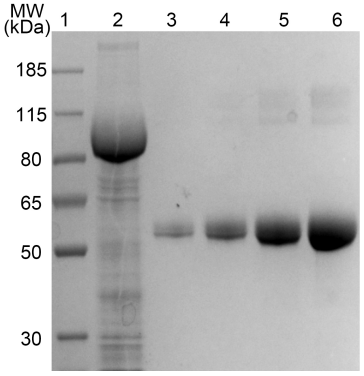

Figure 3-2 SDS-PAGE of purified TALEN monomer (right arm) designed to target human *CCR5* by Ni-NTA affinity chromatography. Lane 1: Molecular weight marker; Lane 2: Purified CCR5 TALEN-R (~100 kDa) as eluted with 250 mM imidazole; Lane 3: BSA standard 1 µg; Lane 4: BSA standard 2 µg; Lane 5: BSA standard 5 µg; Lane 5: BSA standard 10 µg.

3.2.3 *In vitro* cleavage assay

To start with, substrate plasmid pTNT CCR5 R-R was linearized with Nde I (NEB) and purified by Qiagen PCR purification kit. Then in 10 µL of reaction buffer (1×NEBuffer 2.1) containing 100 ng substrate DNA, CCR5 TALEN-R was added to make a final concentration of 100 nM, 75 nM, 50 nM, 25 nM or 10 nM respectively. Samples were incubated at room temperature for 1 h (Table 3-1). Owning to the markedly high activity, TAR TALEN was adjusted to a final concentration of 4.3 pmol, The nuclease cleavage efficiency was monitored by agarose gel electrophoresis and analyzed by Image J. Likewise substrate plasmid CS-CDF-CG-PRE was utilized to assess the cleavage activity of TAR TALEN. The assay was carried out at

37 °C for 2 h in NEB 4 buffer. Besides, the human CCR5 gene sequence can be amplified by PCR with the following primer pairs to serve as substrate DNA evaluate the cleavage performance of CCR5 TALEN pairs. (Table 3-2)

Table 3-1. *In vitro* cleavage assay reaction

Component	Amount per sample	Final
NEBuffer 2.1	1 μL	1×
Substrate DNA	100 ng	10 ng/μL
TALEN	1 μL	Titrate from 100 to 10 nM
Nuclease-free water	Up to 10 μL	

Table 3-2. Primers used to amplify the endogenous CCR5 genes

Primer name	Primer sequence (5'-to-3')
CCR5 external 5'	ACAGTTTGCATTCATGGAGGGC
CCR5 external 3'	AACTGAGCTTGCTCGCTCGG
CCR5 internal 5'(BamHI site underlined)	CGCGGATCCTTAAAAGCCAGGACG GTCAC
CCR5 internal 3' (EcoRI site underlined)	CCGGAATTCTGTAGGGAGCCCAGA AGAGA

3.2.4 Agarose gel electrophoresis and SDS-PAGE

For protein agarose gel electrophoresis, 0.7% (w/v) agarose gel was prepared with 1×TAE buffer (pH 7.4). Prior to loading samples into dry wells, protein (0.2-1 mg/mL) was diluted by 6×gel loading buffer (0.25% bromophenol blue and xylene cyanol, 40% w/v sucrose). Electrophoresis was conducted with a Bio-Rad horizontal electrophoresis system under a constant voltage of 120 V for 20 min. Similarly, for DNA samples, 2% (w/v) agarose gel was prepared with 1×TAE buffer (pH 8.3, Genscript), 6×gel loading buffer was used to load the samples. Prepared DNA samples were subjected to electrophoresis at a constant voltage of 80 V for 40 min, after which, the gel was stained by ethidium bromide and visualized with a fluorescent gel imaging system. SDS-PAGE was performed using a 4-12% (w/v) Bis-Tris protein gels (NuPAGE^{TM}). Briefly, 10 μL of 1 mg/mL protein sample was re-suspended in 2×

loading buffer. After boiling for 10 min, the samples were loaded and the electrophoresis was performed at 120 V and 40 mA for 60 min. The gel was stained and destained with a protein staining system (Genscript).

3.2.5 Cell penetrating peptides conjugation

CCR5 TALEN-R and each of the following cell penetrating peptides were mixed thoroughly in 150 μL sodium phosphate buffer (100 mM sodium phosphate buffer, pH 5.5), where the concentration of TALEN was 3.3 uM and the peptide/protein ratio was 32:1, 16:1 or 8:1 separately. The mixture was left at room temperature to react for 1 h. Then the pH was adjusted by 1 M sodium hydroxide to pH 7.0 and the reaction solution was immediately diluted with 350 μL serum-free DMEM, centrifuged at 10,000 RCF for 5 min at 4 °C to remove the precipitate, and applied directly to Flp-In^{TM}-293 TN-CCR5R cell line.

Table 3-3. CPPs involved in conjugation reactions

Name	Company	Sequence
Cys(Npys)-TAT	Anaspec	C(Npys)YGRKKRRQRRR-NH_2
Cys(Npys)-(Arg)9	Anaspec	C(Npys)RRRRRRRRR-NH_2
Cys(Npys) Antennapedia Peptide	Anaspec	C(Npys)RQIKIWFQNRRMKWKK-NH_2

3.2.6 Restoration of TALEN activity after free radical attack

The DNA binding domain of TALEN contains abundant solvent-exposed cysteine residues that are subjective to radicals attack. To testify that the loss of activity can be restored, the following protocol is established. To 1 mL borate reaction buffer (50 mM, pH 8.6) containing 1.26 mg/ml TALEN protein, pipette 25.2 μL of ammonium persulfate (APS, 10%, w/v) and 8.2 μL of *N,N,N′,N′*- tetramethylethylenediamine (TEMED). The mixture was incubated at room temperature for 2 h, dialyzed against 1×PBS and to remove the free radical and treated with 1

mM Dithiothreitol (DTT). The nuclease activity of TALEN before and after DTT treatment was analyzed via *in vitro* cleavage assay.

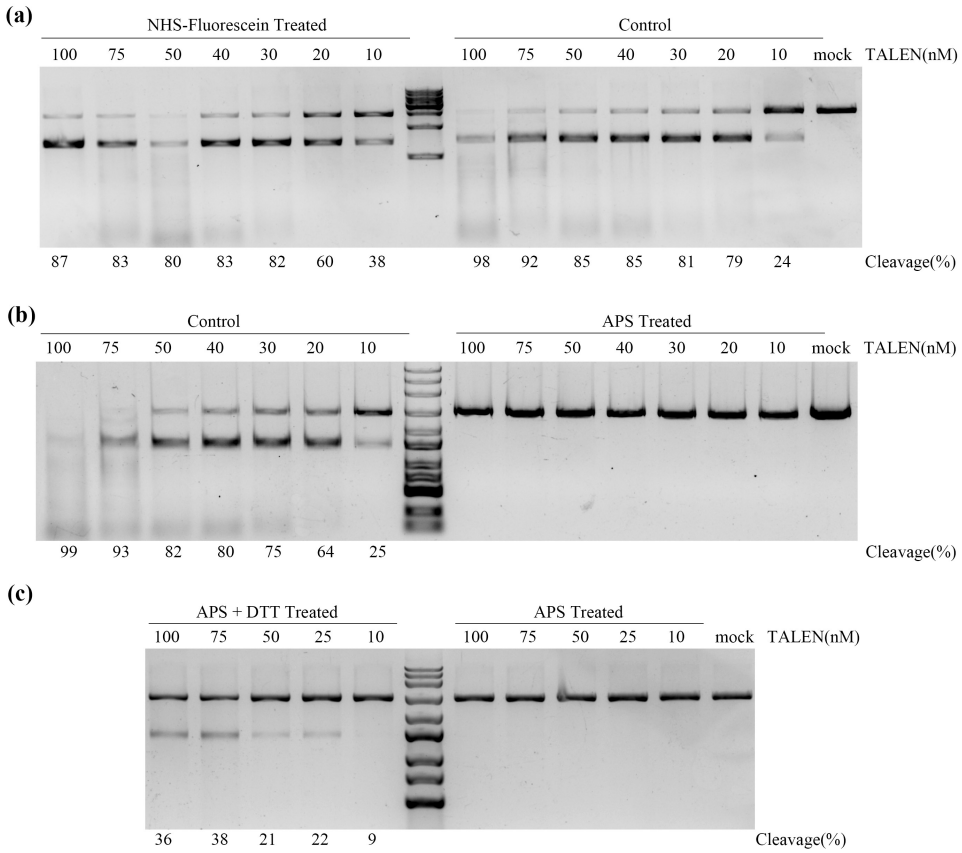

Figure 3-3 (a) *In vitro* cleavage assay of right CCR5 TALEN monomer at different concentrations after being labeled with NHS-fluorescein and stored at 4 °C for one week (left). (b) *In vitro* cleavage assay of right CCR5 TALEN monomer at different concentrations after being treated with free radicals produced by ammonium persulfate (APS) (right). (c) *In vitro* cleavage assay of right CCR5 TALEN monomer at different concentrations after being treated with free radicals produced by ammonium perfulfate (APS) (left) and subsequently rescued with 1 mM DTT.

3.2.7 Synthesis of TALEN nanocapsule (nTALEN)

To begin with, TALEN protein (CCR5 TALEN-R/L, TAR TALEN-R/L) for encapsulation was diluted to 1.26 mg/ml with 50 mM borate buffer (pH 8.6). Next, acrylamide (AAm), *N*-(3-aminopropyl) methacrylamide (APm) and acid-degradable glycerol dimethacrylate

(GDA) were added sequentially into 1 ml of protein solution and mixed thoroughly at 4 °C for 10 min. *In-situ* polymerization was started by the addition of 25.2 μL of ammonium persulfate (APS, 10%, w/v) and 8.2 μL of *N,N,N′,N′*- tetramethylethylenediamine (TEMED). The reaction was maintained at room temperature for 2 h with the molar ratio of AAm/APM/GDA/protein being 8800:8800:675:1. Immediately after polymerization, the solution was dialyzed against 1×PBS buffer to remove unreacted reactants. The Unreacted protein was removed via anion-exchange chromatography (DEAE-Sepharose CL-6B).

3.2.8 TEM and DLS measurement

Transmission electron microscope was employed for directly observing the morphology and sizes of the synthesized nanocapsules. TEM samples were prepared by conducting drop-coating of 2 μL TALEN nanocapsule solutions onto a carbon-coated copper grid for 2 min. The excess amount of samples was removed by filter papers. The grid was then stained with 1% phosphotungstic acid (PTA) solution for 5 min, followed by rinsing the grid three times with DI-water. Once the water was dried out, samples were ready for TEM observation. DLS measurements were performed at 173° scattering angle with a Zetasizer nano instrument equipped with a 10-mW helium-neon laser (λ=632.8 nm) and a thermoelectric temperature controller.

3.2.9 Characterization of protein content

After purification, protein concentration can be roughly estimated by a direct A280 measurement with a Thermo Scientific NanoDrop 2000C Spectrophotometer. Precise protein content in nanocapsules was quantified by the bicinchoninic acid (BCA) colorimetric protein assay. Typically, a tartrate buffer (pH 11.25) containing 25 mM BCA, 3.2 mM CuSO4, and an appropriately diluted protein sample was incubated at 37 °C for 30 min. Absorbance at 562 nm

was determined with a UV/Vis spectrophotometer. BSA solutions with known concentrations were used as standards.

3.2.10 Internalization and nucleus localization of nanocapsules

HEK Flp-In^{TM}-293 cells were cultured in Dulbecco's Modified Eagle's Media (DMEM) supplemented with 10% bovine growth serum (FBS) and 1% penicillin/streptomycin at 37 °C with 98% humidity and 5% CO_2. To visualize internalization and nucleus localization of TALEN nanocapsules, cells were seeded into 24-well plate with a density of 200,000 cells/well. Fluorescein- labeled CCR5 TALEN-R and CCR5 TALEN-R nanocapsule (nCCR5-TALEN-R) were added into each well at a final concentration of 30 nM and incubated at 37 °C for 1 h, 2 h, 4 h, 6 h, 8 h and 12 h respectively. After incubation, the cells were fixed with 1% paraformaldehyde, stained with DAPI nucleic acid stain for 20 min and washed three times with 1×PBS to remove residue dye molecules. Confocal images were acquired on a Zeiss LSM710 confocal microscope system equipped with a Zeiss AXIO Observer Z1 inverted microscope stand with transmitted (HAL), UV(HBO) and laser illumination sources.

3.2.11 Cell proliferation assay

One day prior to the experiment, HEK 293T and Raji cells were seeded at a density of 10,000 cells /well into 96-well plate. CCR5 TALEN-L/R and nCCR5 TALEN-L/R with different concentrations of overall TALEN protein were then added into each well. After incubation of 4 h at 37 °C, 10 μL of CCK-8 solution (Cell Counting Kit-8 assay) was added to each well and continued to incubate for 2 h. The absorbance of each well was recorded at 490 nm using a microplate reader. Untreated cells and fresh medium served as the 100% and 0% cell proliferation control.

3.2.12 Quantification of gene modification by TALEN nanocapsules in reporter cells

EGFP reporter HEK Flp-In-293 cells were seeded into a 24-well plate (200,000 cells/well, 500 μL/well) and cultured in DMEM (10% FBS). 30 min prior to the addition of the samples, the DMEM medium was replaced with a fresh Opti-MEM medium. The cells were then treated with 30 nM nCCR5 TALEN-R and 30 nM CCR5 TALEN-R, respectively. Meanwhile, as a positive control, cells were transfected with 200 ng of pXTNsk-CCR5R (CCR5 TALEN-R expression vector) using lipofectamine 3000 transfection reagent. After incubation for 2 h at 37 °C, samples were removed by replacing Opti-MEM medium with fresh DMEM (10% FBS) and the cells were incubated for another 48 h. Afterward, Cells were collected, fixed with 4% paraformaldehyde and washed three times with 1×PBS prior to flow cytometry analysis. Please note that once properly edited, EGFP expression in HEK Flp-In-293 cells will be restored and fluorescence can be monitored.

3.2.13 Nuclear and cytoplasmic protein extractions

Nuclear and cytoplasmic protein extractions from HEK Flp-In-293 cells were performed using the Nuclear and Cytoplasmic Extraction Reagents according to the manufacturer's instructions. Briefly, cells were harvested with trypsin-EDTA, washed with 1×PBS and pelleted through centrifugation. Thereafter, the cells were resuspended and homogenized in a cytoplasmic protein extraction reagent. After centrifugation at 16,000 g for 5min at 4 °C, the cytoplasmic protein can be derived in the supernatant fraction. To obtain the nuclear protein, the precipitation was resuspended in a nuclear protein extraction reagent followed by centrifugation at 16,000 g for 10 min at 4 °C. The supernatant fraction is collected as the nuclear protein.

3.2.14 Nuclear distribution of TALEN by western blot analysis

Nuclear and cytoplasmic protein extractions were run in 4-12% (w/v) Bis-Tris polyacrylamide gels respectively and transferred to nitrocellulose membranes after electrophoresis. TBS-T blocking buffer (50 mM Tris, 150 mM NaCl, 0.1% Tween-20) containing 5% nonfat milk was applied for 30 min at room temperature to inhibit nonspecific antibody binding. Then nitrocellulose membrane was incubated with a FLAG tag primary antibody in TBS-T blocking buffer with 5% nonfat milk overnight at 4 °C, followed by exposure to an anti-mouse/HRP-conjugated secondary antibody in 5% milk in TBS-T for 1 h at room temperature. An anti-actin antibody and an-anti-lamin B1 antibody were used as loading controls. The Membrane was visualized using the ECL Western Blotting Substrate kit (Pierce) based on the manufacturer's protocol, and the image was captured using a Bio-Rad molecular imager (Bio-Rad).

3.2.15 Gene editing by TAR TALEN nanocapsules (nTAR TALEN) in HEK-293 cells

293 cells were transfected with DA-EGFP lentiviral vectors at MOI 0.5, in which the promoter of EGFP is in LTR. 3 days after vector transduction, 1×10^5 293 cells were transduced with 150 ng nTAR TALEN-L and 150 ng nTAR TALEN-R. After another 5 days of incubation, EGFP expression was examined by cell flow cytometry. Likewise, 293 cells were transfected with FG11-EGFP lentiviral vectors at MOI 0.5, in which EGFP has an internal Ubiquitin C promoter. 1×10^5 293 cells were transduced with 150 ng nTAR TALEN-L and 150 ng nTAR TALEN-R 3 days after the vector transduction. Finally, level of EGFP expression was analyzed 5 days after nanocapsule transduction by cell flow cytometry.

3.2.16 Gene editing by nTAR TALEN in CEM clone

CEM clones were transfected with FG11 EGFP lentiviral vectors at MOI 0.01 to achieve one vector copy per cell. The clones were maintained in RPMI 1640 medium containing 10% FBS and supplemented with 2 mM glutamine and 1% penicillin/streptomycin. The EGFP has an internal Ubiquitin C promoter. 3 days after vector transduction, 1×10^5 CEM clone cells were transduced with 150 ng nTAR TALEN-L and 150 ng nTAR TALEN-R. 5 days later, EGFP expression was checked with cell flow cytometry.

3.2.17 Gene editing by nTAR TALEN in primary macrophages

Monocytes was isolated from the peripheral blood mononuclear cell (PBMC) and stimulated with graulocyte macrophage colony-stimulating factor (GM-GSF) and macrophage colony-stimulating factor (M-CSF). 7 days after stimulation, 5×10^5 macrophages were transduced with Cal-1 EGFP vector, where the EGFP gene has an internal Ubiquitin C promotor. Cells were transduced with 150 ng nTAR TALEN-L and 150 ng nTAR TALEN-R 3 days after vector transduction. EGFP expression was quantified 5 days after nanocapsule transduction by flow cytometry.

3.2.18 Gene Editing by nTAR TALEN in HIV infected primary CD4+ T cells

naïve CD4+ T cells were isolated from PBMC. 2×10^6/mL of naïve CD4+ T cells were infected with 2000 ng/ml of HIV-1 strain NL4-3 or strain AD8 on RetroNectin-coated plates respectively. The infected cells were cultured with 5 ng/mL of IL7/IL15 and 5 ng/mL of TGFβ-1 for 2 weeks to obtain the latently infected primary T cells. Cells were then transduced with nTAR TALEN-L and nTAR TALEN-R for 4 h, followed by virus reactivation with 1 μg/mL of CD3 and CD28 antibody for three days. 7 days after stimulation, intracellular P24 expression

level in latently infected primary T cells were stained by KC57-PE and examined by flow cytometry.

3.3 Results and Discussions

In this work, we selected a His-tagged recombinant TALEN targeting the right half-site of human CCR5 gene (CCR5 TALEN-R) as the model TALEN protein for basic characterization studies. Thereafter with the parameters gained and optimized, we attempted to deliver TAR TALENs that recognize the TAR region of HIV LTRs to evaluate the excision potential of HIV-1 proviral DNA in some real applications. The CCR5 TALEN-R was expressed from *E. coli* and purified to homogeneity by nickel affinity chromatography. The molecular weight was characterized by SDS-PAGE to be approximately 100 Kd (Fig. 4-2). To identify its gene disruption efficiency, a substrate plasmid (pTNT CCR5 R-R) bearing symmetrical left and right TALE-binding sites was generated to facilitate the *in vitro* cleavage assay. As shown in Fig. 4-4 (a), CCR5 TALEN-R exhibited robust cleavage activities *in vitro*, where about 80% of DNA disruption was achieved with merely 20 nM TALEN protein. The editing efficiency dropped abruptly as the TALEN concentration decreased to 10 nM. It is worth to mention that despite 100 nM TALEN protein caused the highest rate of gene disruption, there was a noticeable incidence of off-target cleavage as evidenced by a faint deletion band on the gel map. By contrast, TAR TALEN pairs, designed through the Platinum TALEN platform with the conventional variable repeats (VRs) harboring non-repeat variable di-residue (non-RVD) variations, displayed outstanding gene disruption efficiency and specificity with no detectable off-target cleavage activities (Fig. 4-4 (b)), which is consistent with prior investigations.[186,188]

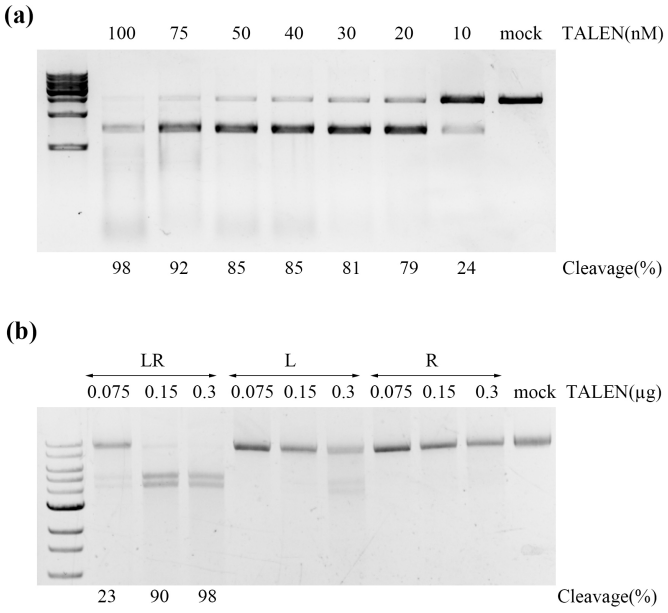

Figure 3-4. (a) *In vitro* cleavage assay of right CCR5 TALEN monomer at different concentrations containing symmetrical left and right target sites. (b) *In vitro* cleavage assay of left and right TAR TALEN monomers designed to target HIV-1 proviral DNA at different TALEN concentrations. The rate of DNA disruption is calculated by dividing the density of the deletion product over the density of total DNA within the same lane.

Next, we conjugated the model CCR5 TALEN-R protein with three distinct cell-penetrating peptides to evaluate the potency of the resulting TALEN proteins to permeate through the cell membrane and induce targeted genetic alterations in HEK 293 EGFP reporter cells. The single-copied EGFP gene was stably integrated into the genome of HEK 293 cells using an Flp-In system (Invitrogen), with its function being disabled by a frameshift resulted from the insertion of CCR5 TALEN-R cleavage sites flanked by symmetrical binding sites. Once unique double-stranded breaks are induced by TALEN, the NHEJ mediated mutagenesis will restore the reading frame and EGFP function in certain cases of nucleotide deletions (e.g., 2, 5, or 8-bp) or insertions (e.g., 1, 4 or 7-bp) (Fig. 4-5 (a)). While this assay only reflects a small

portion of the total mutation events, it has the benefit of being robust and high throughput with minimal background interference.[189,190]

The molar ratio of CPPs to CCR5 TALEN-R protein was adjusted to 8:1, 16:1 and 32:1 to confer the TALEN with different surface charges and CPPs densities. After internalization, the disulfide linkage is disrupted under normal reducing intracellular environment and the exposed nuclear localization signals (NLS) will guide the subsequent import of TALEN protein into the nucleus. As demonstrated in Fig. 4-5 (b), there were varied preferences as to which CPP-TALEN ratio led to the highest gene modification efficiency, with TAT, AnT, and R9 favoring the 8-to-1, 8-to-1 and 16-to-1 CPP-TALEN ratios, respectively. In particular, we note that conjugation at 8-to-1 AnT-to-TALEN ratio gave rise to the maximum EGFP-positive cells (~3.5%) and comparatively, transient transfection with TALEN-expressing plasmid only produced a moderate ratio of gene disruption (1.22 % EGFP-positive cells). Besides, no gene editing occurred without CPPs attached, indicating the pivotal role that CPPs play in guiding the cellular internalization process. However, in line with previous studies,[117] the effective concentration of CPPs was at micromolar levels, which was notably higher than the desired safety dose for therapeutic application.

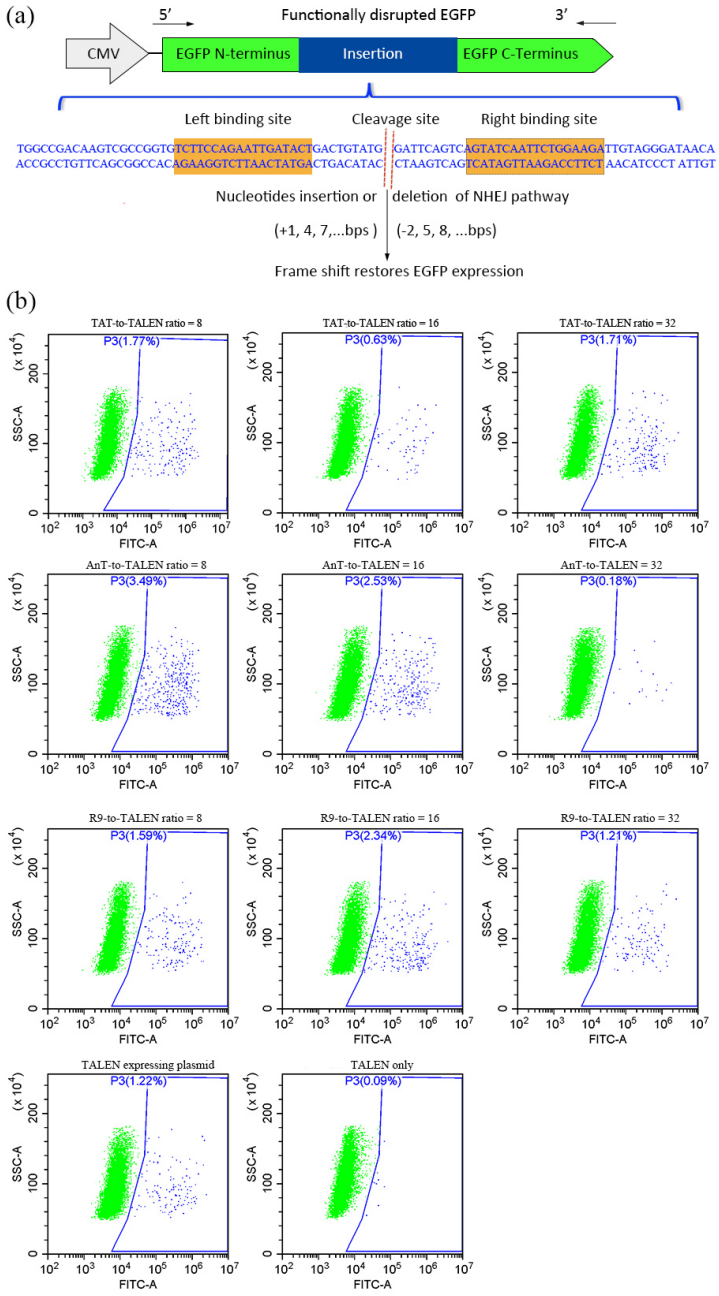

Figure 3-5. (a) Schematic overview of the HEK 293 EGFP reporter system used to assess the efficiency of gene editing. The recognition site together with symmetrical DNA binding sites of the CCR5 TALEN-R protein was inserted between EGFP residues 157 and 158, where 20 amino acid peptide insertions can be accommodated. (b) Quantification of EGFP positive reporter cells by flow cytometry following CPPs-mediated delivery of CCR5 TALEN-R protein. The % of EGFP positive cells represents a small portion of the total mutagenesis events.

The wide range of success of biomacromolecules delivered through polymeric nanocapsules in our previous work has prompted us to reconsider TALEN delivery with responsive nanocapsules.[35,38,129] However, according to previous crystallography studies, each TAL effector repeat possesses a single solvent-exposed Cys residue,[191] which, we speculate may suffer from oxidative attack and protein function loss during polymerization, To prove our hypothesis and explore whether the lost function could be restored in a reductive environment similar to cellular cytosol, CCR5 TALEN-R was exposed to equal dose of free radicals as that during polymerization, followed by gel permeation chromatography to remove free radical initiator and treatment with 1 mM DTT. Just as expected, no cleavage activity of CCR5 TALEN-R could be detected after free radical treatment owing to the loss of free Cys residues, whereas the activity can be rescued after disulfide bonds disruption by DTT (Fig.4-3 (b&c)). Moreover, the amine groups of CCR5 TALEN-R were reacted with tenfold molar excesses of NHS-fluorescein and stored at 4 °C for a week, showing no apparent activity compromise (Fig. 4-3 (a)). Taken together, with the robust activity and stability being identified, we propose that intracellular delivery of TALEN within polymeric nanocapsules would be an appropriate and potential alternative delivery option.

The synthesis strategy for producing TALEN nanocapsule is given in Fig 4-1. Monomers including acrylamide, *N*-(3-aminopropyl) methacrylamide (APm) and the acid labile crosslinker glycerol dimethacrylate (GDMA) were deposited around the TALEN protein in borate buffer (50 mM, pH 8.6) via electrostatic interaction or hydrogen bonding. Subsequent *in situ* free-radical polymerization was initiated with ammonium persulfide, which encapsulated the TALEN protein within a thin polymer network and formed the TALEN protein nanocapsules (nTALEN). The resultant nTALEN containing substantial surface positive charges could effectively enter the

cells and escape the endocytic compartments due to the cation-mediated membrane destabilization and the "proton-sponge" effect respectively. More importantly, the cargo release was facilitated by the acid-sensitive crosslinker-GDMA, which triggers the dissociation of the polymer shells in acidic endosomes, but which stabilizes TALEN protein at normal physiological conditions. Once delivered, the multiple disulfide linkages generated during polymerization were rapidly disputed by the cytoplasmic glutathione (GSH), which recovered the TALEN activity, and the terminal NLS peptides on TALEN protein subsequently guided its transportation and entry into the nucleus to execute specific gene editing tasks. Additionally, it is worth to note that one significant advantage of this polymeric encapsulation platform is tunability such that properties including the rate of cellular internalization and release of TALEN protein can be finely controlled.

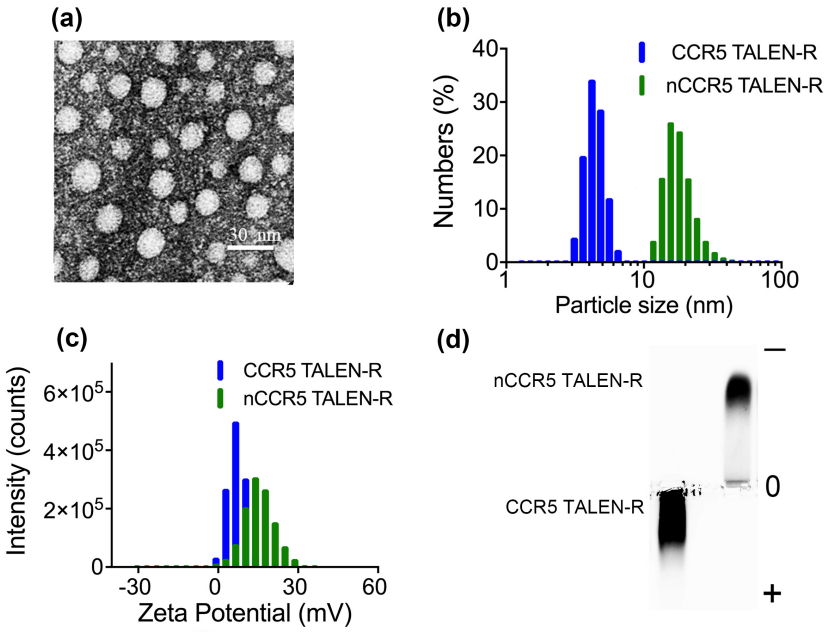

Figure 3-6 Charaterization of CCR5 TALEN-R nanocapsules (nCCR5 TALEN-R). (a) A representative TEM image of nCCR5 TALEN-R. (b) Size distribution and (c) zeta potentials of the native CCR5 TALEN-R and nCCR5 TALEN-R, measured by DLS. (d) Agarose gel electrophoresis of the native CCR5 TALEN-R and nCCR5 TALEN-R.

The morphology of the nCCR5 TALEN-R was initially characterized by transmission electron microscopy, which revealed round shape morphology with a uniform size of ~17 nm in diameter (Fig. 3-5 (a)). The size distribution was also measured by dynamic light scattering (DLS), which, consistent with the TEM observation, displayed a size increase from 4.5 nm for free-form TALEN to 16 nm on average for TALEN nanocapsule (Fig. 3-5 (b)). DLS also demonstrated that the zeta potential of native TALEN was around 6.5 mV at pH 7.4, whereas nTALEN had a mean zeta potential of 14 mV (Fig. 3-5 (c)). Besides, native TALEN and nTALEN were labeled with fluorescein and subjected to agarose gel electrophoresis for surface charge confirmation. As displayed in Fig. 3-5 (d), Native TALEN became anionic due to the consumption of surface amine groups by NHS ester as well as the amount of anions conferred by fluorescein molecules. In comparison, nTALEN harboring a large number of primary amino groups on the polymer shell significantly migrated towards the cathode with no interference by the NHS-fluorescein labeling. These characterizations collectively implied the successful encapsulation of TALEN protein and formation of TALEN nanocapsules.

To ascertain whether the resultant CCR5 TALEN-R nanocapsules (nCC5 TALEN-R) could mediate intracellular TALEN delivery and induce potent targeted gene mutagenesis, HEK 293 EGFP reporter cell line was treated with nCCR5 TALEN-R at various concentrations for 4 h until samples were removed and cells were cultured for another 48 h. According to the flow cytometry results, nTALEN demonstrated dramatically reduced working concentration than CPPs, which was only 30 nM compared to 1 μM for CPPs under the same gene editing efficiency (2% EGFP positive cells). Moreover, as nTALEN concentration increased, the gene modification ratios decreased correspondingly, suggesting a higher intracellular dose may not

necessarily amount to higher gene disruption ratio, probably owing to the concomitant accretion of cellular toxicity or off-targeting effects.

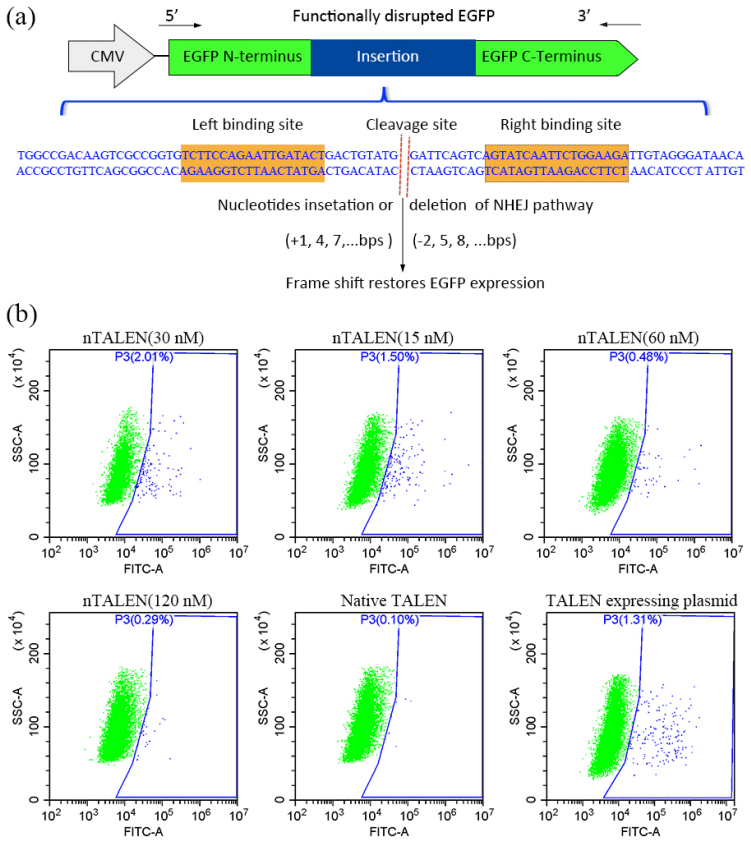

Figure 3-7. (a) Schematic overview of the HEK 293 EGFP reporter system used to assess the efficiency of gene editing. The recognition site together with symmetrical DNA binding sites of the CCR5 TALEN-R protein was inserted between EGFP residues 157 and 158, where 20 amino acid peptide insertions can be accommodated. (b) Quantification of EGFP positive reporter cells by flow cytometry following delivery of CCR5 TALEN-R nanocapsule (nCCR5 TALEN-R), native CCR5 TLANE-R (30 nM) and TALEN expressing plasmid (200 ng). The % of EGFP positive cells represents a small portion of the total mutagenesis events.

Additionally, reducing the optimal working concentration to its half can still result in 1.5% EGFP positive cells, whereas TALEN-expressing plasmid transfection produced only a moderate gene-editing activity (1.31% EGFP positive cells) and no genome modification could be

identified with native CCR5 TALEN-R. Therefore, given that DNA transfection poses the risks of inducing insertional mutagenesis and off-target genome damage, and that the CPPs require rather high working concentration, delivery of TALEN protein within acid-degradable nanocapsule with remarkably lower working concentration and better performance holds enormous promise for further applications.

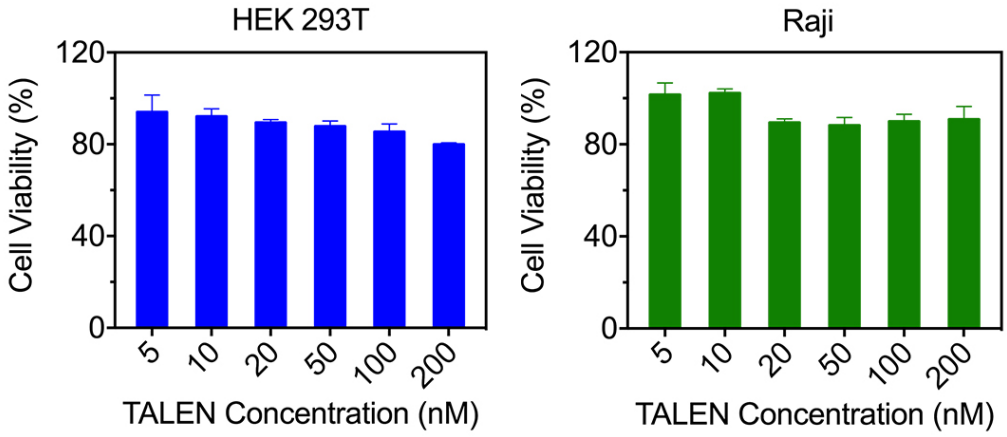

Figure 3-8. The viability of HEK 293T (a) and Raji cells (b) after incubation with nCCR5 TALEN-R for 24 h. The data are presented as the mean ± SEM from six independent experiments.

It is crucial to evaluate the cytotoxicity of a drug especially when it comes to *in vivo* applications. Serial dilutions of nTALEN were incubated with HEK 293T cells (adherence cells) and Raji cancer cells (suspension cells) for 4 h before cell proliferation assay was performed. In general, Raji cancer cells exhibited less sensitivity to TALEN nanocapsules than HEK 293T cells, with overall cell viability above 90% over a broad concentration range. Likewise, within the concentration range between 5 nM and 100 nM, HEK 293T cells retained over 85 % cell viability. These *in vitro* results therefore unequivocally confirmed that nTALEN exhibited low cytotoxicity.

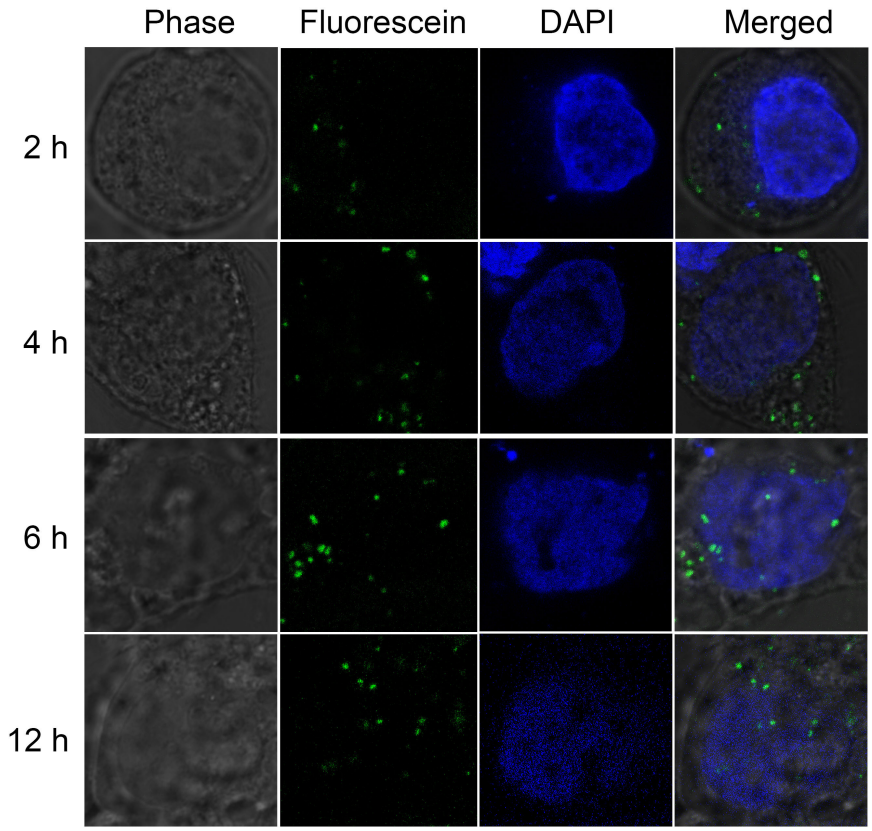

Figure 3-9. Time-course confocal imaging of HEK 293T EGFP reporter cells incubated with 30 nM nCCR5 TALEN-R delivered. nCCR5 TALEN-R were labeled with fluorescein, and the nuclei were stained with DAPI.

To target the internalization and nuclear localization of delivered CCR5 TALEN-R. We conjugated the recombinant CCR5 TALEN-R to fluorescein dye and performed time-course confocal imaging. When added to HEK 293T EGFP reporter cell lines, fluorescein fluorescence appeared inside the cells with short incubation period (2 h). As exposure time extended, the intensity of fluorescence further enhanced, indicating continuous cellular uptake. At 4 h, we observed accumulation of CCR5 TALEN-R around the nucleus and at 6 h inside of the nucleus of targeted cells, which is the expected localization for CCR5 TALEN-R. Moreover, no notable fluorescence intensity enhancement was seen in the nucleus at 12 h interval, likely owing to the

protein degradation occurred concurrently, which confirms that protein therapeutics function in a transient fashion.[134]

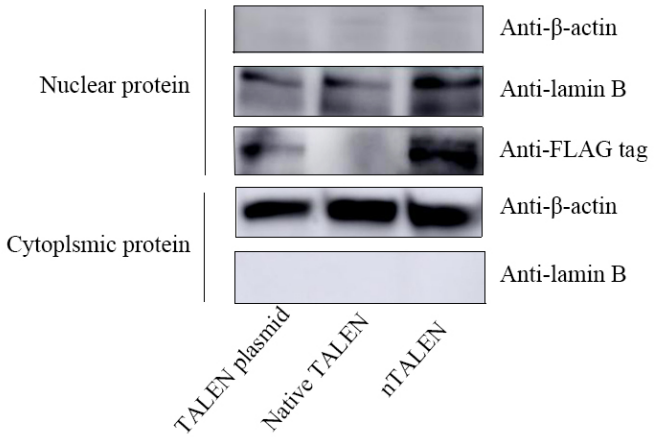

Figure 3-10. Western blot analysis of TALEN protein localization in HEK 293 reporter cells 12 h after sample administration. Anti-β-actin and anti-lamin B were used as loading control and indication of complete nuclear and cytoplasmic protein separations. Anti-FLAG tag antibody was used to detect TALEN proteins bearing 3 × FLAG on its N-terminus.

To further reconfirm the nuclear localization of delivered CCR5 TALEN-R. We conducted nuclear and cytoplasmic protein separations, followed by western blot assay of CCR5 TALEN-R using the anti-FLAG antibody due to the presence of N-terminal 3 × FLAG tag. Anti-Lamin B served as nuclear loading controls for use with nuclear extracts and similarly, β-actin was chosen as cytoplasmic loading controls for use with cytoplasmic extracts. As demonstrated in Fig. 3-10, β-actin steadily appeared in all cytoplasmic extracts but undetectable in nucleus extracts, conversely, lamin B was consistently found in all nucleus fractions but none in the cytoplasm, all of which indicated the successful and complete nuclear and cytoplasmic protein separations. More importantly, CCR5 TALEN-R was detected in the nucleus extracts of nTALEN and the TALEN-expressing plasmid treated cells, where the band intensity was higher for nTALEN than TALEN-expressing plasmid, proving that TALEN protein was indeed

successfully escorted into the nucleus, which functioned rapidly than the DNA transfection method.

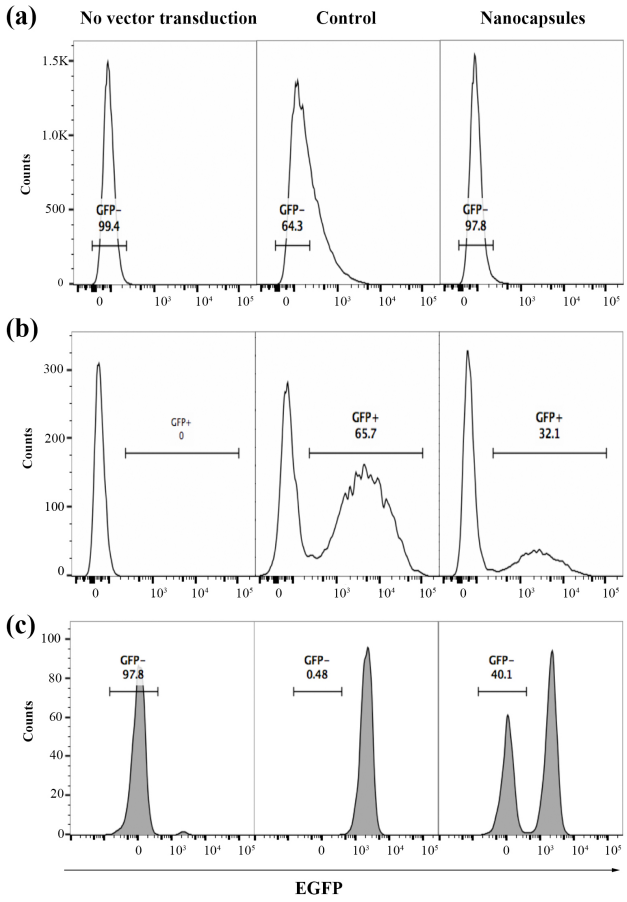

Figure 3-11. Gene Editing by TAR TALEN nanocapsules (nTAR TALEN) targeting HIV-1 LTRs. (a) HEK-293 cells were transfected with DA-EGFP vectors at MOI 0.5, in which the promoter EGFP is in LTR. 3 days after vector transduction, 1×10^5 HEK 293 cells were transduced with 150 ng nTAR TALEN (left arm) and 150 ng nTAR TALEN (right arm). 5 days after nanocapsule transduction, EGFP expression was checked by flow cytometry. (b) HEK-293 cells were transfected with FG11-EGFP vectors at MOI 0.5, in which EGFP has an internal Ubiquitin C promoter. 3 days after vector transduction, 1×10^5 HEK 293 cells were transduced with 150 ng nTAR TALEN (left arm) and 150 ng nTAR TALEN (right arm). After another 5 days, EGFP expression was checked (c) CEM T clones were transfected with FG11-EGFP vectors at MOI 0.01, 3 days after vector transduction, 1×10^5 HEK 293 cells were transduced with 150 ng nTAR TALEN (left arm) and 150 ng nTAR TALEN (right arm). 5 days after nanocapsule transduction, EGFP expression was checked. Control: infected cells not transduced with nanocapsules.

Considering the positive results gained with CCR5 TALEN-R nanocapsules, we further extended our nanocapsule encapsulation to include TAR TALEN pairs engineered via the platinum TALEN platform with extremely high efficiency targeting the trans-activation responsive (TAR) region of HIV-1 LTRs, [188] It is noteworthy that TAR region is crucial for gene expression in HIV proviral genome and an ideal target to abort HIV-1 provirus function effectively.[192]

To start with, we evaluated the LTR-editing efficacy in HEK 293 cells infected with an EGFP lentiviral vector, which integrated into the chromosome with a single-copy EGFP gene bearing its promoter in LTRs. Like wide-type HIV-1 provirus, mutation of only the 5' LTR would abrogate gene transcription. As shown in Fig. 3-11(a), a single dose of 300 ng nTAR TALEN (150 ng for each nTAR TALEN monomer) resulted in a remarkable increase in the average percentage of EGFP negatives cells from 64.3% to 97.8%, implying almost complete gene knockout. Thereafter, we adapted the HEK 293 reporter system to be more stringent by chromosomal integration of a single lentiviral vector FG11-EGFP that expresses EGFP from an internal Ubiquitin C (UbC) promoter, where loss of EGFP expression requires editing both LTRs and coming off of the whole interfering sequences. It is observed that one single treatment (300 ng nTAR TALEN pairs) led to almost 50% knockout of EGFP signal. (Fig.3-11(b)). The vector was also used to transfect CEM T-cell clones, where EGFP expressing disruption was about 40% after a single treatment with the same dose as above. (Fig. 3-11(c)). All these results demonstrated a robust LTR-editing efficacy on integrated lentivirus by the nTAR TALEN.

However, prior study working with mRNAs-encoding TAR TALENs didn't accomplish clear anti-HIV activity in primary human T cells, in which HIV provirus latently sustains as viral reservoirs and presents a great risk to the infected hosts.[188] To evaluate whether nTAR

TALEN can disrupt latent HIV-1 reservoirs in primary cells lines. We isolated primary macrophages by stimulating the peripheral blood mononuclear cell (PBMC) with macrophage colony-stimulating factors (GM-GSF and M-CSF), and then transfected the cells with lentiviral Cal-1 EGFP vector at two different levels of the multiplicity of infection (MOI). Similar to the FG11-EGFP vector, the Cal-1 EGFP vector also contains an internal Ubiquitin C promoter such that blockage of EGFP transcription is contingent on the editing of both LTRs and excision of intervening sequences. According to Fig. 3-12, transfection at MOI of 30 and 50 abolishes 82% and 58% of EGFP expression respectively with a single dosage of nTAR TALEN (300 ng protein in total), manifesting a superior genome-editing activity in primary macrophages.

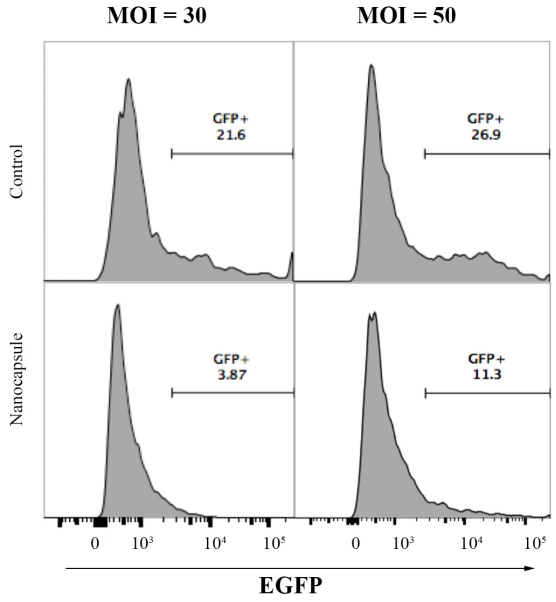

Figure 3-12. Specific elimination of latently infected primary primary cells by nTAR TALEN. Primary macrophages were isolated from PBMC and transfected with Cal-1 EGFP vectors at MOI 30 and 50 respectively. The EGFP has an internal Ubiquitin C promoter. 3 days after vector transduction, 5×10^5 primary macrophage cells were transduced with 150 ng nTAR TALEN (left arm) and 150 ng nTAR TALEN (right arm). 5 days after nanocapsule transduction, EGFP expression was checked by flow cytometry. Control: infected cells not transduced with nTAR TALENs.

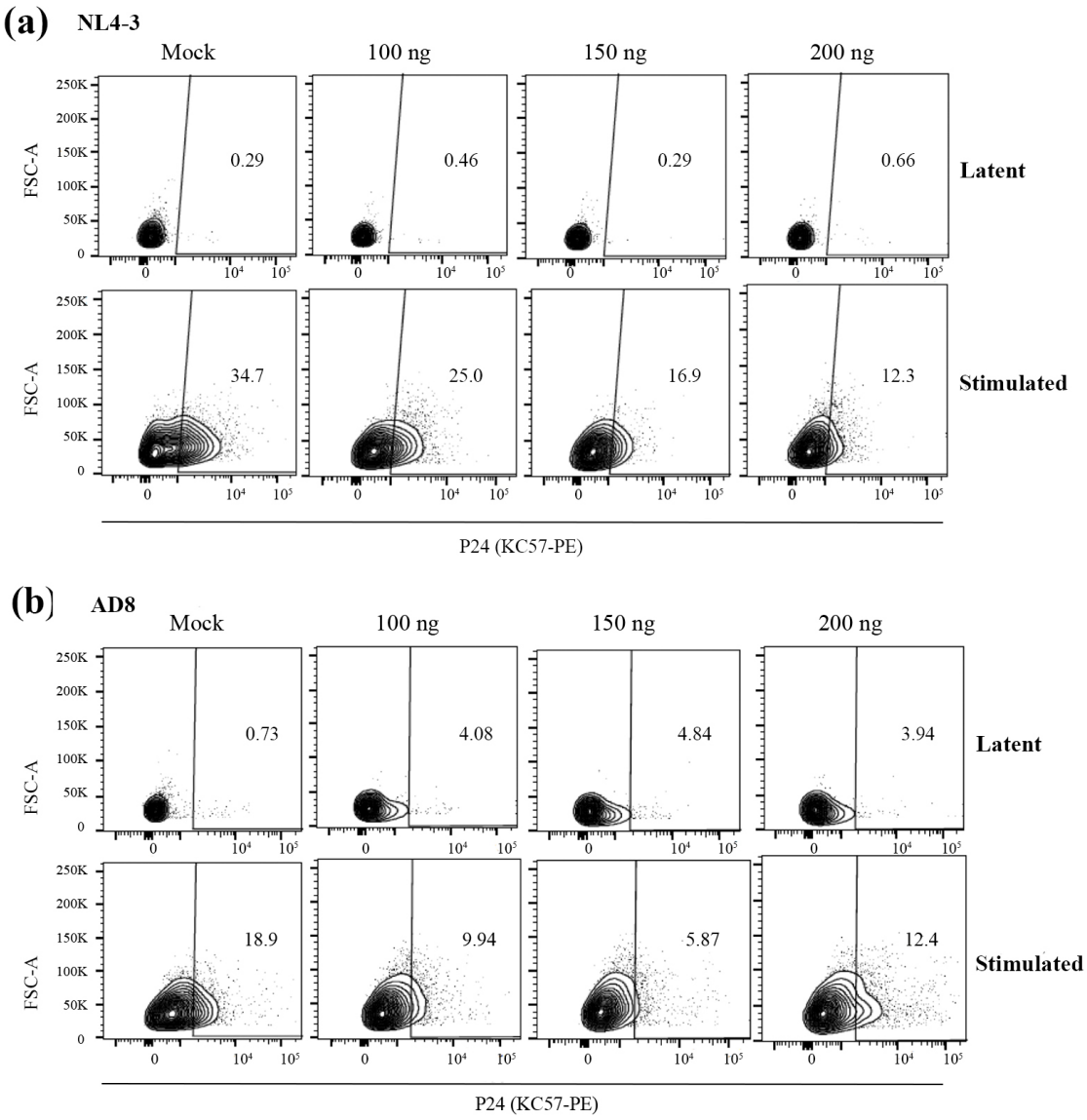

Figure 3-13. Specific elimination of latently infected primary T cells by nTAR TALEN. a) 2×10^6 of naïve CD4+ T cells were infected with 2000 ng of wild type HIV-1 NL4-3 and cultured with 5 ng/mL of IL-7 and IL-15 for 2 weeks to acquire the latently infected primary T cells. Cells were then treated with nanocapsule for 4 hours with or without 1 μg/mL of CD3 and CD28 antibody reactivation for three days, seven days after stimulation, levels of intracellular p24 antigen in latently infected primary T cells were stained by KC57-PE and analyzed by flow cytometry. b) Naïve CD4+ T cells were infected with 2000 ng of HIV AD8 strain. Same procedure as above followed. Mock: cells without virus infection. Control: infected cells not transduced with nTAR TALENs.

Finally, we employed the nTAR TALEN to challenge primary T cells latently infected with wild-type HIV-1 NL4-3 or HIV-1 AD8. The intracellular HIV-1 P24 gag antigen expression, an indicator of HIV-1 replication activity, was quantified by flow cytometry with KC57-PE antibody staining. Without stimulation by CD3 and CD28 antibodies, no apparent viral reactivation could be identified in NL4-3 strain transfected primary T cells, whereas 7 days after stimulation, 34% of cells expressed intracellular p24. Compared to mock, nTAR TALEN exhibited 27% to 64% decrease of p24 positive cells with dosages between 100 ng and 200 ng for each TALEN monomer (Fig. 3-13(a)). In addition, in primary T cells latently infected with AD8 strain, the addition of nTAR TALEN slightly reactivated viral activity, as implied by a multifold augmentation of p24 positive cells. After stimulation, 18.9% of cells were positive for p24 gag in mock, the number of which remarkably dropped after transduction with nTAR TALEN at different levels. Collectively, The nTAR TALEN showed high potential to purge latent viral reservoirs not only in normal T cell lines but also in primary cells.

3.4 Conclusions

In conclusion, we have developed a novel intracellular TALEN delivery approach whereby TALEN protein was encapsulated within a thin layer of pH-sensitive polymer. The cationic surface charge together with acid-labile crosslinkers enables high-efficient transmembrane transportation, cargo release and avoidance of endosome/lysosome sequestration. As a result, the delivered TALEN demonstrated good gene-editing capability under an ultra-low working concentration. In particular, the TAR TALEN efficiently disrupted HIV-1 latent reservoirs particularly in primary T cells, thereby posing a tremendous potential to be a novel therapeutics tool for anti-HIV therapy.

Chapter 4. Design and Fabrication of a Novel Choline Biosensor with Enhanced Sensitivity using Poly(zwitterionic) polymer immobilized choline oxidase

4.1 Introduction

The neurotransmitter plays an important role in memory and behaviors thus is also associated with a wide range of brain disorders such as Alzheimer's disease, Parkinson's disease, and stroke. Multiple neurotransmitters such as acetylcholine (ACh), glutamate (Glut) and dopamine (DA) are frequently released into the synaptic cleft at almost every central and peripheral synapse.[193,194] Real-time techniques for the simultaneous monitor of multiple neurochemicals would greatly facilitate the understanding of the connection between neurochemistry and behaviors in this regard. Microdialysis technique has been widely and clinically applied for the multiple analyte measurements, however, the seconds to minutes time-delay impedes the measurement of the fast extracellular dynamics of some neurotransmitters.[195-197] This limitation has prompted inverstigators to develop sensors capable of monitoring multiple neurochemicals with high spatiotemporal resolution.

Amperometric enzyme-based microsensors have shown promise for real-time measurement of neurotransmitters.[198,199] This technique relies on immobilizing enzyme onto the electrode surface to convert the substrates to electroactive compound such as H_2O_2. In order to simultaneously monitor multiple neurochemicals, various techniques reported such as polymer electrodeposition and electrostatic adsorption have shown their feasibility to selectively immobilize enzyme onto the surface of the micro-electrode array (MEA) in patterned sized down to micro-to-nano range.[200] Microcontact printing (μCP) has proven to be a useful technique in the

patterned functionalization of chemicals onto surfaces, and has been particularly valuable in the patterning of biological materials.[201-203] We previously reported the feasibility of μCP transferring enzyme- glucose oxidase (GOx) and choline oxidase (ChOx) onto targeted sites on MEA. However, those experienced the difficulty on immobilizing sufficient amount of enzyme to prevent the resulting sensors from being kinetic-limited without sacrificing the patterning resolution. To efficiently transfer enzyme to the substrate, the chemistry of the ink is important to make it bind to the new surface more favorable than stay on the stamp.

μCP experienced difficulty to transfer sufficient amount of enzyme at each stamping process and to stamp the second layer directly on the first stamped layer. Each stamping enzyme layer results in a rougher surface which leads to difficult alignment and uneven enzyme transferred. To overcome the obstacles described above, the ChOx ink used in this study has been optimized to be capable of transferring a good amount of enzyme on the substrate for every single stamp and resulting in excellent sensitivity without sacrificing spatial resolution.

4.2 Methods, Experiment, and Characterizations

4.2.1 Materials and instruments

Nafion (5 wt. % in lower aliphatic alcohols and water, contains 15-20% water), m-Phenylenediamine (flakes, 99%), Bovine Serum Albumin (lyophilized powder, ≥96%), Choline Oxidase (ChOx) from *Alcaligenes sp.*, L-glutamic acid, choline chloride, 3-hydroxytyramine (dopamine, DA) anhydrous potassium carbonate, chitosan (from crab shells, minimum 85% deacetylated), glutaraldehye (GAH) (25% in water), sodium chloride and hydrogen peroxide (30 wt% solution in water) were purchased from Sigma-Aldrich.

The PDMS stamps were fabricated by pouring the mixture of monomer and curing agent (the Sylgard®184 silicon elastomer kit) in the ratio of 10:1 onto the SU-8 2075 silicon mold, which was subsequently degassed under vacuum to remove air bubble and cured at 60 °C for 4 hr. The PDMS microstamps were then cut into 1 cm × 1cm pieces and detached from the mold. The fabrication process and the resulting PDMS microstamps are shown in Fig.1. To ensure that the enzyme transferred covers the entire electrode surface (150μm × 40μm), the size of each stamp surface was designed to be (160μm × 50μm).

Electrochemical preparation, *in vitro* calibration and flow cell experiments were performed using Versatile Multichannel Potentiostat (VMP3, Bio-Logic) equipped with the 'p' low current option and low current N stat box. A standard three-electrode system consisting of a separate Pt-wire as a counter electrode (BASi, W. Lafayette, IN), a separate Ag/AgCl reference electrode (BASi, W. Lafayette, IN) modified Pt sites on our MEA as the working electrode was used with the VMP3 system in a Faraday cage. Nova Nano 230 was used for all SEM images.

4.2.2 Synthesis of PAH macroCTA

The PAH macroCTA was synthesized by conjugating the chain transfer agent to the amino groups of PAH. Briefly, 3 mg 4-cyano-4-(phenylcarbonothioylthio) pentanoic acid was dissolved in 400 uL DMSO. The DMSO solution was mixed with 10.5 mg EDC and 2.5 mg NHS in 50 uL MES buffer (pH 5.0), followed by incubation at 4 °C or 1 h. Then 20 mg PAH in 100 uL MES buffer was added in. The mixture was stirred at room temperature for 24 h. Afterwards, the reaction solution was dialyzed against acetate buffer (pH 5.0) for 4 h to remove EDC, NHS, DMSO and unreacted CTA. The conjugation ratio was determined by UV-vis spectra. The final product was obtained by freeze-drying as a pink solid.

4.2.3 Synthesis of PMPC conjugated PAH via RAFT polymerization (PMPC-*g*-PAH)

The PMPC-g-PAH polymer was synthesized via RAFT polymerization. Typically, 10 mg PAH-CTA (CTA, 0.0054 mmol), 80 mg MPC (0.27 mmol), and 8.7 mg VA-044 (0.027 mmol) were dissolved in 500 uL pH 5.0 acetate buffer and added into a schlenk flask. The mixture was deoxygenized through three freeze-pump-thaw processes. Then the flask was placed in water bath at 25 °C and stirred for 6 h. The polymerization was stopped by immersing the flask into liquid nitrogen. Then the reaction solution was dialyzed against DI water to remove the unreacted initiator and monomer. The final product was obtained by freeze drying.

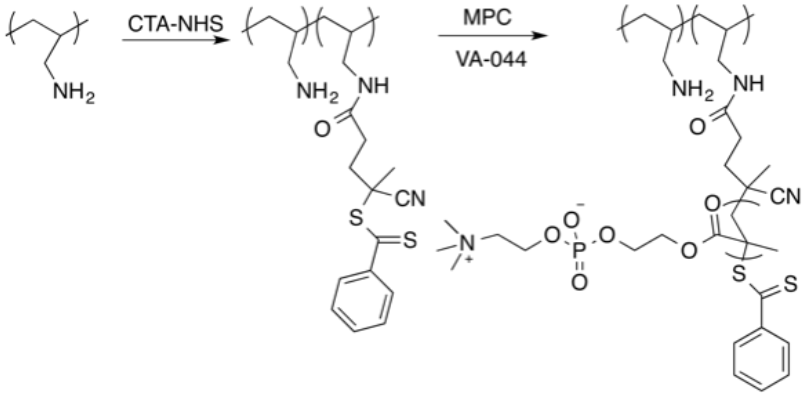

Figure 4-1. Synthesis route of PAH-*g*-PMPC polymer

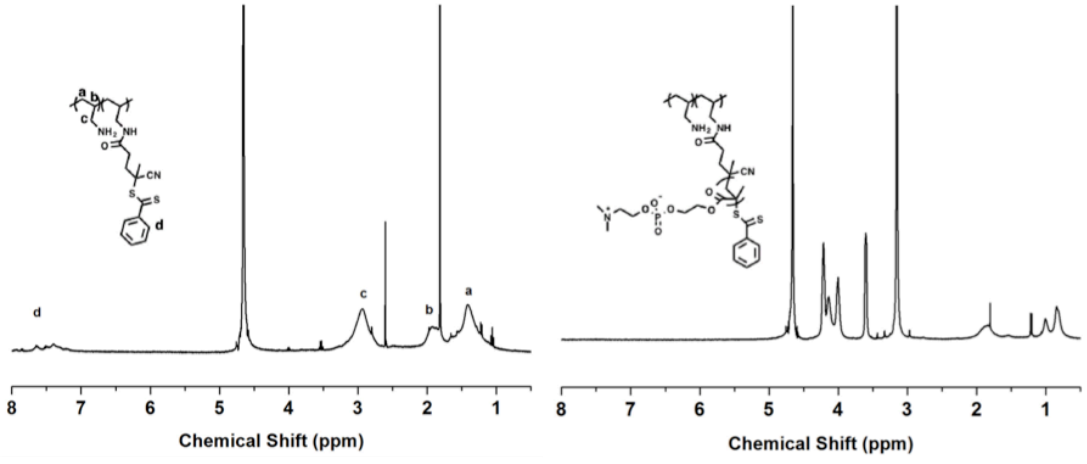

Figure 4-2. Proton NMR of PAH-CTA and PAH-*g*-PMPC

4.2.4 Device fabrication and electrode surface modification

The MEA was 100-150 μm thick, 140 μm wide and 9 mm long, with 4 ~6000 μm^2 Pt recording sites arranged in pairs at the tip. The Si-based wafer processing included the physical vapor deposition of Pt as the electrode material and the chemical vapor deposition of oxide/nitride as insulation. Shaping was done by deep reactive ion etching from the front side.

Poly(m-phenylenediamine) (PPD) was electrodeposited from a 5mM m-Phenylenediamine solution in 1×PBS (pH 7.4) by holding the voltage constant at 0.85V until total charged transferred reached 0.19 nA/hr, followed by 2% Nafion dip-coated over all four sites and annealed at 115 °C for 20min. PPD served as a permselective film by size exclusion, and the anionic polymer, Nafion, was used to further block out negatively charged species such as ascorbic acid (AA) from the electrode surface.

Chitosan was dissolved in a solution (0.1% m/v, pH = 3) and stirred for 48 h to ensure the chitosan flakes dissolved completely. The pH was adjusted to 5 using NaOH solution (0.1M) before the electrodeposition and a constant potential of -0.7 V vs Ag/AgCl was applied at the PPD/Nafion coated Pt electrode for 1 min and repeated twice.

A droplet of ChOx solution (ChOx/BSA/PAH-MPC polymer mixture) was placed on the PDMS stamp and allowed to rest at the room temperature for few minutes. After the “inking” step, alignment of the “inked” stamp and the target microelectrode was achieved by manipulation of the microscope stage, and gently contacted for few seconds to transfer the enzyme from microstamp to microelectrode surface. Followed by exposing the entire tip to 5% GAH vapor for 1 min to cross-link proteins, and then stored dry at 4°C for 48h prior to testing. The whole stamping process is shown in Fig. 4-3.

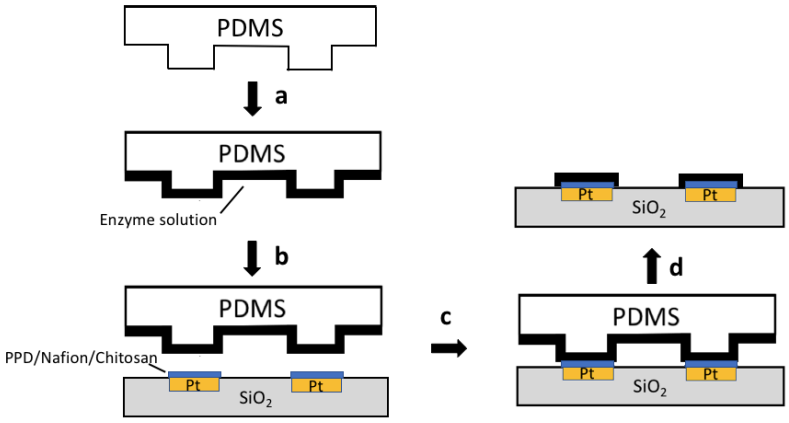

Figure 4-3. Diagram illustrating the enzyme transferring process of µCP. The PDMS stamp is inked with enzyme solution (a), carefully aligned to the target electrode surface under the microscope. (b), and gently contacted for few minutes (c). This transfer (d) formed a patterned enzyme layer on the MEA.

4.2.5 *In vitro* calibration

The MEA was calibrated *in vitro* using constant potential amperometry with the VMP3 system. 0.7 V was applied to the working electrode against the Ag/AgCl reference electrode in 10 mL of stirred PBS at pH 7.4 in a beaker housed in a Faradic cage. After stabilization for a few minutes, the current detected at the electrodes equilibrated to a constant current value. Choline (20-80 µM final concentration), AA (250 µM final concentration) and DA (5-10 µM final concentration) were added to the beaker to assess sensitivity and selectivity. The current choline sensors design is shown in Fig. 4-4. PPD and Nafion permselective layers were used to prevent intervening species such as AA and DA from approaching the Pt surface. Chitosan layer was employed to improve the enzyme adhesion on the electrode surface after crosslinking. The ChOx layer catalyzes choline in the presence of O_2 resulting in the production of H_2O_2 that can be subsequently oxidized at 0.7 V vs Ag/AgCl on the Pt electrode surface.

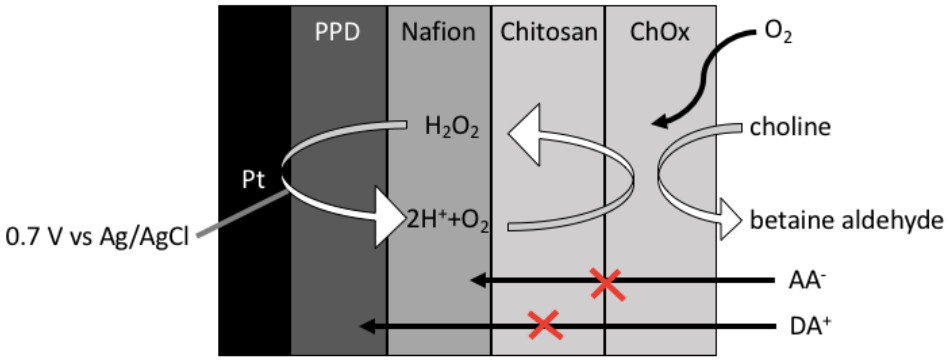

Figure 4-4. Schematic diagram for the preparation of choline sensors by modifying the electrode surface with different permselective layers (PPS and Nafion), chitosan and choline oxidase.

4.3 Results and Discussions

Chitosan was deposited to improve sensor stability via covalent bonding between the stamped enzyme layer and electrode surface after GAH crosslinking. An advantage of using PAH-MPC polymer plus BSA over BSA solely is that the superhydrophilic MPC moieties on PAH-MPC polymer make enzyme ink more transferrable onto hydrophilic chitosan-coated electrode surface than staying on the hydrophobic PDMS stamp (Fig. 4-5). Optical and SEM images of MEA after ChOx and PAH-MPC-ChOx stamping on different electrodes are shown in Fig. 4-6. It is apparent that μCP is capable of transferring and patterning enzyme in micro-range. Greater amount of PAH-MPC-ChOx ink was able to be transfer in each single stamping process than ChOx ink without sacrificing the stamping resolution, which makes PAH-MPC-ChOx ink more favorable in stamping process due to the fact that stamping second layer of enzyme directly onto the first stamped enzyme is difficult (Fig. 4-6a). After crosslinking with GAH, more enzyme stayed on the electrode surface without being washed away after the calibration in the stirring PBS buffer (Fig. 4-6b). For each signal stamp, PAH-MPC-ChOx resulted in around 4 μm thick patterned enzyme layer and ChOx only 4 μm thick.

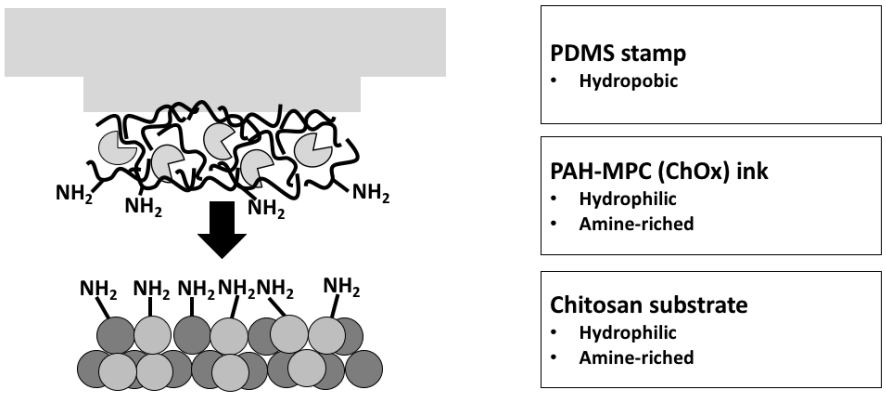

Figure 4-5. Diagram showing the properties of PDMS stamp, enzyme ink and chitosan-coated substrate that makes enzyme more favorable to be transferred onto substrate over staying on the stamp. Extra amine-group in the polymer chain resulted in stronger crosslinking of enzyme layer and the electrode surface.

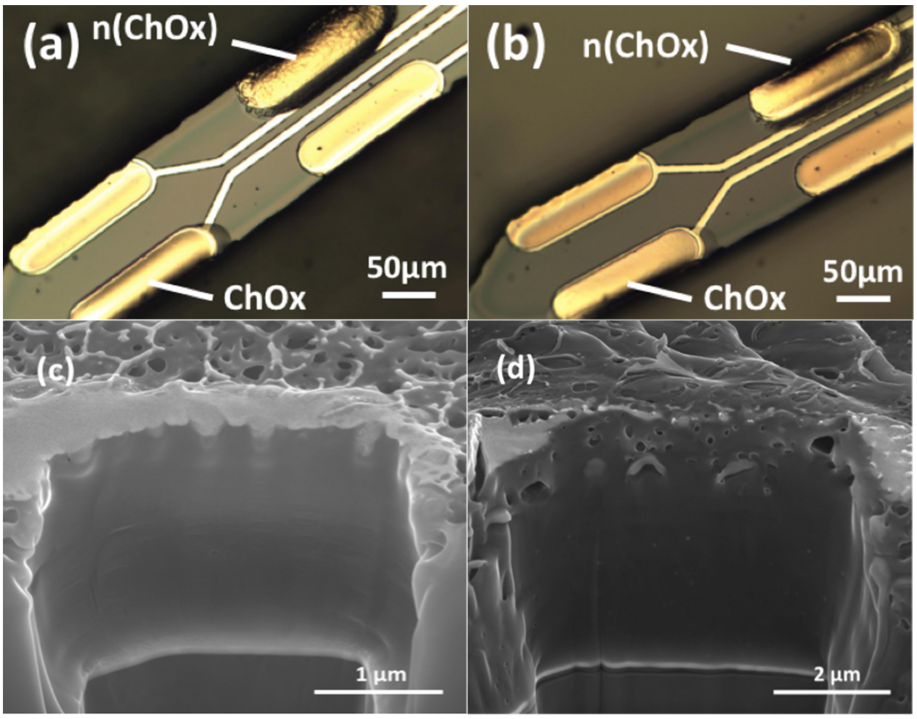

Figure 4-6. Optical microscope image of MEA after PDMS stamping of ChOx (lower right) and n(ChOx) (upper left) (a) before calibration and (b) after calibration. (c) 32500 SEM image of the

cross-section of ChOx stamped. (d) 17500 SEM image of the cross-section of n(ChOx) stamped microprobe after calibration in PBS buffer. n(ChOx) represents PAH-MPC-ChOx.

Typical calibration curves for the choline sensors are presented as Fig. 4-7. Biosensors made from ChOx and PAH-MPC-ChOx exhibited repeatable, improved sensitivity from 294±19 nA/μM.cm^2 (n=9) to 503±21nA/μM.cm^2 (n=12) and detection limit from 0.83±0.12 μM (n=9) to 0.45±0.05 (n=12) μM at a signal-to-noise ratio of 3, respectively. Those sensors were also tested with common interferent presenting in the extracellular fluid in the CNS at physiological concentration, such as 250 μM AA and 10 μM DA, and no detectable response was observed (the first two injection in Fig. 4-7(a)).

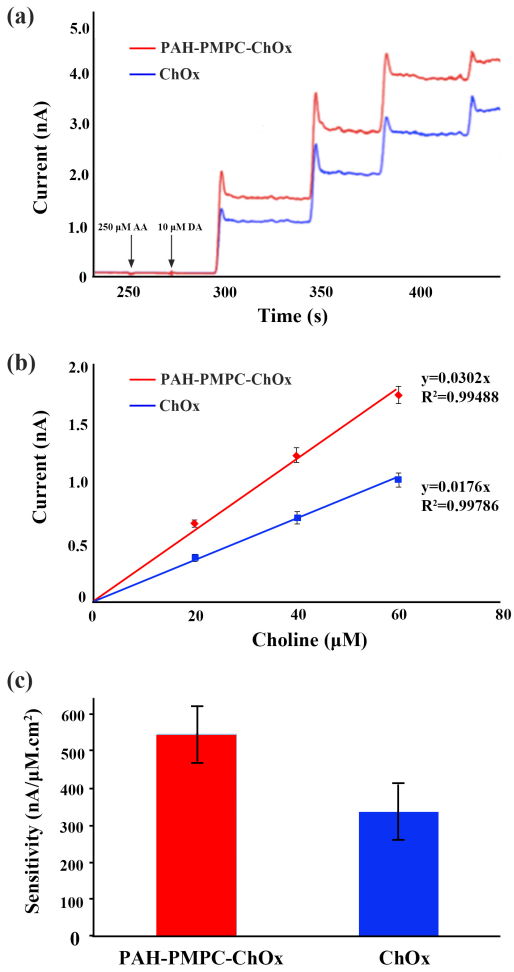

Figure 4-7. Representative current response of stamped ChOx (Blue trace) and stamped PAH-MPC-ChOx (Red trace) sensors to choline chloride (chcl). (a) The sensors response was recorded in stirred 1×PBS (pH 7.4) solution for 250 µM AA, 10 µM DA and sequential injection of choline and finally 20 µM H_2O_2 at a constant potential of 0.7 V (vs Ag/AgCl). (b) Biosensors made from ChOx and PAH-MPC-ChOx exhibited repeatable, improved sensitivity of 294±19 nA/µM·cm (n=9) to 294±19 nA/µM·cm (n=12). (c) Comparison of sensitivity of PAH-MPC-ChOx and ChOx sensors with 95% confidential interval.

To verify the factor that caused 2-fold improvement in sensitivity of PAH-PMPC-ChOx microsensors, the value of Km were measured and compared in Fig. 4-8. Before stamping onto the electrode surface, PAH-PMPC-ChOx and ChOx ink solution showed similar Km value with 2.42×10^{-3} and 2.69×10^{-3} M, respectively. This Km value proved the improved sensitivity of PAH-PMPC-ChOx microsensors was mainly due to the greater amount of enzyme transferred.

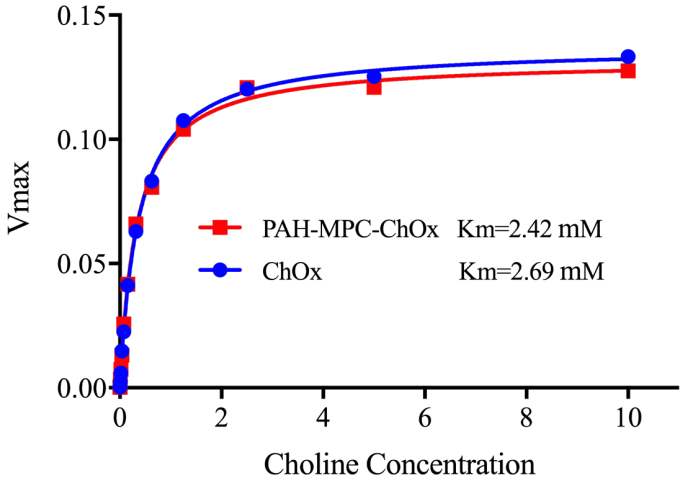

Figure 4-8. Km measurement of PAH-PMPC-ChOx and ChOx

The resulting PAH-PMPC-ChOx also displayed a fast response time (~1.4s) to a choline step change of 20 µM in a flow cell as shown in Fig 4-9.

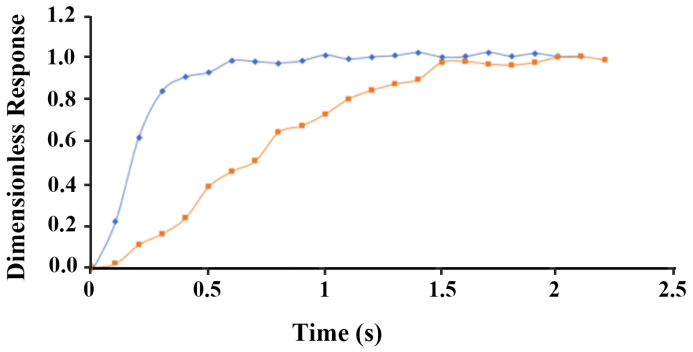

Figure 4-9. Response time measurement of H_2O_2 (blue trace) and choline (yellow trace) in flow cell system

4.4 Conclusions

PAH-PMPC polymer coated ChOx ink could improve the transfer of enzyme from PDMS stamp to the chitosan-coated electrode surface during choline biosensor fabrication. The increased enzyme loading capacity on electrodes as well as the abundant amine groups available for crosslinking effectively prevents ChOx from being washed away during the biosensor calibration process. As a result, the novel choline biosensor displayed improved sensitivity from 294±19 nA/μM·cm^2 (n=9) to 503±21 nA/μM·cm^2 (n=12) and improved detection limit from 0.83±0.12 μM (n=9) to 0.45±0.05 nA/μM·cm^2 (n=12). The employment of PAH-PMPC polymer to facilitate and improve the PDMS stamping process is expected to contribute to neuroscience research by enabling the controlled deposition of different enzymes on the selected microelectrode sites on one microprobe with enhanced sensitivity, thereby enabling the combined sensing of multiple neurotransmitters at the same location simultaneously.

Chapter 5. Conclusion

In this dissertation, recent advances in "nanocarriers for systemic protein delivery", "nanocarriers for intracellular protein delivery", "approaches for gene-editing nucleases delivery" and "polymer-based biosensors" are systemically reviewed. Three projects related to oxalate oxidase nanocapsules for hyperoxaluria treatment, TALEN nanocapsules against integrated HIV-1 and zwitterionic polymer-coated choline biosensor are specifically described. In this chapter, the novelty, significance, and outlook of each project are summarized as follows:

1) We have developed a delivery vehicle for the native OxO by encapsulating it within a layer of zwitterionic polymers. The encapsulation endowed nOxO with robust activity, increased stability and resistance to protein adsorption. In addition, we demonstrated that nOxO could also reduce phagocytosis, while significantly increasing the circulation half-life, without eliciting significant immune responses due to the antifouling properties. Therefore, our platform offers a potential route for the systemic delivery of OxO to treat hyperoxaluria, as well as various therapeutic enzymes for the treatment of other systemic disorders. For future work, a diseased animal model of hyperoxaluria is highly needed to evaluate the therapeutic efficacy of nOxO. Moreover, the proposed mechanism that PMPC covering enhances OxO bioactivity may need further elucidation by experiments and molecular dynamics simulations.

2) We have proved that TALEN protein can be delivered into the cellular cytosol via CPPs or nanocapsules. The type and surface density of CPPs significantly impact the cellular uptake and subsequent gene-editing outcome. The TALEN nanocapsules (nTALEN) harboring substantial surface positive charges could effectively enter the cells and escape the endocytic compartments. The cargo release is facilitated by the acid-sensitive crosslinker GDMA, which triggers the dissociation of the polymer shells in acidic endosomes. Once delivered, the multiple

disulfide linkages generated during polymerization are rapidly disrupted by the cytoplasmic glutathione, which recovers the TALEN activity. The N-terminal NLS on TALEN surface subsequently guides its transportation and entry into the nucleus to implement the specific gene-editing task. In HEK 293 reporter cells, we demonstrated that CCR5 TALEN nanocapsule could induce targeted gene mutagenesis at a much lower working concentration (30 nM) than CPPs under the same ratio of gene disruption. More importantly, the TAR TALEN nanocapsule demonstrated high excision potential to purge HIV provirus in primary T cell lines. For future work, HIV-infected humanized animal models are desired for tropical and *ex vivo* delivery studies and therapeutic evaluation of the TAR TALEN nanocapsules. In addition, a smart delivery system that could specifically target CD4+ cells is in demand so that TAR TALEN can be delivered through intravenous administration.

3) We have generated a novel choline biosensor that choline oxidase is immobilized by PAH-PMPC polymer on the electrode surface. The abundant amine groups from PAH-PMPC enable sufficient crosslinking of the enzyme layer with the chitosan layer underneath such that the enzyme loading capacity is significantly increased, leading to improved sensitivity and detection limit. Moreover, the hydrophilicity of the MPC moiety facilitates enzyme transfer from the hydrophobic PDMS stamp to the hydrophilic electrode surface. For future work, whether the advanced properties of PMPC polymer such as reducing immune response and extending *in vivo* half-life are applicable to biosensors as well need further confirmation via animal experiments.

Appendix: DNA Sequences

pTNT CCR5 RR (2740 bp)

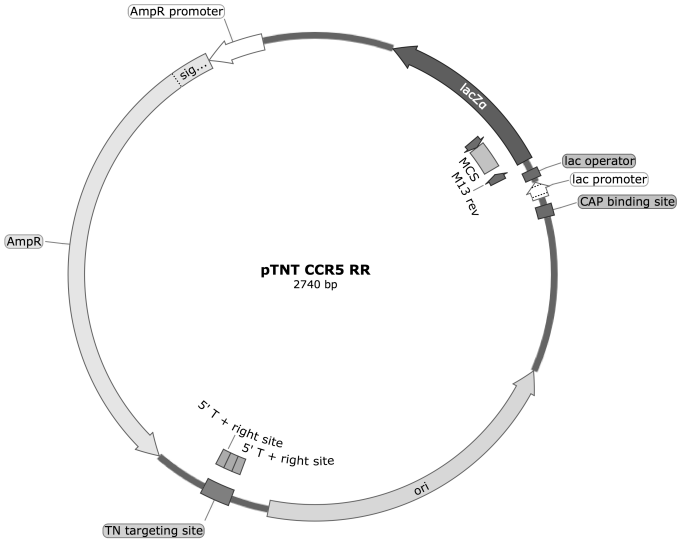

TCGCGCGTTTCGGTGATGACGGTGAAAACCTCTGACACATGCAGCTCCCGGAGACGGTCACAGCTTGT
CTGTAAGCGGATGCCGGGAGCAGACAAGCCCGTCAGGGCGCGTCAGCGGGTGTTGGCGGGTGTCGGG
GCTGGCTTAACTATGCGGCATCAGAGCAGATTGTACTGAGAGTGCACCATATGCGGTGTGAAATACCG
CACAGATGCGTAAGGAGAAAATACCGCATCAGGCGCCATTCGCCATTCAGGCTGCGCAACTGTTGGGA
AGGGCGATCGGTGCGGGCCTCTTCGCTATTACGCCAGCTGGCGAAAGGGGGATGTGCTGCAAGGCGAT
TAAGTTGGGTAACGCCAGGGTTTTCCCAGTCACGACGTTGTAAAACGACGGCCAGTGAATTCGAGCTC
GGTACCCGGGGATCCTCTAGAGTCGACCTGCAGGCATGCAAGCTTGGCGTAATCATGGTCATAGCTGT
TTCCTGTGTGAAATTGTTATCCGCTCACAATTCCACACAACATACGAGCCGGAAGCATAAAGTGTAAA
GCCTGGGGTGCCTAATGAGTGAGCTAACTCACATTAATTGCGTTGCGCTCACTGCCCGCTTTCCAGTCG
GGAAACCTGTCGTGCCAGCTGCATTAATGAATCGGCCAACGCGCGGGGAGAGGCGGTTTGCGTATTGG
GCGCTCTTCCGCTTCCTCGCTCACTGACTCGCTGCGCTCGGTCGTTCGGCTGCGGCGAGCGGTATCAGC
TCACTCAAAGGCGGTAATACGGTTATCCACAGAATCAGGGGATAACGCAGGAAAGAACATGTGAGCA
AAAGGCCAGCAAAAGGCCAGGAACCGTAAAAAGGCCGCGTTGCTGGCGTTTTTCCATAGGCTCCGCCC
CCCTGACGAGCATCACAAAAATCGACGCTCAAGTCAGAGGTGGCGAAACCCGACAGGACTATAAAGA
TACCAGGCGTTTCCCCCTGGAAGCTCCCTCGTGCGCTCTCCTGTTCCGACCCTGCCGCTTACCGGATAC
CTGTCCGCCTTTCTCCCTTCGGGAAGCGTGGCGCTTTCTCATAGCTCACGCTGTAGGTATCTCAGTTCG
GTGTAGGTCGTTCGCTCCAAGCTGGGCTGTGTGCACGAACCCCCCGTTCAGCCCGACCGCTGCGCCTTA
TCCGGTAACTATCGTCTTGAGTCCAACCCGGTAAGACACGACTTATCGCCACTGGCAGCAGCCACTGG
TAACAGGATTAGCAGAGCGAGGTATGTAGGCGGTGCTACAGAGTTCTTGAAGTGGTGGCCTAACTACG
GCTACACTAGAAGAACAGTATTTGGTATCTGCGCTCTGCTGAAGCCAGTTACCTTCGGAAAAAGAGTT
GGTAGCTCTTGATCCGGCAAACAAACCACCGCTGGTAGCGGTGGTTTTTTTGTTTGCAAGCAGCAGATT
ACGCGCAGAAAAAAAGGATCTCAAGAAGATCCTTTGATCTTTTCTACGGGGTCTGACGCTCAGTGGAA
CGAAAACTCACGTTAAGGGATTTTGGTTCTTCCAGAATTGATACTCTCATTTTCCATACAGTCAGTATC
AATTCTGGAAGACATGAGATTATCAAAAAGGATCTTCACCTAGATCCTTTTAAATTAAAAATGAAGTT
TTAAATCAATCTAAAGTATATATGAGTAAACTTGGTCTGACAGTTACCAATGCTTAATCAGTGAGGCA
CCTATCTCAGCGATCTGTCTATTTCGTTCATCCATAGTTGCCTGACTCCCCGTCGTGTAGATAACTACG
ATACGGGAGGGCTTACCATCTGGCCCCAGTGCTGCAATGATACCGCGAGACCCACGCTCACCGGCTCC
AGATTTATCAGCAATAAACCAGCCAGCCGGAAGGGCCGAGCGCAGAAGTGGTCCTGCAACTTTATCCG
CCTCCATCCAGTCTATTAATTGTTGCCGGGAAGCTAGAGTAAGTAGTTCGCCAGTTAATAGTTTGCGCA
ACGTTGTTGCCATTGCTACAGGCATCGTGGTGTCACGCTCGTCGTTTGGTATGGCTTCATTCAGCTCCG
GTTCCCAACGATCAAGGCGAGTTACATGATCCCCCATGTTGTGCAAAAAAGCGGTTAGCTCCTTCGGT

CCTCCGATCGTTGTCAGAAGTAAGTTGGCCGCAGTGTTATCACTCATGGTTATGGCAGCACTGCATAAT
TCTCTTACTGTCATGCCATCCGTAAGATGCTTTTCTGTGACTGGTGAGTACTCAACCAAGTCATTCTGA
GAATAGTGTATGCGGCGACCGAGTTGCTCTTGCCCGGCGTCAATACGGGATAATACCGCGCCACATAG
CAGAACTTTAAAAGTGCTCATCATTGGAAAACGTTCTTCGGGGCGAAAACTCTCAAGGATCTTACCGC
TGTTGAGATCCAGTTCGATGTAACCCACTCGTGCACCCAACTGATCTTCAGCATCTTTTACTTTCACCA
GCGTTTCTGGGTGAGCAAAAACAGGAAGGCAAAATGCCGCAAAAAAGGGAATAAGGGCGACACGGA
AATGTTGAATACTCATACTCTTCCTTTTTCAATATTATTGAAGCATTTATCAGGGTTATTGTCTCATGAG
CGGATACATATTTGAATGTATTTAGAAAAATAAACAAATAGGGGTTCCGCGCACATTTCCCCGAAAAG
TGCCACCTGACGTCTAAGAAACCATTATTATCATGACATTAACCTATAAAAATAGGCGTATCACGAGG
CCCTTTCGTC

pET21a-TNsk-CCR5R (8449 bp)

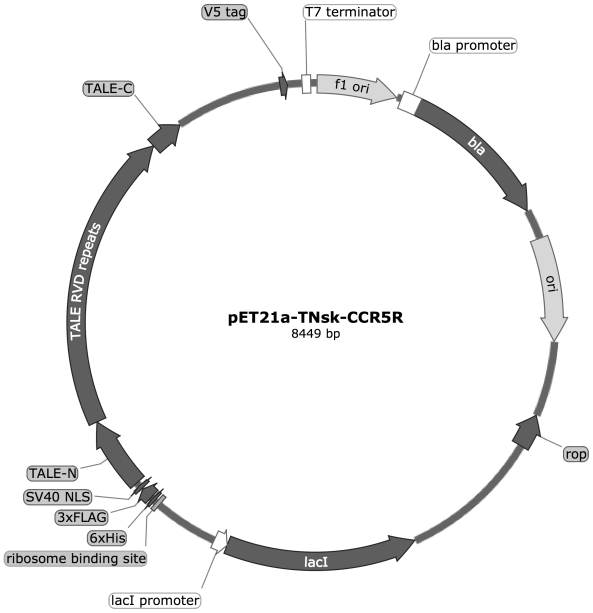

TGGCGAATGGGACGCGCCCTGTAGCGGCGCATTAAGCGCGGCGGGTGTGGTGGTTACGCGCAGCGTG
ACCGCTACACTTGCCAGCGCCCTAGCGCCCGCTCCTTTCGCTTTCTTCCCTTCCTTTCTCGCCACGTTCG
CCGGCTTTCCCCGTCAAGCTCTAAATCGGGGGCTCCCTTTAGGGTTCCGATTTAGTGCTTTACGGCACC
TCGACCCCAAAAAACTTGATTAGGGTGATGGTTCACGTAGTGGGCCATCGCCCTGATAGACGGTTTTT
CGCCCTTTGACGTTGGAGTCCACGTTCTTTAATAGTGGACTCTTGTTCCAAACTGGAACAACACTCAAC
CCTATCTCGGTCTATTCTTTTGATTTATAAGGGATTTTGCCGATTTCGGCCTATTGGTTAAAAAATGAGC
TGATTTAACAAAAATTTAACGCGAATTTTAACAAAATATTAACGTTTACAATTTCAGGTGGCACTTTTC
GGGGAAATGTGCGCGGAACCCCTATTTGTTTATTTTTCTAAATACATTCAAATATGTATCCGCTCATGA
GACAATAACCCTGATAAATGCTTCAATAATATTGAAAAAGGAAGAGTATGAGTATTCAACATTTCCGT
GTCGCCCTTATTCCCTTTTTTGCGGCATTTTGCCTTCCTGTTTTTGCTCACCCAGAAACGCTGGTGAAAG
TAAAAGATGCTGAAGATCAGTTGGGTGCACGAGTGGGTTACATCGAACTGGATCTCAACAGCGGTAA
GATCCTTGAGAGTTTTCGCCCCGAAGAACGTTTTCCAATGATGAGCACTTTTAAAGTTCTGCTATGTGG
CGCGGTATTATCCCGTATTGACGCCGGGCAAGAGCAACTCGGTCGCCGCATACACTATTCTCAGAATG
ACTTGGTTGAGTACTCACCAGTCACAGAAAAGCATCTTACGGATGGCATGACAGTAAGAGAATTATGC
AGTGCTGCCATAACCATGAGTGATAACACTGCGGCCAACTTACTTCTGACAACGATCGGAGGACCGAA
GGAGCTAACCGCTTTTTTGCACAACATGGGGGATCATGTAACTCGCCTTGATCGTTGGGAACCGGAGC
TGAATGAAGCCATACCAAACGACGAGCGTGACACCACGATGCCTGCAGCAATGGCAACAACGTTGCG
CAAACTATTAACTGGCGAACTACTTACTCTAGCTTCCCGGCAACAATTAATAGACTGGATGGAGGCGG
ATAAAGTTGCAGGACCACTTCTGCGCTCGGCCCTTCCGGCTGGCTGGTTTATTGCTGATAAATCTGGAG
CCGGTGAGCGTGGGTCTCGCGGTATCATTGCAGCACTGGGGCCAGATGGTAAGCCCTCCCGTATCGTA
GTTATCTACACGACGGGGAGTCAGGCAACTATGGATGAACGAAATAGACAGATCGCTGAGATAGGTG

CCTCACTGATTAAGCATTGGTAACTGTCAGACCAAGTTTACTCATATATACTTTAGATTGATTTAAAAC
TTCATTTTTAATTTAAAAGGATCTAGGTGAAGATCCTTTTTGATAATCTCATGACCAAAATCCCTTAAC
GTGAGTTTTCGTTCCACTGAGCGTCAGACCCCGTAGAAAAGATCAAAGGATCTTCTTGAGATCCTTTTT
TTCTGCGCGTAATCTGCTGCTTGCAAACAAAAAAACCACCGCTACCAGCGGTGGTTTGTTTGCCGGATC
AAGAGCTACCAACTCTTTTTCCGAAGGTAACTGGCTTCAGCAGAGCGCAGATACCAAATACTGTCCTT
CTAGTGTAGCCGTAGTTAGGCCACCACTTCAAGAACTCTGTAGCACCGCCTACATACCTCGCTCTGCTA
ATCCTGTTACCAGTGGCTGCTGCCAGTGGCGATAAGTCGTGTCTTACCGGGTTGGACTCAAGACGATA
GTTACCGGATAAGGCGCAGCGGTCGGGCTGAACGGGGGGTTCGTGCACACAGCCCAGCTTGGAGCGA
ACGACCTACACCGAACTGAGATACCTACAGCGTGAGCTATGAGAAAGCGCCACGCTTCCCGAAGGGA
GAAAGGCGGACAGGTATCCGGTAAGCGGCAGGGTCGGAACAGGAGAGCGCACGAGGGAGCTTCCAG
GGGGAAACGCCTGGTATCTTTATAGTCCTGTCGGGTTTCGCCACCTCTGACTTGAGCGTCGATTTTTGT
GATGCTCGTCAGGGGGGCGGAGCCTATGGAAAAACGCCAGCAACGCGGCCTTTTTACGGTTCCTGGCC
TTTTGCTGGCCTTTTGCTCACATGTTCTTTCCTGCGTTATCCCCTGATTCTGTGGATAACCGTATTACCG
CCTTTGAGTGAGCTGATACCGCTCGCCGCAGCCGAACGACCGAGCGCAGCGAGTCAGTGAGCGAGGA
AGCGGAAGAGCGCCTGATGCGGTATTTTCTCCTTACGCATCTGTGCGGTATTTCACACCGCATATATGG
TGCACTCTCAGTACAATCTGCTCTGATGCCGCATAGTTAAGCCAGTATACACTCCGCTATCGCTACGTG
ACTGGGTCATGGCTGCGCCCCGACACCCGCCAACACCCGCTGACGCGCCCTGACGGGCTTGTCTGCTC
CCGGCATCCGCTTACAGACAAGCTGTGACCGTCTCCGGGAGCTGCATGTGTCAGAGGTTTTCACCGTC
ATCACCGAAACGCGCGAGGCAGCTGCGGTAAAGCTCATCAGCGTGGTCGTGAAGCGATTCACAGATG
TCTGCCTGTTCATCCGCGTCCAGCTCGTTGAGTTTCTCCAGAAGCGTTAATGTCTGGCTTCTGATAAAG
CGGGCCATGTTAAGGGCGGTTTTTTCCTGTTTGGTCACTGATGCCTCCGTGTAAGGGGGATTTCTGTTC
ATGGGGGTAATGATACCGATGAAACGAGAGAGGATGCTCACGATACGGGTTACTGATGATGAACATG
CCCGGTTACTGGAACGTTGTGAGGGTAAACAACTGGCGGTATGGATGCGGCGGGACCAGAGAAAAAT
CACTCAGGGTCAATGCCAGCGCTTCGTTAATACAGATGTAGGTGTTCCACAGGGTAGCCAGCAGCATC
CTGCGATGCAGATCCGGAACATAATGGTGCAGGGCGCTGACTTCCGCGTTTCCAGACTTTACGAAACA
CGGAAACCGAAGACCATTCATGTTGTTGCTCAGGTCGCAGACGTTTTGCAGCAGCAGTCGCTTCACGT
TCGCTCGCGTATCGGTGATTCATTCTGCTAACCAGTAAGGCAACCCCGCCAGCCTAGCCGGGTCCTCA
ACGACAGGAGCACGATCATGCGCACCCGTGGGGCCGCCATGCCGGCGATAATGGCCTGCTTCTCGCCG
AAACGTTTGGTGGCGGGACCAGTGACGAAGGCTTGAGCGAGGGCGTGCAAGATTCCGAATACCGCAA
GCGACAGGCCGATCATCGTCGCGCTCCAGCGAAAGCGGTCCTCGCCGAAAATGACCCAGAGCGCTGC
CGGCACCTGTCCTACGAGTTGCATGATAAAGAAGACAGTCATAAGTGCGGCGACGATAGTCATGCCCC
GCGCCCACCGGAAGGAGCTGACTGGGTTGAAGGCTCTCAAGGGCATCGGTCGAGATCCCGGTGCCTA
ATGAGTGAGCTAACTTACATTAATTGCGTTGCGCTCACTGCCCGCTTTCCAGTCGGGAAACCTGTCGTG
CCAGCTGCATTAATGAATCGGCCAACGCGCGGGGAGAGGCGGTTTGCGTATTGGGCGCCAGGGTGGTT
TTTCTTTTCACCAGTGAGACGGGCAACAGCTGATTGCCCTTCACCGCCTGGCCCTGAGAGAGTTGCAGC
AAGCGGTCCACGCTGGTTTGCCCCAGCAGGCGAAAATCCTGTTTGATGGTGGTTAACGGCGGGATATA
ACATGAGCTGTCTTCGGTATCGTCGTATCCCACTACCGAGATATCCGCACCAACGCGCAGCCCGGACT
CGGTAATGGCGCGCATTGCGCCCAGCGCCATCTGATCGTTGGCAACCAGCATCGCAGTGGGAACGATG
CCCTCATTCAGCATTTGCATGGTTTGTTGAAAACCGGACATGGCACTCCAGTCGCCTTCCCGTTCCGCT
ATCGGCTGAATTTGATTGCGAGTGAGATATTTATGCCAGCCAGCCAGACGCAGACGCCCGAGACAGAA
CTTAATGGGCCCGCTAACAGCGCGATTTGCTGGTGACCCAATGCGACCAGATGCTCCACGCCCAGTCG
CGTACCGTCTTCATGGGAGAAAATAATACTGTTGATGGGTGTCTGGTCAGAGACATCAAGAAATAACG
CCGGAACATTAGTGCAGGCAGCTTCCACAGCAATGGCATCCTGGTCATCCAGCGGATAGTTAATGATC
AGCCCACTGACGCGTTGCGCGAGAAGATTGTGCACCGCCGCTTTACAGGCTTCGACGCCGCTTCGTTCT
ACCATCGACACCACCACGCTGGCACCCAGTTGATCGGCGCGAGATTTAATCGCCGCGACAATTTGCGA
CGGCGCGTGCAGGGCCAGACTGGAGGTGGCAACGCCAATCAGCAACGACTGTTTGCCCGCCAGTTGTT
GTGCCACGCGGTTGGGAATGTAATTCAGCTCCGCCATCGCCGCTTCCACTTTTTCCCGCGTTTTCGCAG
AAACGTGGCTGGCCTGGTTCACCACGCGGGAAACGGTCTGATAAGAGACACCGGCATACTCTGCGAC
ATCGTATAACGTTACTGGTTTCACATTCACCACCCTGAATTGACTCTCTTCCGGGCGCTATCATGCCAT
ACCGCGAAAGGTTTTGCGCCATTCGATGGTGTCCGGGATCTCGACGCTCTCCCTTATGCGACTCCTGCA
TTAGGAAGCAGCCCAGTAGTAGGTTGAGGCCGTTGAGCACCGCCGCCGCAAGGAATGGTGCATGCAA
GGAGATGGCGCCCAACAGTCCCCCGGCCACGGGGCCTGCCACCATACCCACGCCGAAACAAGCGCTC
ATGAGCCCGAAGTGGCGAGCCCGATCTTCCCCATCGGTGATGTCGGCGATATAGGCGCCAGCAACCGC
ACCTGTGGCGCCGGTGATGCCGGCCACGATGCGTCCGGCGTAGAGGATCGAGATCTCGATCCCGCGAA
ATTAATACGACTCACTATAGGGGAATTGTGAGCGGATAACAATTCCCCTCTAGAAATAATTTTGTTTAA
CTTTAAGAAGGAGATATACATATGGCTCATCATCATCATCATCATGCTAGCATGGACTACAAAGACCA

TGACGGTGATTATAAAGATCATGACATCGATTACAAGGATGACGATGACAAGATGGCCCCCAAGAAG
AAGAGGAAGGTGGGCATTCACCGCGGGGTACCTATGGTGGACTTGAGGACACTCGGTTATTCGCAACA
GCAACAGGAGAAAATCAAGCCTAAGGTCAGGAGCACCGTCGCGCAACACCACGAGGCGCTTGTGGGG
CATGGCTTCACTCATGCGCATATTGTCGCGCTTTCACAGCACCCTGCGGCGCTTGGGACGGTGGCTGTC
AAATACCAAGATATGATTGCGGCCCTGCCCGAAGCCACGCACGAGGCAATTGTAGGGGTCGGTAAAC
AGTGGTCGGGAGCGCGAGCACTTGAGGCGCTGCTGACTGTGGCGGGTGAGCTTAGGGGGCCTCCGCTC
CAGCTCGACACCGGGCAGCTGCTGAAGATCGCGAAGAGAGGGGGAGTAACAGCGGTAGAGGCAGTGC
ACGCCTGGCGCAATGCGCTCACCGGGGCCCCCTTGAACCTGACCCCAGACCAGGTAGTCGCAATCGCG
TCACATGACGGGGGAAAGCAAGCCCTGGAAACCGTGCAAAGGTTGTTGCCGGTCCTTTGTCAAGACCA
CGGCCTTACACCGGAGCAAGTCGTGGCCATTGCAAGCAATGGGGGGTGGCAAACAGGCTCTTGAGACG
GTTCAGAGACTTCTCCCAGTTCTCTGTCAAGCCCACGGGCTGACTCCCGATCAAGTTGTAGCGATTGCG
TCCAACGGTGGAGGGAAACAAGCATTGGAGACTGTCCAACGGCTCCTTCCCGTGTTGTGTCAAGCCCA
CGGTTTGACGCCTGCACAAGTGGTCGCCATCGCCAGCCATGATGGCGGTAAGCAGGCGCTGGAAACA
GTACAGCGCCTGCTGCCTGTACTGTGCCAGGATCATGGACTGACCCCAGACCAGGTAGTCGCAATCGC
GTCAACATGACGGGGGAAAGCAAGCCCTGGAAACCGTGCAAAGGTTGTTGCCGGTCCTTTGTCAAGACC
ACGGCCTTACACCGGAGCAAGTCGTGGCCATTGCAAGCAACATCGGTGGCAAACAGGCTCTTGAGAC
GGTTCAGAGACTTCTCCCAGTTCTCTGTCAAGCCCACGGGCTGACTCCCGATCAAGTTGTAGCGATTGC
GAATAACAATGGAGGGAAACAAGCATTGGAGACTGTCCAACGGCTCCTTCCCGTGTTGTGTCAAGCCC
ACGGTTTGACGCCTGCACAAGTGGTCGCCATCGCCTCCAATATTGGCGGTAAGCAGGCGCTGGAAACA
GTACAGCGCCTGCTGCCTGTACTGTGCCAGGATCATGGACTGACCCCAGACCAGGTAGTCGCAATCGC
GTCGAACATTGGGGGAAAGCAAGCCCTGGAAACCGTGCAAAGGTTGTTGCCGGTCCTTTGTCAAGACC
ACGGCCTTACACCGGAGCAAGTCGTGGCCATTGCAAGCAATGGGGGTGGCAAACAGGCTCTTGAGAC
GGTTCAGAGACTTCTCCCAGTTCTCTGTCAAGCCCACGGGCTGACTCCCGATCAAGTTGTAGCGATTGC
GTCCAACGGTGGAGGGAAACAAGCATTGGAGACTGTCCAACGGCTCCTTCCCGTGTTGTGTCAAGCCC
ACGGTTTGACGCCTGCACAAGTGGTCGCCATCGCCAACAACAACGGCGGTAAGCAGGCGCTGGAAAC
AGTACAGCGCCTGCTGCCTGTACTGTGCCAGGATCATGGACTGACCCCAGACCAGGTAGTCGCAATCG
CGTCGAACATTGGGGGAAAGCAAGCCCTGGAAACCGTGCAAAGGTTGTTGCCGGTCCTTTGTCAAGAC
CACGGCCTTACACCGGAGCAAGTCGTGGCCATTGCAAGCAATGGGGGTGGCAAACAGGCTCTTGAGA
CGGTTCAGAGACTTCTCCCAGTTCTCTGTCAAGCCCACGGGCTGACTCCCGATCAAGTTGTAGCGATTG
CGTCGAACATTGGAGGGAAACAAGCATTGGAGACTGTCCAACGGCTCCTTCCCGTGTTGTGTCAAGCC
CACGGTTTGACGCCTGCACAAGTGGTCGCCATCGCCAGCCATGATGGCGGTAAGCAGGCGCTGGAAAC
AGTACAGCGCCTGCTGCCTGTACTGTGCCAGGATCATGGACTGACACCCGAACAGGTGGTCGCCATTG
CTTCTAATGGGGGAGGACGGCCAGCCTTGGAGTCCATCGTAGCCCAATTGTCCAGGCCCGATCCCGCG
TTGGCTGCGTTAACGAATGACCATCTGGTGGCGTTGGCATGTCTTGGTGGACGACCCGCGCTCGATGC
AGTCAAAAAGGGTCTGCCTCATGCTCCCGCATTGATCAAAAGAACCAACCGGCGGATTCCCGAGAGA
ACTTCCCATCGAGTCGCGGGATCCCAACTAGTCAAAAGTGAACTGGAGGAGAAGAAATCTGAACTTCG
TCATAAATTGAAATATGTGCCTCATGAATATATTGAATTAATTGAAATTGCCAGAAATCCCACTCAGG
ATAGAATTCTTGAAATGAAGGTAATGGAATTTTTTATGAAAGTTTATGGATATAGAGGTGAACATTTG
GGTGGATCAAGGAAACCGGACGGAGCAATTTATACTGTCGGATCTCCTATTGATTACGGTGTGATCGT
GGATACTAAAGCTTATAGCGGAGGTTATAATCTGCCAATTGGCCAAGCAGATGAAATGCAACGATATG
TCGAAGAAAATCAAACACGAAACAAACATATCAACCCTAATGAATGGTGGAAAGTCTATCCATCTTCT
GTAACGGAATTTAAGTTTTTATTTGTGAGTGGTCACTTTAAAGGAAACTACAAAGCTCAGCTTACACG
ATTAAATCATATCACTAATTGTAATGGAGCTGTTCTTAGTGTAGAAGAGCTTTTAATTGGTGGAGAAAT
GATTAAAGCCGGCACATTAACCTTAGAGGAAGTGAGACGGAAATTTAATAACGGCGAGATAAACTTTT
AAGGGCCCTTCGAAGGTAAGCCTATCCCTAACCCTCTCCTCGGTCTCGATTCTACGCGTACCGGTCTCG
AGTTAAGATCCGGCTGCTAACAAAGCCCGAAAGGAAGCTGAGTTGGCTGCTGCCACCGCTGAGCAAT
AACTAGCATAACCCCTTGGGGCCTCTAAACGGGTCTTGAGGGGTTTTTTGCTGAAAGGAGGAACTATA
TCCGGAT

pXTNsk-CCR5R (8055 bp)

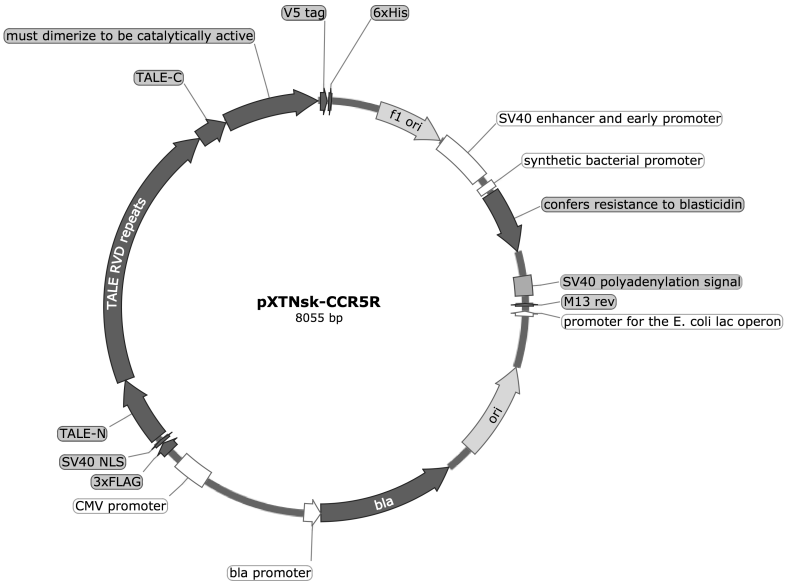

GGGCCCTTCGAAGGTAAGCCTATCCCTAACCCTCTCCTCGGTCTCGATTCTACGCGTACCGGTCATCAT
CACCATCACCATTGAGTTTAAACCCGCTGATCAGCCTCGACTGTGCCTTCTAGTTGCCAGCCATCTGTT
GTTTGCCCCTCCCCCGTGCCTTCCTTGACCCTGGAAGGTGCCACTCCCACTGTCCTTTCCTAATAAAAT
GAGGAAATTGCATCGCATTGTCTGAGTAGGTGTCATTCTATTCTGGGGGGTGGGGTGGGGCAGGACAG
CAAGGGGGAGGATTGGGAAGACAATAGCAGGCATGCTGGGGATGCGGTGGGCTCTATGGCTTCTGAG
GCGGAAAGAACCAGCTGGGGCTCTAGGGGGTATCCCCACGCGCCCTGTAGCGGCGCATTAAGCGCGG
CGGGTGTGGTGGTTACGCGCAGCGTGACCGCTACACTTGCCAGCGCCCTAGCGCCCGCTCCTTTCGCTT
TCTTCCCTTCCTTTCTCGCCACGTTCGCCGGCTTTCCCCGTCAAGCTCTAAATCGGGGCATCCCTTTAGG
GTTCCGATTTAGTGCTTTACGGCACCTCGACCCCAAAAAACTTGATTAGGGTGATGGTTCACGTAGTGG
GCCATCGCCCTGATAGACGGTTTTTCGCCCTTTGACGTTGGAGTCCACGTTCTTTAATAGTGGACTCTT
GTTCCAAACTGGAACAACACTCAACCCTATCTCGGTCTATTCTTTTGATTTATAAGGGATTTTGGGGAT
TTCGGCCTATTGGTTAAAAAATGAGCTGATTTAACAAAAATTTAACGCGAATTAATTCTGTGGAATGT
GTGTCAGTTAGGGTGTGGAAAGTCCCCAGGCTCCCCAGGCAGGCAGAAGTATGCAAAGCATGCATCTC
AATTAGTCAGCAACCAGGTGTGGAAAGTCCCCAGGCTCCCCAGCAGGCAGAAGTATGCAAAGCATGC
ATCTCAATTAGTCAGCAACCATAGTCCCGCCCCTAACTCCGCCCATCCCGCCCCTAACTCCGCCCAGTT
CCGCCCATTCTCCGCCCCATGGCTGACTAATTTTTTTTATTTATGCAGAGGCCGAGGCCGCCTCTGCCT
CTGAGCTATTCCAGAAGTAGTGAGGAGGCTTTTTTGGAGGCCTAGGCTTTTGCAAAAAGCTCCCGGGA
GCTTGTATATCCATTTTCGGATCTGATCAGCACGTGTTGACAATTAATCATCGGCATAGTATATCGGCA
TAGTATAATACGACAAGGTGAGGAACTAAACCATGGCCAAGCCTTTGTCTCAAGAAGAATCCACCCTC
ATTGAAAGAGCAACGGCTACAATCAACAGCATCCCCATCTCTGAAGACTACAGCGTCGCCAGCGCAGC
TCTCTCTAGCGACGGCCGCATCTTCACTGGTGTCAATGTATATCATTTTACTGGGGGACCTTGTGCAGA
ACTCGTGGTGCTGGGCACTGCTGCTGCTGCGGCAGCTGGCAACCTGACTTGTATCGTCGCGATCGGAA
ATGAGAACAGGGGCATCTTGAGCCCCTGCGGACGGTGTCGACAGGTGCTTCTCGATCTGCATCCTGGG
ATCAAAGCGATAGTGAAGGACAGTGATGGACAGCCGACGGCAGTTGGGATTCGTGAATTGCTGCCCTC
TGGTTATGTGTGGGAGGGCTAAGCACTTCGTGGCCGAGGAGCAGGACTGACACGTGCTACGAGATTTC
GATTCCACCGCCGCCTTCTATGAAAGGTTGGGCTTCGGAATCGTTTTCCGGGACGCCGGCTGGATGATC
CTCCAGCGCGGGGATCTCATGCTGGAGTTCTTCGCCCACCCCAACTTGTTTATTGCAGCTTATAATGGT
TACAAATAAAGCAATAGCATCACAAATTTCACAAATAAAGCATTTTTTTCACTGCATTCTAGTTGTGGT
TTGTCCAAACTCATCAATGTATCTTATCATGTCTGTATACCGTCGACCTCTAGCTAGAGCTTGGCGTAA
TCATGGTCATAGCTGTTTCCTGTGTGAAATTGTTATCCGCTCACAATTCCACACAACATACGAGCCGGA
AGCATAAAGTGTAAAGCCTGGGGTGCCTAATGAGTGAGCTAACTCACATTAATTGCGTTGCGCTCACT
GCCCGCTTTCCAGTCGGGAAACCTGTCGTGCCAGCTGCATTAATGAATCGGCCAACGCGCGGGGAGAG
GCGGTTTGCGTATTGGGCGCTCTTCCGCTTCCTCGCTCACTGACTCGCTGCGCTCGGTCGTTCGGCTGC
GGCGAGCGGTATCAGCTCACTCAAAGGCGGTAATACGGTTATCCACAGAATCAGGGGATAACGCAGG
AAAGAACATGTGAGCAAAAGGCCAGCAAAAGGCCAGGAACCGTAAAAAGGCCGCGTTGCTGGCGTTT

TTCCATAGGCTCCGCCCCCCTGACGAGCATCACAAAAATCGACGCTCAAGTCAGAGGTGGCGAAACCC
GACAGGACTATAAAGATACCAGGCGTTTCCCCCTGGAAGCTCCCTCGTGCGCTCTCCTGTTCCGACCCT
GCCGCTTACCGGATACCTGTCCGCCTTTCTCCCTTCGGGAAGCGTGGCGCTTTCTCAATGCTCACGCTG
TAGGTATCTCAGTTCGGTGTAGGTCGTTCGCTCCAAGCTGGGCTGTGTGCACGAACCCCCCGTTCAGCC
CGACCGCTGCGCCTTATCCGGTAACTATCGTCTTGAGTCCAACCCGGTAAGACACGACTTATCGCCACT
GGCAGCAGCCACTGGTAACAGGATTAGCAGAGCGAGGTATGTAGGCGGTGCTACAGAGTTCTTGAAG
TGGTGGCCTAACTACGGCTACACTAGAAGGACAGTATTTGGTATCTGCGCTCTGCTGAAGCCAGTTAC
CTTCGGAAAAAGAGTTGGTAGCTCTTGATCCGGCAAACAAACCACCGCTGGTAGCGGTGGTTTTTTTG
TTTGCAAGCAGCAGATTACGCGCAGAAAAAAAGGATCTCAAGAAGATCCTTTGATCTTTTCTACGGGG
TCTGACGCTCAGTGGAACGAAAACTCACGTTAAGGGATTTTGGTCATGAGATTATCAAAAAGGATCTT
CACCTAGATCCTTTTAAATTAAAAATGAAGTTTTAAATCAATCTAAAGTATATATGAGTAAACTTGGTC
TGACAGTTACCAATGCTTAATCAGTGAGGCACCTATCTCAGCGATCTGTCTATTTCGTTCATCCATAGT
TGCCTGACTCCCCGTCGTGTAGATAACTACGATACGGGAGGGCTTACCATCTGGCCCCAGTGCTGCAA
TGATACCGCGAGACCCACGCTCACCGGCTCCAGATTTATCAGCAATAAACCAGCCAGCCGGAAGGGCC
GAGCGCAGAAGTGGTCCTGCAACTTTATCCGCCTCCATCCAGTCTATTAATTGTTGCCGGGAAGCTAG
AGTAAGTAGTTCGCCAGTTAATAGTTTGCGCAACGTTGTTGCCATTGCTACAGGCATCGTGGTGTCACG
CTCGTCGTTTGGTATGGCTTCATTCAGCTCCGGTTCCCAACGATCAAGGCGAGTTACATGATCCCCCAT
GTTGTGCAAAAAAGCGGTTAGCTCCTTCGGTCCTCCGATCGTTGTCAGAAGTAAGTTGGCCGCAGTGTT
ATCACTCATGGTTATGGCAGCACTGCATAATTCTCTTACTGTCATGCCATCCGTAAGATGCTTTTCTGT
GACTGGTGAGTACTCAACCAAGTCATTCTGAGAATAGTGTATGCGGCGACCGAGTTGCTCTTGCCCGG
CGTCAATACGGGATAATACCGCGCCACATAGCAGAACTTTAAAAGTGCTCATCATTGGAAAACGTTCT
TCGGGGCGAAAACTCTCAAGGATCTTACCGCTGTTGAGATCCAGTTCGATGTAACCCACTCGTGCACC
CAACTGATCTTCAGCATCTTTTACTTTCACCAGCGTTTCTGGGTGAGCAAAAACAGGAAGGCAAAATG
CCGCAAAAAAGGGAATAAGGGCGACACGGAAATGTTGAATACTCATACTCTTCCTTTTTCAATATTAT
TGAAGCATTTATCAGGGTTATTGTCTCATGAGCGGATACATATTTGAATGTATTTAGAAAAATAAACA
AATAGGGGTTCCGCGCACATTTCCCCGAAAAGTGCCACCTGACGTCGACGGATCGGGAGATCTCCCGA
TCCCCTATGGTCGACTCTCAGTACAATCTGCTCTGATGCCGCATAGTTAAGCCAGTATCTGCTCCCTGC
TTGTGTGTTGGAGGTCGCTGAGTAGTGCGCGAGCAAAATTTAAGCTACAACAAGGCAAGGCTTGACCG
ACAATTGCATGAAGAATCTGCTTAGGGTTAGGCGTTTTGCGCTGCTTCGCGATGTACGGGCCAGATAT
ACGCGTTGACATTGATTATTGACTAGTTATTAATAGTAATCAATTACGGGGTCATTAGTTCATAGCCCA
TATATGGAGTTCCGCGTTACATAACTTACGGTAAATGGCCCGCCTGGCTGACCGCCCAACGACCCCCG
CCCATTGACGTCAATAATGACGTATGTTCCCATAGTAACGCCAATAGGGACTTTCCATTGACGTCAATG
GGTGGACTATTTACGGTAAACTGCCCACTTGGCAGTACATCAAGTGTATCATATGCCAAGTACGCCCC
CTATTGACGTCAATGACGGTAAATGGCCCGCCTGGCATTATGCCCAGTACATGACCTTATGGGACTTTC
CTACTTGGCAGTACATCTACGTATTAGTCATCGCTATTACCATGGTGATGCGGTTTTGGCAGTACATCA
ATGGGCGTGGATAGCGGTTTGACTCACGGGGATTTCCAAGTCTCCACCCCATTGACGTCAATGGGAGT
TTGTTTTGGCACCAAAATCAACGGGACTTTCCAAAATGTCGTAACAACTCCGCCCCATTGACGCAAAT
GGGCGGTAGGCGTGTACGGTGGGAGGTCTATATAAGCAGAGCTCTCTGGCTAACTAGAGAACCCACTG
CTTACTGGCTTATCGAAATTAATACGACTCACTATAGGGAGACCCAAGCTGGCTAGCATGGACTACAA
AGACCATGACGGTGATTATAAAGATCATGACATCGATTACAAGGATGACGATGACAAGATGGCCCCC
AAGAAGAAGAGGAAGGTGGGCATTCACCGCGGGGTACCTATGGTGGACTTGAGGACACTCGGTTATT
CGCAACAGCAACAGGAGAAAATCAAGCCTAAGGTCAGGAGCACCGTCGCGCAACACCACGAGGCGCT
TGTGGGGCATGGCTTCACTCATGCGCATATTGTCGCGCTTTCACAGCACCCTGCGGCGCTTGGGACGGT
GGCTGTCAAATACCAAGATATGATTGCGGCCCTGCCCGAAGCCACGCACGAGGCAATTGTAGGGGTCG
GTAAACAGTGGTCGGGAGCGCGAGCACTTGAGGCGCTGCTGACTGTGGCGGGTGAGCTTAGGGGGCC
TCCGCTCCAGCTCGACACCGGGCAGCTGCTGAAGATCGCGAAGAGAGGGGGAGTAACAGCGGTAGAG
GCAGTGCACGCCTGGCGCAATGCGCTCACCGGGGCCCCCTTGAACCTGACCCCAGACCAGGTAGTCGC
AATCGCGTCACATGACGGGGGAAAGCAAGCCCTGGAAACCGTGCAAAGGTTGTTGCCGGTCCTTTGTC
AAGACCACGGCCTTACACCGGAGCAAGTCGTGGCCATTGCAAGCAATGGGGGTGGCAAACAGGCTCT
TGAGACGGTTCAGAGACTTCTCCCAGTTCTCTGTCAAGCCCACGGGCTGACTCCCGATCAAGTTGTAGC
GATTGCGTCCAACGGTGGAGGGAAACAAGCATTGGAGACTGTCCAACGGCTCCTTCCCGTGTTGTGTC
AAGCCCACGGTTTGACGCCTGCACAAGTGGTCGCCATCGCCAGCCATGATGGCGGTAAGCAGGCGCTG
GAAACAGTACAGCGCCTGCTGCCTGTACTGTGCCAGGATCATGGACTGACCCCAGACCAGGTAGTCGC
AATCGCGTCACATGACGGGGGAAAGCAAGCCCTGGAAACCGTGCAAAGGTTGTTGCCGGTCCTTTGTC
AAGACCACGGCCTTACACCGGAGCAAGTCGTGGCCATTGCAAGCAACATCGGTGGCAAACAGGCTCTT
GAGACGGTTCAGAGACTTCTCCCAGTTCTCTGTCAAGCCCACGGGCTGACTCCCGATCAAGTTGTAGC

GATTGCGAATAACAATGGAGGGAAACAAGCATTGGAGACTGTCCAACGGCTCCTTCCCGTGTTGTGTC
AAGCCCACGGTTTGACGCCTGCACAAGTGGTCGCCATCGCCTCCAATATTGGCGGTAAGCAGGCGCTG
GAAACAGTACAGCGCCTGCTGCCTGTACTGTGCCAGGATCATGGACTGACCCCAGACCAGGTAGTCGC
AATCGCGTCGAACATTGGGGGAAAGCAAGCCCTGGAAACCGTGCAAAGGTTGTTGCCGGTCCTTTGTC
AAGACCACGGCCTTACACCGGAGCAAGTCGTGGCCATTGCAAGCAATGGGGGTGGCAAACAGGCTCT
TGAGACGGTTCAGAGACTTCTCCCAGTTCTCTGTCAAGCCCACGGGCTGACTCCCGATCAAGTTGTAGC
GATTGCGTCCAACGGTGGAGGGAAACAAGCATTGGAGACTGTCCAACGGCTCCTTCCCGTGTTGTGTC
AAGCCCACGGTTTGACGCCTGCACAAGTGGTCGCCATCGCCAACAACAACGGCGGTAAGCAGGCGCT
GGAAACAGTACAGCGCCTGCTGCCTGTACTGTGCCAGGATCATGGACTGACCCCAGACCAGGTAGTCG
CAATCGCGTCGAACATTGGGGGAAAGCAAGCCCTGGAAACCGTGCAAAGGTTGTTGCCGGTCCTTTGT
CAAGACCACGGCCTTACACCGGAGCAAGTCGTGGCCATTGCAAGCAATGGGGGTGGCAAACAGGCTC
TTGAGACGGTTCAGAGACTTCTCCCAGTTCTCTGTCAAGCCCACGGGCTGACTCCCGATCAAGTTGTAG
CGATTGCGTCGAACATTGGAGGGAAACAAGCATTGGAGACTGTCCAACGGCTCCTTCCCGTGTTGTGT
CAAGCCCACGGTTTGACGCCTGCACAAGTGGTCGCCATCGCCAGCCATGATGGCGGTAAGCAGGCGCT
GGAAACAGTACAGCGCCTGCTGCCTGTACTGTGCCAGGATCATGGACTGACACCCGAACAGGTGGTCG
CCATTGCTTCTAATGGGGGAGGACGGCCAGCCTTGGAGTCCATCGTAGCCCAATTGTCCAGGCCCGAT
CCCGCGTTGGCTGCGTTAACGAATGACCATCTGGTGGCGTTGGCATGTCTTGGTGGACGACCCGCGCT
CGATGCAGTCAAAAAGGGTCTGCCTCATGCTCCCGCATTGATCAAAAGAACCAACCGGCGGATTCCCG
AGAGAACTTCCCATCGAGTCGCGGGATCCCAACTAGTCAAAAGTGAACTGGAGGAGAAGAAATCTGA
ACTTCGTCATAAATTGAAATATGTGCCTCATGAATATATTGAATTAATTGAAATTGCCAGAAATCCCAC
TCAGGATAGAATTCTTGAAATGAAGGTAATGGAATTTTTTATGAAAGTTTATGGATATAGAGGTGAAC
ATTTGGGTGGATCAAGGAAACCGGACGGAGCAATTTATACTGTCGGATCTCCTATTGATTACGGTGTG
ATCGTGGATACTAAAGCTTATAGCGGAGGTTATAATCTGCCAATTGGCCAAGCAGATGAAATGCAACG
ATATGTCGAAGAAAATCAAACACGAAACAAACATATCAACCCTAATGAATGGTGGAAAGTCTATCCA
TCTTCTGTAACGGAATTTAAGTTTTTATTTGTGAGTGGTCACTTTAAAGGAAACTACAAAGCTCAGCTT
ACACGATTAAATCATATCACTAATTGTAATGGAGCTGTTCTTAGTGTAGAAGAGCTTTTAATTGGTGGA
GAAATGATTAAAGCCGGCACATTAACCTTAGAGGAAGTGAGACGGAAATTTAATAACGGCGAGATAA
ACTTTTAA

pTAR TALEN-L (7864 bp)

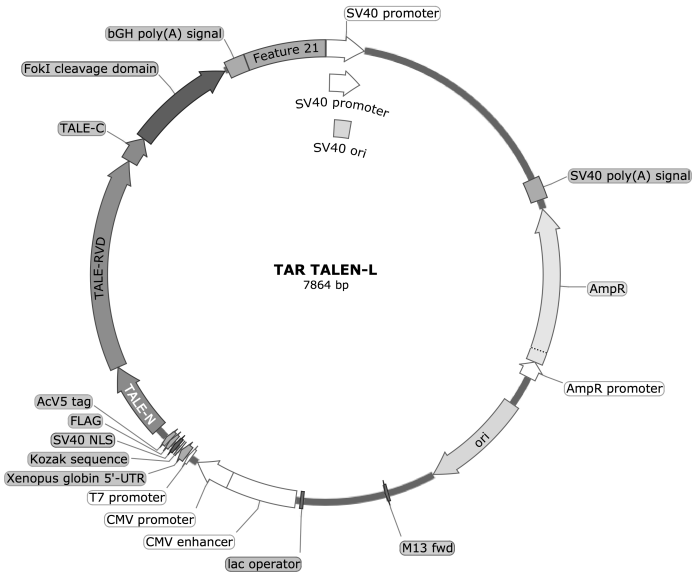

CTCCAGCAGGCAGAAGTATGCAAAGCATGCATCTCAATTAGTCAGCAACCATAGTCCCGCCCCTAACT
CCGCCCATCCCGCCCCTAACTCCGCCCAGTTCCGCCCATTCTCCGCCCCATGGCTGACTAATTTTTTTTA
TTTATGCAGAGGCCGAGGCCGCCTCTGCCTCTGAGCTATTCCAGAAGTAGTGAGGAGGCTTTTTTGGA

GGCCTAGGCTTTTGCAAAAAGCTCCCGGGAGCTTGTATATCCATTTTCGGATCTGATCAGCACGTGATG
AAAAAGCCTGAACTCACCGCGACGTCTGTCGAGAAGTTTCTGATCGAAAAGTTCGACAGCGTCCGACC
TGATGCAGCTCTCGGAGGGCGAAGAATCTCGTGCTTTCAGCTTCGATGTAGGAGGGCGTGGATATGTC
CTGCGGGTAAATAGCTGCGCCGATGGTTTCTACAAAGATCGTTATGTTTATCGGCACTTTGCATCGGCC
GCGCTCCCGATTCCGGAAGTGCTTGACATTGGGGAATTCAGCGAGAGCCTGACCTATTGCATCTCCCG
CCGTGCACAGGGTGTCACGTTGCAAGACCTGCCTGAAACCGAACTGCCCGCTGTTCTGCAGCCGGTCG
CGGAGGCCATGGATGCGATCGCTGCGGCCGATCTTAGCCAGACGAGCGGGTTCGGCCCATTCGGACCG
CAAGGAATCGGTCAATACACTACATGGCGTGATTTCATATGCGCGATTGCTGATCCCCATGTGTATCAC
TGGCAAACTGTGATGGACGACACCGTCAGTGCGTCCGTCGCGCAGGCTCTCGATGAGCTGATGCTTTG
GGCCGAGGACTGCCCCGAAGTCCGGCACCTCGTGCACGCGGATTTCGGCTCCAACAATGTCCTGACGG
ACAATGGCCGCATAACAGCGGTCATTGACTGGAGCGAGGCGATGTTCGGGGATTCCCAATACGAGGTC
GCCAACATCTTCTTCTGGAGGCCGTGGTTGGCTTGTATGGAGCAGCAGACGCGCTACTTCGAGCGGAG
GCATCCGGAGCTTGCAGGATCGCCGCGGCTCCGGGCGTATATGCTCCGCATTGGTCTTGACCAACTCT
ATCAGAGCTTGGTTGACGGCAATTTCGATGATGCAGCTTGGGCGCAGGGTCGATGCGACGCAATCGTC
CGATCCGGAGCCGGGACTGTCGGGCGTACACAAATCGCCCGCAGAAGCGCGGCCGTCTGGACCGATG
GCTGTGTAGAAGTACTCGCCGATAGTGGAAACCGACGCCCCAGCACTCGTCCGAGGGCAAAGGAATA
GCACGTGCTACGAGATTTCGATTCCACCGCCGCCTTCTATGAAAGGTTGGGCTTCGGAATCGTTTTCCG
GGACGCCGGCTGGATGATCCTCCAGCGCGGGGATCTCATGCTGGAGTTCTTCGCCCACCCCAACTTGTT
TATTGCAGCTTATAATGGTTACAAATAAAGCAATAGCATCACAAATTTCACAAATAAAGCATTTTTTTC
ACTGCATTCTAGTTGTGGTTTGTCCAAACTCATCAATGTATCTTATCATGTCTGTATACCGTCGACCTCT
AGCTAGAGCTTGGCGTAATCATGGTCATTACCAATGCTTAATCAGTGAGGCACCTATCTCAGCGATCT
GTCTATTTCGTTCATCCATAGTTGCCTGACTCCCCGTCGTGTAGATAACTACGATACGGGAGGGCTTAC
CATCTGGCCCCAGCGCTGCGATGATACCGCGAGAACCACGCTCACCGGCTCCGGATTTATCAGCAATA
AACCAGCCAGCCGGAAGGGCCGAGCGCAGAAGTGGTCCTGCAACTTTATCCGCCTCCATCCAGTCTAT
TAATTGTTGCCGGGAAGCTAGAGTAAGTAGTTCGCCAGTTAATAGTTTGCGCAACGTTGTTGCCATCGC
TACAGGCATCGTGGTGTCACGCTCGTCGTTTGGTATGGCTTCATTCAGCTCCGGTTCCCAACGATCAAG
GCGAGTTACATGATCCCCCATGTTGTGCAAAAAAGCGGTTAGCTCCTTCGGTCCTCCGATCGTTGTCAG
AAGTAAGTTGGCCGCAGTGTTATCACTCATGGTTATGGCAGCACTGCATAATTCTCTTACTGTCATGCC
ATCCGTAAGATGCTTTTCTGTGACTGGTGAGTACTCAACCAAGTCATTCTGAGAATAGTGTATGCGGCG
ACCGAGTTGCTCTTGCCCGGCGTCAATACGGGATAATACCGCGCCACATAGCAGAACTTTAAAAGTGC
TCATCATTGGAAAACGTTCTTCGGGGCGAAAACTCTCAAGGATCTTACCGCTGTTGAGATCCAGTTCG
ATGTAACCCACTCGTGCACCCAACTGATCTTCAGCATCTTTTACTTTCACCAGCGTTTCTGGGTGAGCA
AAAACAGGAAGGCAAAATGCCGCAAAAAAGGGAATAAGGGCGACACGGAAATGTTGAATACTCATA
TTCTTCCTTTTTCAATATTATTGAAGCATTTATCAGGGTTATTGTCTCATGAGCGGATACATATTTGAAT
GTATTTAGAAAAATAAACAAATAGGGGTCAGTGTTACAACCAATTAACCAATTCTGAACATTATCGCG
AGCCCATTTATACCTGAATATGGCTCATAACACCCCTTGCTCATGACCAAAATCCCTTAACGTGAGTTA
CGCGCGCGTCGTTCCACTGAGCGTCAGACCCCGTAGAAAAGATCAAAGGATCTTCTTGAGATCCTTTTT
TTCTGCGCGTAATCTGCTGCTTGCAAACAAAAAAACCACCGCTACCAGCGGTGGTTTGTTTGCCGGATC
AAGAGCTACCAACTCTTTTTCCGAAGGTAACTGGCTTCAGCAGAGCGCAGATACCAAATACTGTTCTT
CTAGTGTAGCCGTAGTTAGCCCACCACTTCAAGAACTCTGTAGCACCGCCTACATACCTCGCTCTGCTA
ATCCTGTTACCAGTGGCTGCTGCCAGTGGCGATAAGTCGTGTCTTACCGGGTTGGACTCAAGACGATA
GTTACCGGATAAGGCGCAGCGGTCGGGCTGAACGGGGGGTTCGTGCACACAGCCCAGCTTGGAGCGA
ACGACCTACACCGAACTGAGATACCTACAGCGTGAGCTATGAGAAAGCGCCACGCTTCCCGAAGGGA
GAAAGGCGGACAGGTATCCGGTAAGCGGCAGGGTCGGAACAGGAGAGCGCACGAGGGAGCTTCCAG
GGGGAAACGCCTGGTATCTTTATAGTCCTGTCGGGTTTCGCCACCTCTGACTTGAGCGTCGATTTTTGT
GATGCTCGTCAGGGGGGCGGAGCCTATGGAAAAACGCCAGCAACGCGGCCTTTTTACGGTTCCTGGCC
TTTTGCTGGCCTTTTGCTCACATGTTCTTTCCTGCGTTATCCCCTGATTCTGTGGATAACCGTATTACCG
CCTTTGAGTGAGCTGATACCGCTCGCCGCAGCCGAACGACCGAGCGCAGCGAGTCAGTGAGCGAGGA
AGCGGAAGGCGAGAGTAGGGAACTGCCAGGCATCAAACTAAGCAGAAGGCCCCTGACGGATGGCCTT
TTTGCGTTTCTACAAACTCTTTCTGTGTTGTAAAACGACGGCCAGTCTTAAGCTCGGGCCCCCTGGGCG
GTTCTGATAACGAGTAATCGTTAATCCGCAAATAACGTAAAAACCCGCTTCGGCGGGTTTTTTTATGGG
GGGAGTTTAGGGAAAGAGCATTTGTCAGAATATTTAAGGGCGCCTGTCACTTTGCTTGATATATGAGA
ATTATTTAACCTTATAAATGAGAAAAAAGCAACGCACTTTAAATAAGATACGTTGCTTTTTCGATTGAT
GAACACCTATAATTAAACTATTCATCTATTATTTATGATTTTTTGTATATACAATATTTCTAGTTTGTTA
AAGAGAATTAAGAAAATAAATCTCGAAAATAATAAAGGGAAAATCAGTTTTTGATATCAAAATTATA
CATGTCAACGATAATACAAAATATAATACAAACTATAAGATGTTATCAGTATTTATTATCATTTAGAAT

AAATTTTGTGTCGCCCTTAATTGTGAGCGGATAACAATTACGAGCTTCATGCACAGTGGCGTTGACATT
GATTATTGACTAGTTATTAATAGTAATCAATTACGGGGTCATTAGTTCATAGCCCATATATGGAGTTCC
GCGTTACATAACTTACGGTAAATGGCCCGCCTGGCTGACCGCCCAACGACCCCCGCCCATTGACGTCA
ATAATGACGTATGTTCCCATAGTAACGCCAATAGGGACTTTCCATTGACGTCAATGGGTGGAGTATTT
ACGGTAAACTGCCCACTTGGCAGTACATCAAGTGTATCATATGCCAAGTACGCCCCCTATTGACGTCA
ATGACGGTAAATGGCCCGCCTGGCATTATGCCCAGTACATGACCTTATGGGACTTTCCTACTTGGCAGT
ACATCTACGTATTAGTCATCGCTATTACCATGGTGATGCGGTTTTGGCAGTACATCAATGGGCGTGGAT
AGCGGTTTGACTCACGGGGATTTCCAAGTCTCCACCCCATTGACGTCAATGGGAGTTTGTTTTGGCACC
AAAATCAACGGGACTTTCCAAAATGTCGTAACAACTCCGCCCCATTGACGCAAATGGGCGGTAGGCGT
GTACGGTGGGAGGTCTATATAAGCAGAGCTCTCTGGCTAACTAGAGAACCCACTGCTTACTGGCTTAT
CGAAATTAATACGACTCACTATAGGGAAGCTTCTTGTTCTTTTTGCAGAAGCTCAGAATAAACGCTCA
ACTTTGGCCTCGAGGCCACCATGGCTTCCTCCCCTCCAAAGAAAAAGAGAAAGGTTGCGGCCGCTGAC
TACAAGGATGACGACGATAAAAGTTGGAAGGACGCAAGTGGTTGGTCTAGAATGCATGCGGCCCCGC
GACGGCGTGCTGCGCAACCCTCCGACGCTTCGCCGGCCGCGCAGGTGGATCTACGCACGCTCGGCTAC
AGTCAGCAGCAGCAAGAGAAGATCAAACCGAAGGTGCGTTCGACAGTGGCGCAGCACCACGAGGCAC
TGGTGGGCCATGGGTTTACACACGCGCACATCGTTGCGCTCAGCCAACACCCGGCAGCGTTAGGGACC
GTCGCTGTCACGTATCAGCACATAATCACGGCGTTGCCAGAGGCGACACACGAAGACATCGTTGGCGT
CGGCAAACAGTGGTCCGGCGCACGCGCCCTGGAGGCCTTGCTCACGGATGCGGGGGAGTTGAGAGGT
CCGCCGTTACAGTTGGACACAGGCCAACTTGTGAAGATTGCAAAACGTGGCGGCGTGACCGCAATGG
AGGCAGTGCATGCATCGCGCAATGCGCTCACGGGAGCACCCCTCAACCTGACCCCGGACCAGGTGGTT
GCAATCGCGTCACACGATGGGGGAAAGCAGGCCCTAGAAACCGTTCAGCGACTCCTGCCCGTCCTGTG
CCAGGACCACGGCCTGACCCCCGAACAGGTTGTCGCTATTGCTAGTAACGGCGGAGGCAAACAGGCG
CTGGAAACAGTTCAGCGCCTCTTGCCGGTCTTGTGTCAGGCCCACGGCCTGACCCCGGACCAGGTGGT
TGCAATCGCGTCACACGATGGGGGAAAGCAGGCCCTAGAAACCGTTCAGCGACTCCTGCCCGTCCTGT
GCCAGGCCCACGGCCTGACCCCCGCCCAGGTTGTCGCTATTGCTAGTAACGGCGGAGGCAAACAGGCG
CTGGAAACAGTTCAGCGCCTCTTGCCGGTCTTGTGTCAGGACCACGGCCTGACCCCAGACCAAGTTGT
CGCGATTGCAAGCAACAACGGAGGCAAACAAGCCTTAGAAACAGTCCAGAGATTGTTGCCGGTGCTG
TGCCAAGACCACGGCCTGACCCCAGAACAAGTTGTCGCGATTGCAAGCAACAACGGAGGCAAACAAG
CCTTAGAAACAGTCCAGAGATTGTTGCCGGTGCTGTGCCAAGCCCACGGCCTGACCCCAGACCAGGTT
GTGGCCATCGCCAGCAACATAGGTGGCAAGCAGGCCCTCGAAACCGTCCAGAGACTGTTACCGGTTCT
CTGCCAGGCCCACGGCCTGACCCCGGCCCAGGTGGTTGCAATCGCGTCACACGATGGGGGAAAGCAG
GCCCTAGAAACCGTTCAGCGACTCCTGCCCGTCCTGTGCCAGGACCACGGCCTGACCCCGGACCAGGT
GGTTGCAATCGCGTCACACGATGGGGGAAAGCAGGCCCTAGAAACCGTTCAGCGACTCCTGCCCGTCC
TGTGCCAGGACCACGGCCTGACCCCAGAACAGGTTGTGGCCATCGCCAGCAACATAGGTGGCAAGCA
GGCCCTCGAAACCGTCCAGAGACTGTTACCGGTTCTCTGCCAGGCCCACGGCCTGACCCCAGACCAAG
TTGTCGCGATTGCAAGCAACAACGGAGGCAAACAAGCCTTAGAAACAGTCCAGAGATTGTTGCCTGTG
CTGTGCCAAGCCCACGGCCTGACCCCTGAGCAGGTAGTGGCTATTGCATCCAACATAGGGGGCAGACC
CGCACTGGAGTCAATCGTGGCCCAGCTTTCGAGGCCGGACCCCGCGCTGGCCGCACTCACTAATGATC
ATCTTGTAGCGCTGGCCTGCCTCGGCGGACGTCCTGCCATGGATGCAGTGAAAAAGGGATTGCCGCAC
GCGCCGGAATTGATCAGATCCCAGCTAGTGAAATCTGAATTGGAAGAGAAGAAATCTGAACTTAGAC
ATAAATTGAAATATGTGCCACATGAATATATTGAATTGATTGAAATCGCAAGAAATTCAACTCAGGAT
AGAATCCTTGAAATGAAGGTGATGGAGTTCTTTATGAAGGTTTATGGTTATCGTGGTAAACATTTGGGT
GGATCAAGGAAACCAGACGGAGCAATTTATACTGTCGGATCTCCTATTGATTACGGTGTGATCGTTGA
TACTAAGGCATATTCAGGAGGTTATAATCTTCCAATTGGTCAAGCAGATGAAATGCAAAGATATGTCG
AAGAGAATCAAACAAGAAACAAGCATATCAACCCTAATGAATGGTGGAAAGTCTATCCATCTTCAGT
AACAGAATTTAAGTTCTTGTTTGTGAGTGGTCATTTCAAAGGAAACTACAAAGCTCAGCTTACAAGAT
TGAATCATATCACTAATTGTAATGGAGCTGTTCTTAGTGTAGAAGAGCTTTTGATTGGTGGAGAAATG
ATTAAAGCTGGTACATTGACACTTGAGGAAGTGAGAAGGAAATTTAATAACGGCGAGATAAACTTTTA
AAAAATCAGCCTCGACTGTGCCTTCTAGTTGCCAGCCATCTGTTGTTTGCCCCTCCCCCGTGCCTTCCTT
GACCCTGGAAGGTGCCACTCCCACTGTCCTTTCCTAATAAAATGAGGAAATTGCATCACAACACTCAA
CCCTATCTCGGTCTATTCTTTTGATTTATAAGGGATTTTGCCGATTTCGGCCTATTGGTTAAAAAATGAG
CTGATTTAACAAAAATTTAACGCGAATTAATTCTGTGGAATGTGTGTCAGTTAGGGTGTGGAAAGTCC
CCAGGCTCCCCAGCAGGCAGAAGTATGCAAAGCATGCATCTCAATTAGTCAGCAACCAGGTGTGGAA
AGTCCCCAGGCTCCCCAGCAGGCAGAAGTATGCAAAGCATGCATCTCAATTAGTCAGCAACCATAGTC
CCGCCCCTAACTCCGCCCATCCCGCCCCTAACTCCGCCCAGTTCCGCCCATTCTCCGCCCCATGGCTGA
CTAATTTTTTTTATTTATGCAGAGGCCGAGGCCGCCTCTGCCTCTGAGCTATTCCAGAAGTAGTGAGG

AGGCTTTTTGGAGCCTAGCTCAGA

pTAR TALEN-R (8073 bp)

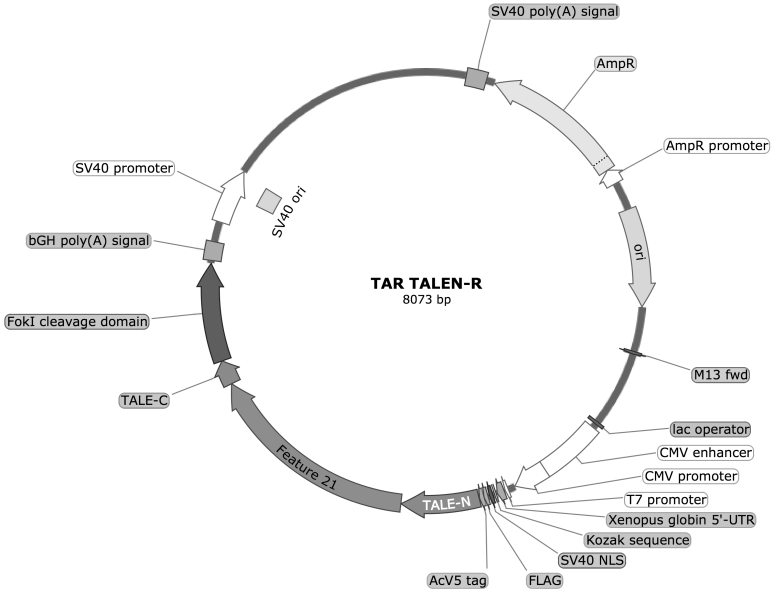

GGGGTCCCAAATCGCCCGCAGAAGCGCGGCCGTCTGGACCGATGCCTGGTAGAAGTACTCGCCGATA
GTGAAACCGACGCCCCAGCACTCGTCCGAGGGCAAAGGAATAGCACGTGCTACGAGATTTCGATTCCA
CCGCCGCCTTCTATGAAAGGTTGGGCTTCGGAATCGTTTTCCGGGACGCCGGCTGGATGATCCTCCAGC
GCGGGGATCTCATGCTGGAGTTCTTCGCCCACCCCAACTTGTTTATTGCAGCTTATAATGGTTACAAAT
AAAGCAATAGCATCACAAATTTCACAAATAAAGCATTTTTTTCACTGCATTCTAGTTGTGGTTTGTCCA
AACTCATCAATGTATCTTATCATGTCTGTATACCGTCGACCTCTAGCTAGAGCTTGGCGTAATCATGGT
CATTACCAATGCTTAATCAGTGAGGCACCTATCTCAGCGATCTGTCTATTTCGTTCATCCATAGTTGCC
TGACTCCCCGTCGTGTAGATAACTACGATACGGGAGGGCTTACCATCTGGCCCCAGCGCTGCGATGAT
ACCGCGAGAACCACGCTCACCGGCTCCGGATTTATCAGCAATAAACCAGCCAGCCGGAAGGGCCGAG
CGCAGAAGTGGTCCTGCAACTTTATCCGCCTCCATCCAGTCTATTAATTGTTGCCGGGAAGCTAGAGTA
AGTAGTTCGCCAGTTAATAGTTTGCGCAACGTTGTTGCCATCGCTACAGGCATCGTGGTGTCACGCTCG
TCGTTTGGTATGGCTTCATTCAGCTCCGGTTCCCAACGATCAAGGCGAGTTACATGATCCCCCATGTTG
TGCAAAAAAGCGGTTAGCTCCTTCGGTCCTCCGATCGTTGTCAGAAGTAAGTTGGCCGCAGTGTTATC
ACTCATGGTTATGGCAGCACTGCATAATTCTCTTACTGTCATGCCATCCGTAAGATGCTTTTCTGTGAC
TGGTGAGTACTCAACCAAGTCATTCTGAGAATAGTGTATGCGGCGACCGAGTTGCTCTTGCCCGGCGT
CAATACGGGATAATACCGCGCCACATAGCAGAACTTTAAAAGTGCTCATCATTGGAAAACGTTCTTCG
GGGCGAAAACTCTCAAGGATCTTACCGCTGTTGAGATCCAGTTCGATGTAACCCACTCGTGCACCCAA
CTGATCTTCAGCATCTTTTACTTTCACCAGCGTTTCTGGGTGAGCAAAAACAGGAAGGCAAAATGCCG
CAAAAAAGGGAATAAGGGCGACACGGAAATGTTGAATACTCATATTCTTCCTTTTTCAATATTATTGA
AGCATTTATCAGGGTTATTGTCTCATGAGCGGATACATATTTGAATGTATTTAGAAAAATAAACAAAT
AGGGGTCAGTGTTACAACCAATTAACCAATTCTGAACATTATCGCGAGCCCATTTATACCTGAATATG
GCTCATAACACCCCTTGCTCATGACCAAAATCCCTTAACGTGAGTTACGCGCGCGTCGTTCCACTGAGC
GTCAGACCCCGTAGAAAAGATCAAAGGATCTTCTTGAGATCCTTTTTTTCTGCGCGTAATCTGCTGCTT
GCAAACAAAAAAACCACCGCTACCAGCGGTGGTTTGTTTGCCGGATCAAGAGCTACCAACTCTTTTTC
CGAAGGTAACTGGCTTCAGCAGAGCGCAGATACCAAATACTGTTCTTCTAGTGTAGCCGTAGTTAGCC
CACCACTTCAAGAACTCTGTAGCACCGCCTACATACCTCGCTCTGCTAATCCTGTTACCAGTGGCTGCT
GCCAGTGGCGATAAGTCGTGTCTTACCGGGTTGGACTCAAGACGATAGTTACCGGATAAGGCGCAGCG
GTCGGGCTGAACGGGGGGTTCGTGCACACAGCCCAGCTTGGAGCGAACGACCTACACCGAACTGAGA
TACCTACAGCGTGAGCTATGAGAAAGCGCCACGCTTCCCGAAGGGAGAAAGGCGGACAGGTATCCGG
TAAGCGGCAGGGTCGGAACAGGAGAGCGCACGAGGGAGCTTCCAGGGGGAAACGCCTGGTATCTTTA

TAGTCCTGTCGGGTTTCGCCACCTCTGACTTGAGCGTCGATTTTTGTGATGCTCGTCAGGGGGGCGGAG
CCTATGGAAAAACGCCAGCAACGCGGCCTTTTTACGGTTCCTGGCCTTTTGCTGGCCTTTTGCTCACAT
GTTCTTTCCTGCGTTATCCCCTGATTCTGTGGATAACCGTATTACCGCCTTTGAGTGAGCTGATACCGCT
CGCCGCAGCCGAACGACCGAGCGCAGCGAGTCAGTGAGCGAGGAAGCGGAAGGCGAGAGTAGGGAA
CTGCCAGGCATCAAACTAAGCAGAAGGCCCCTGACGGATGGCCTTTTTGCGTTTCTACAAACTCTTTCT
GTGTTGTAAAACGACGGCCAGTCTTAAGCTCGGGCCCCCTGGGCGGTTCTGATAACGAGTAATCGTTA
ATCCGCAAATAACGTAAAAACCCGCTTCGGCGGGTTTTTTTATGGGGGGAGTTTAGGGAAAGAGCATT
TGTCAGAATATTTAAGGGCGCCTGTCACTTTGCTTGATATATGAGAATTATTTAACCTTATAAATGAGA
AAAAAGCAACGCACTTTAAATAAGATACGTTGCTTTTTCGATTGATGAACACCTATAATTAAACTATTC
ATCTATTATTTATGATTTTTTGTATATACAATATTTCTAGTTTGTTAAAGAGAATTAAGAAAATAAATCT
CGAAAATAATAAAGGGAAAATCAGTTTTTGATATCAAAATTATACATGTCAACGATAATACAAAATAT
AATACAAACTATAAGATGTTATCAGTATTTATTATCATTTAGAATAAATTTTGTGTCGCCCTTAATTGT
GAGCGGATAACAATTACGAGCTTCATGCACAGTGGCGTTGACATTGATTATTGACTAGTTATTAATAG
TAATCAATTACGGGGTCATTAGTTCATAGCCCATATATGGAGTTCCGCGTTACATAACTTACGGTAAAT
GGCCCGCCTGGCTGACCGCCCAACGACCCCCGCCCATTGACGTCAATAATGACGTATGTTCCCATAGT
AACGCCAATAGGGACTTTCCATTGACGTCAATGGGTGGAGTATTTACGGTAAACTGCCCACTTGGCAG
TACATCAAGTGTATCATATGCCAAGTACGCCCCCTATTGACGTCAATGACGGTAAATGGCCCGCCTGG
CATTATGCCCAGTACATGACCTTATGGGACTTTCCTACTTGGCAGTACATCTACGTATTAGTCATCGCT
ATTACCATGGTGATGCGGTTTTGGCAGTACATCAATGGGCGTGGATAGCGGTTTGACTCACGGGGATT
TCCAAGTCTCCACCCCATTGACGTCAATGGGAGTTTGTTTTGGCACCAAAATCAACGGGACTTTCCAAA
ATGTCGTAACAACTCCGCCCCATTGACGCAAATGGGCGGTAGGCGTGTACGGTGGGAGGTCTATATAA
GCAGAGCTCTCTGGCTAACTAGAGAACCCACTGCTTACTGGCTTATCGAAATTAATACGACTCACTAT
AGGGAAGCTTCTTGTTCTTTTTGCAGAAGCTCAGAATAAACGCTCAACTTTGGCCTCGAGGCCACCATG
GCTTCCTCCCCTCCAAAGAAAAAGAGAAAGGTTGCGGCCGCTGACTACAAGGATGACGACGATAAAA
GTTGGAAGGACGCAAGTGGTTGGTCTAGAATGCATGCGGCCCCGCGACGGCGTGCTGCGCAACCCTCC
GACGCTTCGCCGGCCGCGCAGGTGGATCTACGCACGCTCGGCTACAGTCAGCAGCAGCAAGAGAAGA
TCAAACCGAAGGTGCGTTCGACAGTGGCGCAGCACCACGAGGCACTGGTGGGCCATGGGTTTACACA
CGCGCACATCGTTGCGCTCAGCCAACACCCGGCAGCGTTAGGGACCGTCGCTGTCACGTATCAGCACA
TAATCACGGCGTTGCCAGAGGCGACACACGAAGACATCGTTGGCGTCGGCAAACAGTGGTCCGGCGC
ACGCGCCCTGGAGGCCTTGCTCACGGATGCGGGGGAGTTGAGAGGTCCGCCGTTACAGTTGGACACAG
GCCAACTTGTGAAGATTGCAAAACGTGGCGGCGTGACCGCAATGGAGGCAGTGCATGCATCGCGCAA
TGCGCTCACGGGAGCACCCCTCAACCTGACCCCGGACCAGGTGGTTGCAATCGCGTCACACGATGGGG
GAAAGCAGGCCCTAGAAACCGTTCAGCGACTCCTGCCCGTCCTGTGCCAGGACCACGGCCTGACCCCG
GAACAGGTGGTTGCAATCGCGTCACACGATGGGGGAAAGCAGGCCCTAGAAACCGTTCAGCGACTCC
TGCCCGTCCTGTGCCAGGCCCACGGCCTGACCCCGGACCAGGTGGTTGCAATCGCGTCACACGATGGG
GGAAAGCAGGCCCTAGAAACCGTTCAGCGACTCCTGCCCGTCCTGTGCCAGGCCCACGGCCTGACCCC
CGCCCAGGTTGTCGCTATTGCTAGTAACGGCGGAGGCAAACAGGCGCTGGAAACAGTTCAGCGCCTCT
TGCCGGTCTTGTGTCAGGACCACGGCCTGACCCCAGACCAGGTTGTGGCCATCGCCAGCAACATAGGT
GGCAAGCAGGCCCTCGAAACCGTCCAGAGACTGTTACCGGTTCTCTGCCAGGACCACGGCCTGACCCC
AGAACAAGTTGTCGCGATTGCAAGCAACAACGGAGGCAAACAAGCCTTAGAAACAGTCCAGAGATTG
TTGCCGGTGCTGTGCCAAGCCCACGGCCTGACCCCGGACCAGGTGGTTGCAATCGCGTCACACGATGG
GGGAAAGCAGGCCCTAGAAACCGTTCAGCGACTCCTGCCCGTCCTGTGCCAGGCCCACGGCCTGACCC
CGGCCCAGGTGGTTGCAATCGCGTCACACGATGGGGGAAAGCAGGCCCTAGAAACCGTTCAGCGACT
CCTGCCCGTCCTGTGCCAGGACCACGGCCTGACCCCAGACCAGGTTGTGGCCATCGCCAGCAACATAG
GTGGCAAGCAGGCCCTCGAAACCGTCCAGAGACTGTTACCGGTTCTCTGCCAGGACCACGGCCTGACC
CCAGAACAAGTTGTCGCGATTGCAAGCAACAACGGAGGCAAACAAGCCTTAGAAACAGTCCAGAGAT
TGTTGCCGGTGCTGTGCCAAGCCCACGGCCTGACCCCAGACCAGGTTGTGGCCATCGCCAGCAACATA
GGTGGCAAGCAGGCCCTCGAAACCGTCCAGAGACTGTTACCGGTTCTCTGCCAGGCCCACGGCCTGAC
CCCAGCCCAAGTTGTCGCGATTGCAAGCAACAACGGAGGCAAACAAGCCTTAGAAACAGTCCAGAGA
TTGTTGCCGGTGCTGTGCCAAGACCACGGCCTGACCCCTGAGCAGGTAGTGGCTATTGCATCCAACAT
AGGGGGCAGACCCGCACTGGAGTCAATCGTGGCCCAGCTTTCGAGGCCGGACCCCGCGCTGGCCGCA
CTCACTAATGATCATCTTGTAGCGCTGGCCTGCCTCGGCGGACGTCCTGCCATGGATGCAGTGAAAAA
GGGATTGCCGCACGCGCCGGAATTGATCAGATCCCAGCTAGTGAAATCTGAATTGGAAGAGAAGAAA
TCTGAACTTAGACATAAATTGAAATATGTGCCACATGAATATATTGAATTGATTGAAATCGCAAGAAA
TTCAACTCAGGATAGAATCCTTGAAATGAAGGTGATGGAGTTCTTTATGAAGGTTTATGGTTATCGTGG
TAAACATTTGGGTGGATCAAGGAAACCAGACGGAGCAATTTATACTGTCGGATCTCCTATTGATTACG

GTGTGATCGTTGATACTAAGGCATATTCAGGAGGTTATAATCTTCCAATTGGTCAAGCAGATGAAATG
CAAAGATATGTCGAAGAGAATCAAACAAGAAACAAGCATATCAACCCTAATGAATGGTGGAAAGTCT
ATCCATCTTCAGTAACAGAATTTAAGTTCTTGTTTGTGAGTGGTCATTTCAAAGGAAACTACAAAGCTC
AGCTTACAAGATTGAATCATATCACTAATTGTAATGGAGCTGTTCTTAGTGTAGAAGAGCTTTTGATTG
GTGGAGAAATGATTAAAGCTGGTACATTGACACTTGAGGAAGTGAGAAGGAAATTTAATAACGGCGA
GATAAACTTTTAAAAAATCAGCCTCGACTGTGCCTTCTAGTTGCCAGCCATCTGTTGTTTGCCCCTCCC
CCGTGCCTTCCTTGACCCTGGAAGGTGCCACTCCCACTGTCCTTTCCTAATAAAATGAGGAAATTGCAT
CACAACACTCAACCCTATCTCGGTCTATTCTTTTGATTTATAAGGGATTTTGCCGATTTCGGCCTATTGG
TTAAAAAATGAGCTGATTTAACAAAAATTTAACGCGAATTAATTCTGTGGAATGTGTGTCAGTTAGGG
TGTGGAAAGTCCCCAGGCTCCCCAGCAGGCAGAAGTATGCAAAGCATGCATCTCAATTAGTCAGCAAC
CAGGTGTGGAAAGTCCCCAGGCTCCCCAGCAGGCAGAAGTATGCAAAGCATGCATCTCAATTAGTCAG
CAACCATAGTCCCGCCCCTAACTCCGCCCATCCCGCCCCTAACTCCGCCCAGTTCCGCCCATTCTCCGC
CCCATGGCTGACTAATTTTTTTTTATTTATGCAGAGGCCGAGGCCGCCTCTGCCTCTGAGCTATTCCAG
AAGTAGTGAGGAGGCTTTTTTGGAGGCCTAGGCTTTTGCAAAAAGCTCCCGGGAGCTTGTATATCCAT
TTTCGGATCTGATCAGCACGTGATGAAAAAGCCTGAACTCACCGCGACGTCTGTCGAGAAGTTTCTGA
TCGAAAAGTTCGACAGCGTCCGACCTGATGCAGCTCTCGGAGGGCGAAGAATCTCGTGCTTTCAGCTT
CGATGTAGGAGGGCGTGGATATGTCCTGCGGGTAAATAGCTGCGCCGATGGTTTCTACAAAGATCGTT
ATGTTTATCGGCACTTTGCATCGGCCGCGCTCCCGATTCCGGAAGTGCTTGACATTGGGGAATTCAGCG
AGAGCCTGACCTATTGCATCTCCCGCCGTGCACAGGGTGTCACGTTGCAAGACCTGCCTGAAACCGAA
CTGCCCGCTGTTCTGCAGCCGGTCGCGGAGGCCATGGATGCGATCGCTGCGGCCGATCTTAGCCAGAC
GAGCGGGTTCGGCCCATTCGGACCGCAAGGAATCGGTCAATACACTACATGGCGTGATTTCATATGCG
CGATTGCTGATCCCCATGTGTATCACTGGCAAACTGTGATGGACGACACCGTCAGTGCGTCCGTCGCG
CAGGCTCTCGATGAGCTGATGCTTTGGGCCGAGGACTGCCCCGAAGTCCGGCACCTCGTGCACGCGGA
TTTCGGCTCCAACAATGTCCTGACGGACAATGGCCGCATAACAGCGGTCATTGACTGGAGCGAGGCGA
TGTTCGGGGATTCCCAATACGAGGTCGCCAACATCTTCTTCTGGAGGCCGTGGTTGGCTTGTATGGAGC
AGCAGACGCGCTACTTCGAGCGGAGGCATCCGGAGCTTGCAGGATCGCCGCGGCTCCGGGCGTATATG
CTCCGCATTGGTCTTGACCAACTCTATCAGAGCTTGGTTGACGGCAATTTCGATGATGCAGCTTGGGCG
CAGGGTCGATGCGACGCAATCGTCCGATCCGGAGCCGGGACTGTCGGGCGTACACAAATCGCCCGCA
GAAGCGCGGCCGTCTGGACCGATGGCTGTGTAGAAGTACTCGCCGATAGTGGAAACCGACGCCCCAG
CACTCGTCCGAGGGCAAAGGAATAGCACGTGCTACGAGATTTCGATTCCACCGCCGCCTTCTATGAAA
GGTTGGGCTTCGGAATCGTTTTCCGGGACGCCGGCTGGATGATCCTCCAGCGCGGGGATCTCATGCTG
GAGTTCTTCGCCCACCCCAACTTGTTTATTGCAGCTTATAATGGTTACAAATAAAGCAATAGCATCACA
AATTTCACAAATAAAGCATTTTTCACGCATTCT

References

1 Lu, Y., Sun, W. J. & Gu, Z. Stimuli-responsive nanomaterials for therapeutic protein delivery. *J Control Release* **194**, 1-19, doi:10.1016/j.jconrel.2014.08.015 (2014).

2 Leader, B., Baca, Q. J. & Golan, D. E. Protein therapeutics: A summary and pharmacological classification. *Nat Rev Drug Discov* **7**, 21-39, doi:10.1038/nrd2399 (2008).

3 Banting, F. G., Best, C. H., Collip, J. B., Campbell, W. R. & Fletcher, A. A. Pancreatic extracts in the treatment of diabetes mellitus. *Can Med Assoc J* **7**, 141-146 (1922).

4 Li, C. H. & Papkoff, H. Preparation and Properties of Growth Hormone from Human and Monkey Pituitary Glands. *Science* **124**, 1293-1294, doi:DOI 10.1126/science.124.3235.1293 (1956).

5 Gemzell, C. A., Diczfalusy, E. & Tillinger, G. Clinical effect of human pituitary follicle-stimulating hormone (FSH). *J Clin Endocrinol Metab* **18**, 1333-1348, doi:10.1210/jcem-18-12-1333 (1958).

6 Johnson, I. S. Human insulin from recombinant DNA technology. *Science* **219**, 632-637 (1983).

7 Buckel, P. Recombinant proteins for therapy. *Trends Pharmacol Sci* **17**, 450-456, doi:Doi 10.1016/S0165-6147(96)01011-5 (1996).

8 Baneyx, F. Recombinant protein expression in Escherichia coli. *Curr Opin Biotech* **10**, 411-421, doi:Doi 10.1016/S0958-1669(99)00003-8 (1999).

9 Cregg, J. M., Vedvick, T. S. & Raschke, W. C. Recent Advances in the Expression of Foreign Genes in Pichia-Pastoris. *Bio-Technol* **11**, 905-910, doi:DOI 10.1038/nbt0893-905 (1993).

10 Kawakami, S., Sato, A., Nishikawa, M., Yamashita, F. & Hashida, M. Mannose receptor-mediated gene transfer into macrophages using novel mannosylated cationic liposomes. *Gene Ther* **7**, 292-299, doi:DOI 10.1038/sj.gt.3301089 (2000).

11 Wurm, F. M. Production of recombinant protein therapeutics in cultivated mammalian cells. *Nat Biotechnol* **22**, 1393-1398, doi:10.1038/nbt1026 (2004).

12 Chica, R. A., Doucet, N. & Pelletier, J. N. Semi-rational approaches to engineering enzyme activity: combining the benefits of directed evolution and rational design. *Curr Opin Biotechnol* **16**, 378-384, doi:10.1016/j.copbio.2005.06.004 (2005).

13 Lutz, S. Beyond directed evolution-semi-rational protein engineering and design. *Curr Opin Biotech* **21**, 734-743, doi:10.1016/j.copbio.2010.08.011 (2010).

14 Ness, J. E. *et al.* DNA shuffling of subgenomic sequences of subtilisin. *Nat Biotechnol* **17**, 893-896 (1999).

15 Giver, L., Gershenson, A., Freskgard, P. O. & Arnold, F. H. Directed evolution of a thermostable esterase. *P Natl Acad Sci USA* **95**, 12809-12813, doi:DOI 10.1073/pnas.95.22.12809 (1998).

16 Estell, D. A., Graycar, T. P. & Wells, J. A. Engineering an Enzyme by Site-Directed Mutagenesis to Be Resistant to Chemical Oxidation. *J Biol Chem* **260**, 6518-6521 (1985).

17 Ozaki, S. I. & Demontellano, P. R. O. Molecular Engineering of Horseradish-Peroxidase - Highly Enantioselective Sulfoxidation of Aryl Alkyl Sulfides by the Phe-41-]Leu Mutant. *J Am Chem Soc* **116**, 4487-4488, doi:DOI 10.1021/ja00089a052 (1994).

18 Loida, P. J. & Sligar, S. G. Engineering Cytochrome-P-450 (Cam) to Increase the Stereospecificity and Coupling of Aliphatic Hydroxylation. *Protein Eng* **6**, 207-212, doi:DOI 10.1093/protein/6.2.207 (1993).

19 Sawano, A. & Miyawaki, A. Directed evolution of green fluorescent protein by a new versatile PCR strategy for site-directed and semi-random mutagenesis. *Nucleic Acids Res* **28**, E78 (2000).

20 Kim, T. *et al.* Shifting the pH profile of Aspergillus niger PhyA phytase to match the stomach pH enhances its effectiveness as an animal feed additive. *Appl Environ Microb* **72**, 4397-4403, doi:10.1128/Aem.02612-05 (2006).

21 Chirino, A. J., Ary, M. L. & Marshall, S. A. Minimizing the immunogenicity of protein therapeutics. *Drug Discov Today* **9**, 82-90, doi:Pii S1359-6446(03)02953-2

Doi 10.1016/S1359-6446(03)02953-2 (2004).

22 Osipovitch, D. C. *et al.* Design and analysis of immune-evading enzymes for ADEPT therapy. *Protein Eng Des Sel* **25**, 613-623, doi:10.1093/protein/gzs044 (2012).

23 Kermekchiev, M. B., Kirilova, L. I., Vail, E. E. & Barnes, W. M. Mutants of Taq DNA polymerase resistant to PCR inhibitors allow DNA amplification from whole blood and crude soil samples. *Nucleic Acids Research* **37**, doi:ARTN e40

10.1093/nar/gkn1055 (2009).

24 Horvath, C. M., Wen, Z. L. & Darnell, J. E. A Stat Protein Domain That Determines DNA-Sequence Recognition Suggests a Novel DNA-Binding Domain. *Gene Dev* **9**, 984-994, doi:DOI 10.1101/gad.9.8.984 (1995).

25 Lawrence, M. S., Phillips, K. J. & Liu, D. R. Supercharging proteins can impart unusual resilience. *J Am Chem Soc* **129**, 10110-+, doi:10.1021/ja071641y (2007).

26 Zuris, J. A. *et al.* Cationic lipid-mediated delivery of proteins enables efficient protein-based genome editing in vitro and in vivo. *Nat Biotechnol* **33**, 73-80, doi:10.1038/nbt.3081 (2015).

27 Gilbert, M. *et al.* The synthesis of sialylated oligosaccharides using a CMP-Neu5Ac synthetase/sialyltransferase fusion. *Nat Biotechnol* **16**, 769-772, doi:DOI 10.1038/nbt0898-769 (1998).

28 Wang, J. Q. *et al.* Enhanced inhibition of human anti-Gal antibody binding to mammalian cells by synthetic alpha-Gal epitope polymers. *J Am Chem Soc* **121**, 8174-8181, doi:DOI 10.1021/ja990219h (1999).

29 Moks, T. *et al.* Expression of Human Insulin-Like Growth Factor-I in Bacteria - Use of Optimized Gene Fusion Vectors to Facilitate Protein-Purification. *Biochemistry-Us* **26**, 5239-5244, doi:DOI 10.1021/bi00391a005 (1987).

30 Choi, B. K. *et al.* Use of combinatorial genetic libraries to humanize N-linked glycosylation in the yeast Pichia pastoris. *P Natl Acad Sci USA* **100**, 5022-5027, doi:10.1073/pnas.0931263100 (2003).

31 Jacobs, P. P., Geysens, S., Vervecken, W., Contreras, R. & Callewaert, N. Engineering complex-type N-glycosylation in Pichia pastoris using GlycoSwitch technology. *Nat Protoc* **4**, 58-70, doi:10.1038/nprot.2008.213 (2009).

32 Gai, S. A. & Wittrup, K. D. Yeast surface display for protein engineering and characterization. *Curr Opin Struc Biol* **17**, 467-473, doi:10.1016/j.sbi.2007.08.012 (2007).

33 Wang, H. Y. & Chong, S. R. Visualization of coupled protein folding and binding in bacteria and purification of the heterodimeric complex. *P Natl Acad Sci USA* **100**, 478-483, doi:DOI 10.1073/pnas.0236088100 (2003).

34 Farokhzad, O. C. & Langer, R. Impact of Nanotechnology on Drug Delivery. *Acs Nano* **3**, 16-20, doi:10.1021/nn900002m (2009).

35 Zhao, M. *et al.* Nanocapsules of oxalate oxidase for hyperoxaluria treatment. *Nano Research*, doi:10.1007/s12274-017-1898-3 (2017).

36 Zhang, P. *et al.* Zwitterionic gel encapsulation promotes protein stability, enhances pharmacokinetics, and reduces immunogenicity. *P Natl Acad Sci USA* **112**, 12046-12051, doi:10.1073/pnas.1512465112 (2015).

37 Ho, D. H. *et al.* Clinical-Pharmacology of Polyethylene Glycol-L-Asparaginase. *Drug Metab Dispos* **14**, 349-352 (1986).

38 Tian, H. J. *et al.* Growth-Factor Nanocapsules That Enable Tunable Controlled Release for Bone Regeneration. *Acs Nano* **10**, 7362-7369, doi:10.1021/acsnano.5b07950 (2016).

39 Zhu, S. W., Nih, L., Carmichael, S. T., Lu, Y. F. & Segura, T. Enzyme-Responsive Delivery of Multiple Proteins with Spatiotemporal Control. *Adv Mater* **27**, 3620-3625, doi:10.1002/adma.201500417 (2015).

40 Owens, D. E. & Peppas, N. A. Opsonization, biodistribution, and pharmacokinetics of polymeric nanoparticles. *Int J Pharm* **307**, 93-102, doi:10.1016/j.ijpharm.2005.10.010 (2006).

41 Moghimi, S. M., Hunter, A. C. & Murray, J. C. Long-circulating and target-specific nanoparticles: Theory to practice. *Pharmacological Reviews* **53**, 283-318 (2001).

42 Albanese, A., Tang, P. S. & Chan, W. C. W. The Effect of Nanoparticle Size, Shape, and Surface Chemistry on Biological Systems. *Annu Rev Biomed Eng* **14**, 1-16, doi:10.1146/annurev-bioeng-071811-150124 (2012).

43 Choi, H. S. *et al.* Renal clearance of quantum dots. *Nat Biotechnol* **25**, 1165-1170, doi:10.1038/nbt1340 (2007).

44 Davis, M. E., Chen, Z. & Shin, D. M. Nanoparticle therapeutics: an emerging treatment modality for cancer. *Nat Rev Drug Discov* **7**, 771-782, doi:10.1038/nrd2614 (2008).

45 Lundqvist, M. *et al.* Nanoparticle size and surface properties determine the protein corona with possible implications for biological impacts. *P Natl Acad Sci USA* **105**, 14265-14270, doi:10.1073/pnas.0805135105 (2008).

46 Champion, J. A., Katare, Y. K. & Mitragotri, S. Particle shape: A new design parameter for micro- and nanoscale drug delivery carriers. *J Control Release* **121**, 3-9, doi:10.1016/j.jconrel.2007.03.022 (2007).

47 Walkey, C. D., Olsen, J. B., Guo, H. B., Emili, A. & Chan, W. C. W. Nanoparticle Size and Surface Chemistry Determine Serum Protein Adsorption and Macrophage Uptake. *J Am Chem Soc* **134**, 2139-2147, doi:10.1021/ja2084338 (2012).

48 Veronese, F. M. & Pasut, G. PEGylation, successful approach to drug delivery. *Drug Discov Today* **10**, 1451-1458, doi:Doi 10.1016/S1359-6446(05)03575-0 (2005).

49 Abuchowski, A., Mccoy, J. R., Palczuk, N. C., Vanes, T. & Davis, F. F. Effect of Covalent Attachment of Polyethylene-Glycol on Immunogenicity and Circulating Life of Bovine Liver Catalase. *J Biol Chem* **252**, 3582-3586 (1977).

50 Lawrence, P. B. & Price, J. L. How PEGylation influences protein conformational stability. *Curr Opin Chem Biol* **34**, 88-94, doi:10.1016/j.cbpa.2016.08.006 (2016).

51 Veronese, F. M. *et al.* Site-specific pegylation of G-CSF by reversible denaturation. *Bioconjugate Chem* **18**, 1824-1830, doi:10.1021/bc070123 (2007).

52 Binazadeh, M., Kabiri, M. & Unsworth, L. D. Poly(ethylene glycol) and Poly(carboxy betaine) Based Nonfouling Architectures: Review and Current Efforts. *Acs Sym Ser* **1120**, 621-643 (2012).

53 Szleifer, I. Polymers and proteins: Interactions at interfaces. *Curr Opin Solid St M* **2**, 337-344, doi:Doi 10.1016/S1359-0286(97)80125-8 (1997).

54 Storm, G., Belliot, S. O., Daemen, T. & Lasic, D. D. Surface Modification of Nanoparticles to Oppose Uptake by the Mononuclear Phagocyte System. *Adv Drug Deliver Rev* **17**, 31-48, doi:Doi 10.1016/0169-409x(95)00039-A (1995).

55 Peracchia, M. T. Stealth nanoparticles for intravenous administration. *Stp Pharma Sci* **13**, 155-161 (2003).

56 Peracchia, M. T. *et al.* Stealth (R) PEGylated polycyanoacrylate nanoparticles for intravenous administration and splenic targeting. *J Control Release* **60**, 121-128, doi:Doi 10.1016/S0168-3659(99)00063-2 (1999).

57 Liu, Y., Li, J. & Lu, Y. F. Enzyme therapeutics for systemic detoxification. *Adv Drug Deliver Rev* **90**, 24-39, doi:10.1016/j.addr.2015.05.005 (2015).

58 Moghimi, S. M. Chemical camouflage of nanospheres with a poorly reactive surface: towards development of stealth and target-specific nanocarriers. *Bba-Mol Cell Res* **1590**, 131-139, doi:Pii S0167-4889(02)00204-5

Doi 10.1016/S0167-4889(02)00204-5 (2002).

59 Ganson, N. J., Kelly, S. J., Scarlett, E., Sundy, J. S. & Hershfield, M. S. Control of hyperuricemia in subjects with refractory gout, and induction of antibody against

poly(ethylene glycol) (PEG), in a phase I trial of subcutaneous PEGylated urate oxidase. *Arthritis Res Ther* **8**, doi:ARTN R12
10.1186/ar1861 (2006).

60 Wang, X. Y., Ishida, T. & Kiwada, H. Anti-PEG IgM elicited by injection of liposomes is involved in the enhanced blood clearance of a subsequent dose of PEGylated liposomes. *J Control Release* **119**, 236-244, doi:10.1016/j.jconrel.2007.02.010 (2007).

61 Gregoriadis, G. Drug Entrapment in Liposomes. *Febs Lett* **36**, 292-296, doi:Doi 10.1016/0014-5793(73)80394-1 (1973).

62 Zylberberg, C. & Matosevic, S. Pharmaceutical liposomal drug delivery: a review of new delivery systems and a look at the regulatory landscape. *Drug Deliv* **23**, 3319-3329, doi:10.1080/10717544.2016.1177136 (2016).

63 Scherphof, G. L., Dijkstra, J., Spanjer, H. H., Derksen, J. T. P. & Roerdink, F. H. Uptake and Intracellular Processing of Targeted and Nontargeted Liposomes by Rat Kupffer Cells Invivo and Invitro. *Ann Ny Acad Sci* **446**, 368-384, doi:DOI 10.1111/j.1749-6632.1985.tb18414.x (1985).

64 Hu, C. M. J., Fang, R. H., Copp, J., Luk, B. T. & Zhang, L. F. A biomimetic nanosponge that absorbs pore-forming toxins. *Nat Nanotechnol* **8**, 336-340, doi:10.1038/Nnano.2013.54 (2013).

65 Dehaini, D. *et al.* Ultra-small lipid-polymer hybrid nanoparticles for tumor-penetrating drug delivery. *Nanoscale* **8**, 14411-14419, doi:10.1039/c6nr04091h (2016).

66 Gao, W. W. *et al.* Hydrogel Containing Nanoparticle-Stabilized Liposomes for Topical Antimicrobial Delivery. *Acs Nano* **8**, 2900-2907, doi:10.1021/nn500110a (2014).

67 Fan, C. *et al.* Enhanced Topical Delivery of Tetrandrine by Ethosomes for Treatment of Arthritis. *Biomed Res Int*, doi:Artn 161943
10.1155/2013/161943 (2013).

68 Gabizon, A. & Papahadjopoulos, D. Liposome Formulations with Prolonged Circulation Time in Blood and Enhanced Uptake by Tumors. *P Natl Acad Sci USA* **85**, 6949-6953, doi:DOI 10.1073/pnas.85.18.6949 (1988).

69 Klibanov, A. L., Maruyama, K., Torchilin, V. P. & Huang, L. Amphipathic Polyethyleneglycols Effectively Prolong the Circulation Time of Liposomes. *Febs Lett* **268**, 235-237, doi:Doi 10.1016/0014-5793(90)81016-H (1990).

70 Nag, O. K. & Awasthi, V. Surface engineering of liposomes for stealth behavior. *Pharmaceutics* **5**, 542-569, doi:10.3390/pharmaceutics5040542 (2013).

71 Papahadjopoulos, D. *et al.* Sterically Stabilized Liposomes - Improvements in Pharmacokinetics and Antitumor Therapeutic Efficacy. *P Natl Acad Sci USA* **88**, 11460-11464, doi:DOI 10.1073/pnas.88.24.11460 (1991).

72 Henry, B. D. *et al.* Engineered liposomes sequester bacterial exotoxins and protect from severe invasive infections in mice. *Nat Biotechnol* **33**, 81-U295, doi:10.1038/nbt.3037 (2015).

73 Kroll, A. V. *et al.* Nanoparticulate Delivery of Cancer Cell Membrane Elicits Multiantigenic Antitumor Immunity. *Adv Mater* **29**, doi:10.1002/adma.201703969 (2017).

74 Xue, J. W. *et al.* Neutrophil-mediated anticancer drug delivery for suppression of postoperative malignant glioma recurrence. *Nat Nanotechnol* **12**, 692-+, doi:10.1038/Nnano.2017.54 (2017).

75 Matsuno, R. & Ishihara, K. Integrated functional nanocolloids covered with artificial cell membranes for biomedical applications. *Nano Today* **6**, 61-74, doi:10.1016/j.nantod.2010.12.009 (2011).

76 Zhang, P. *et al.* Butyrylcholinesterase nanocapsule as a long circulating bioscavenger with reduced immune response. *J Control Release* **230**, 73-78, doi:10.1016/j.jconrel.2016.04.008 (2016).

77 Jiang, S. Y. & Cao, Z. Q. Ultralow-Fouling, Functionalizable, and Hydrolyzable Zwitterionic Materials and Their Derivatives for Biological Applications. *Adv Mater* **22**, 920-932, doi:10.1002/adma.200901407 (2010).

78 Leng, C. *et al.* In Situ Probing of the Surface Hydration of Zwitterionic Polymer Brushes: Structural and Environmental Effects. *J Phys Chem C* **118**, 15840-15845, doi:10.1021/jp504293r (2014).

79 Keefe, A. J. & Jiang, S. Y. Poly(zwitterionic)protein conjugates offer increased stability without sacrificing binding affinity or bioactivity. *Nat Chem* **4**, 60-64, doi:10.1038/nchem.1213 (2012).

80 Vaisocherova, H. *et al.* Ultralow fouling and functionalizable surface chemistry based on a zwitterionic polymer enabling sensitive and specific protein detection in undiluted blood plasma. *Anal Chem* **80**, 7894-7901, doi:10.1021/ac8015888 (2008).

81 Cheng, G., Xite, H., Zhang, Z., Chen, S. F. & Jiang, S. Y. A Switchable Biocompatible Polymer Surface with Self-Sterilizing and Nonfouling Capabilities. *Angew Chem Int Edit* **47**, 8831-8834, doi:10.1002/anie.200803570 (2008).

82 Lewis, A., Tang, Y. Q., Brocchini, S., Choi, J. W. & Godwin, A. Poly(2-methacryloyloxyethyl phosphorylcholine) for Protein Conjugation. *Bioconjugate Chem* **19**, 2144-2155, doi:10.1021/bc800242t (2008).

83 Chiba, N. *et al.* Development of gene vectors for pinpoint targeting to human hepatocytes by cationically modified polymer complexes. *Eur Surg Res* **39**, 23-34, doi:10.1159/000098437 (2007).

84 Sundy, J. S. *et al.* Pharmacokinetics and pharmacodynamics of intravenous PEGylated recombinant mammalian urate oxidase in patients with refractory gout. *Arthritis Rheum* **56**, 1021-1028, doi:10.1002/art.22403 (2007).

85 Liu, S. J. & Jiang, S. Y. Chemical conjugation of zwitterionic polymers protects immunogenic enzyme and preserves bioactivity without polymer-specific antibody response. *Nano Today* **11**, 285-291, doi:10.1016/j.nantod.2016.05.006 (2016).

86 Liang, S. *et al.* Phosphorylcholine polymer nanocapsules prolong the circulation time and reduce the immunogenicity of therapeutic proteins. *Nano Research* **9**, 1022-1031, doi:10.1007/s12274-016-0991-3 (2016).

87 Bernstein, A. *et al.* Higher antitumor efficacy of daunomycin when linked to dextran: in vivo and in vitro studies. *J Natl Cancer Inst* **60**, 379-384 (1978).

88 Yasuda, Y., Fujita, T., Takakura, Y., Hashida, M. & Sezaki, H. Biochemical and Biopharmaceutical Properties of Macromolecular Conjugates of Uricase with Dextran and Polyethylene-Glycol. *Chem Pharm Bull* **38**, 2053-2056 (1990).

89 Wileman, T. E., Foster, R. L. & Elliott, P. N. C. Soluble Asparaginase-Dextran Conjugates Show Increased Circulatory Persistence and Lowered Antigen Reactivity. *J Pharm Pharmacol* **38**, 264-271 (1986).

90 Lam, W., Chan, H. L., Yang, M. S., Cheng, S. K. & Fong, W. F. Synergism of energy starvation and dextran-conjugated doxorubicin in the killing of multidrug-resistant KB carcinoma cells. *Anti-Cancer Drug* **10**, 171-178, doi:Doi 10.1097/00001813-199902000-00005 (1999).

91 Danhauser-Riedl, S. *et al.* Phase I clinical and pharmacokinetic trial of dextran conjugated doxorubicin (AD-70, DOX-OXD). *Invest New Drugs* **11**, 187-195 (1993).

92 Zinderman, C. E., Landow, L. & Wise, R. P. Anaphylactoid reactions to Dextran 40 and 70: Reports to the United States Food and Drug Administration, 1969 to 2004. *J Vasc Surg* **43**, 1004-1009, doi:10.1016/j.jvs.2006.01.006 (2006).

93 Lemarchand, C. *et al.* Influence of polysaccharide coating on the interactions of nanoparticles with biological systems. *Biomaterials* **27**, 108-118, doi:10.1016/j.biomaterials.2005.04.041 (2006).

94 Weiler, J. M., Edens, R. E., Linhardt, R. J. & Kapelanski, D. P. Heparin and modified heparin inhibit complement activation in vivo. *J Immunol* **148**, 3210-3215 (1992).

95 Freedman, M. D. Pharmacodynamics, Clinical Indications, and Adverse-Effects of Heparin. *J Clin Pharmacol* **32**, 584-596, doi:DOI 10.1002/j.1552-4604.1992.tb05765.x (1992).

96 Higa, O. Z., Rogero, S. O., Machado, L. D. B., Mathor, M. B. & Lugao, A. B. Biocompatibility study for PVP wound dressing obtained in different conditions. *Radiat Phys Chem* **55**, 705-707, doi:Doi 10.1016/S0969-806x(99)00215-7 (1999).

97 Zhang, X. P. *et al.* Nanocapsules of therapeutic proteins with enhanced stability and long blood circulation for hyperuricemia management. *J Control Release* **255**, 54-61, doi:10.1016/j.jconrel.2017.03.019 (2017).

98 Ravin, H. A., Seligman, A. M. & Fine, J. Polyvinyl Pyrrolidone as a Plasma Expander - Studies on Its Excretion, Distribution and Metabolism. *New Engl J Med* **247**, 921-929, doi:Doi 10.1056/Nejm195212112472403 (1952).

99 Kamada, H. *et al.* Antitumor activity of tumor necrosis factor-alpha conjugated with polyvinylpyrrolidone on solid tumors in mice. *Cancer Res* **60**, 6416-6420 (2000).

100 Caliceti, P. *et al.* Physicochemical and Biological Properties of Monofunctional Hydroxy Terminating Poly(N-Vinylpyrrolidone) Conjugated Superoxide-Dismutase. *J Bioact Compat Pol* **10**, 103-120, doi:Doi 10.1177/088391159501000202 (1995).

101 Duncan, R. & Vicent, M. J. Do HPMA copolymer conjugates have a future as clinically useful nanomedicines? A critical overview of current status and future opportunities. *Adv Drug Deliver Rev* **62**, 272-282, doi:10.1016/j.addr.2009.12.005 (2010).

102 Morgan, S. M., Subr, V., Ulbrich, K., Woodley, J. F. & Duncan, R. Evaluation of N-(2-hydroxypropyl)methacrylamide copolymer-peptide conjugates as potential oral vaccines.

Studies on their degradation by isolated rat small intestinal peptidases and their uptake by adult rat small intestinal tissue in vitro. *Int J Pharm* **128**, 99-111, doi:Doi 10.1016/0378-5173(95)04228-8 (1996).

103 Liu, Y. *et al.* Biomimetic enzyme nanocomplexes and their use as antidotes and preventive measures for alcohol intoxication. *Nat Nanotechnol* **8**, 187-192, doi:10.1038/Nnano.2012.264 (2013).

104 Veronese, F. M., Largajolli, R., Visco, C., Ferruti, P. & Miucci, A. Surface Modification of Proteins by Covalent Binding of Acrylic Polymers. *Appl Biochem Biotech* **11**, 269-277, doi:Doi 10.1007/Bf02798441 (1985).

105 Caliceti, P., Schiavon, O. & Veronese, F. M. Immunological properties of uricase conjugated to neutral soluble polymers. *Bioconjugate Chem* **12**, 515-522, doi:10.1021/bc000119x (2001).

106 Tobio, M., Gref, R., Sanchez, A., Langer, R. & Alonso, M. J. Stealth PLA-PEG nanoparticles as protein carriers for nasal administration. *Pharmaceut Res* **15**, 270-275, doi:Doi 10.1023/A:1011922819926 (1998).

107 Stewart, M. P. *et al.* In vitro and ex vivo strategies for intracellular delivery. *Nature* **538**, 183-192, doi:10.1038/nature19764 (2016).

108 Foged, C. & Nielsen, H. M. Cell-penetrating peptides for drug delivery across membrane barriers. *Expert Opin Drug Del* **5**, 105-117, doi:10.1517/17425247.5.1.105 (2008).

109 Chou, L. Y. T., Ming, K. & Chan, W. C. W. Strategies for the intracellular delivery of nanoparticles. *Chem Soc Rev* **40**, 233-245, doi:10.1039/c0cs00003e (2011).

110 Gurtovenko, A. A., Anwar, J. & Vattulainen, I. Defect-Mediated Trafficking across Cell Membranes: Insights from in Silico Modeling. *Chem Rev* **110**, 6077-6103, doi:10.1021/cr1000783 (2010).

111 Thomas, C. E., Ehrhardt, A. & Kay, M. A. Progress and problems with the use of viral vectors for gene therapy. *Nat Rev Genet* **4**, 346-358, doi:10.1038/nrg1066 (2003).

112 Walrant, A., Cardon, S., Burlina, F. & Sagan, S. Membrane Crossing and Membranotropic Activity of Cell-Penetrating Peptides: Dangerous Liaisons? *Accounts Chem Res* **50**, 2968-2975, doi:10.1021/acs.accounts.7b00455 (2017).

113 Kalafatovic, D. & Giralt, E. Cell-Penetrating Peptides: Design Strategies beyond Primary Structure and Amphipathicity. *Molecules* **22**, doi:ARTN 1929

10.3390/molecules22111929 (2017).

114 Vives, E., Brodin, P. & Lebleu, B. A truncated HIV-1 Tat protein basic domain rapidly translocates through the plasma membrane and accumulates in the cell nucleus. *J Biol Chem* **272**, 16010-16017, doi:DOI 10.1074/jbc.272.25.16010 (1997).

115 Derossi, D., Joliot, A. H., Chassaing, G. & Prochiantz, A. The 3rd Helix of the Antennapedia Homeodomain Translocates through Biological-Membranes. *J Biol Chem* **269**, 10444-10450 (1994).

116 Morris, M. C., Depollier, J., Mery, J., Heitz, F. & Divita, G. A peptide carrier for the delivery of biologically active proteins into mammalian cells. *Nat Biotechnol* **19**, 1173-1176, doi:DOI 10.1038/nbt1201-1173 (2001).

117 Liu, J., Gaj, T., Patterson, J. T., Sirk, S. J. & Barbas, C. F. Cell-Penetrating Peptide-Mediated Delivery of TALEN Proteins via Bioconjugation for Genome Engineering. *Plos One* **9**, doi:ARTN e85755

10.1371/journal.pone.0085755 (2014).

118 Heitz, F., Morris, M. C. & Divita, G. Twenty years of cell-penetrating peptides: from molecular mechanisms to therapeutics. *Brit J Pharmacol* **157**, 195-206, doi:10.1111/j.1476-5381.2009.00057.x (2009).

119 Futaki, S., Nakase, I., Tadokoro, A., Takeuchi, T. & Jones, A. T. Arginine-rich peptides and their internalization mechanisms. *Biochemical Society Transactions* **35**, 784-787, doi:10.1042/bst0350784 (2007).

120 Vendeville, A. *et al.* HIV-1 Tat enters T cells using coated pits before translocating from acidified endosomes and eliciting biological responses. *Mol Biol Cell* **15**, 2347-2360, doi:10.1091/mbc.E03-12-0921 (2004).

121 Patel, L. N., Zaro, J. L. & Shen, W. C. Cell penetrating peptides: intracellular pathways and pharmaceutical perspectives. *Pharm Res* **24**, 1977-1992, doi:10.1007/s11095-007-9303-7 (2007).

122 Abu Lila, A. S. & Ishida, T. Liposomal Delivery Systems: Design Optimization and Current Applications. *Biol Pharm Bull* **40**, 1-10 (2017).

123 Torchilin, V. P. *Handbook of nanobiomedical research : fundamentals, applications, and recent developments*. (World Scientific, 2014).

124 Bungener, L. *et al.* Virosome-mediated delivery of protein antigens to dendritic cells. *Vaccine* **20**, 2287-2295, doi:Pii S0264-410x(02)00103-2
Doi 10.1016/S0264-410x(02)00103-2 (2002).

125 Kabanov, A. V. & Vinogradov, S. V. Nanogels as Pharmaceutical Carriers: Finite Networks of Infinite Capabilities. *Angew Chem Int Edit* **48**, 5418-5429, doi:10.1002/anie.200900441 (2009).

126 Gu, Z., Biswas, A., Zhao, M. X. & Tang, Y. Tailoring nanocarriers for intracellular protein delivery. *Chem Soc Rev* **40**, 3638-3655, doi:10.1039/c0cs00227e (2011).

127 Sun, W. J. *et al.* Self-Assembled DNA Nanoclews for the Efficient Delivery of CRISPR-Cas9 for Genome Editing. *Angew Chem Int Edit* **54**, 12029-12033, doi:10.1002/anie.201506030 (2015).

128 Murata, H. *et al.* Denatured and reversibly cationized p53 readily enters cells and simultaneously folds to the functional protein in the cells. *Biochemistry-Us* **45**, 6124-6132, doi:10.1021/bi052642a (2006).

129 Yan, M. *et al.* A novel intracellular protein delivery platform based on single-protein nanocapsules. *Nat Nanotechnol* **5**, 48-53, doi:10.1038/Nnano.2009.341 (2010).

130 Zhao, M. X. *et al.* Clickable Protein Nanocapsules for Targeted Delivery of Recombinant p53 Protein. *J Am Chem Soc* **136**, 15319-15325, doi:10.1021/ja508083g (2014).

131 Kim, S. H., Jeong, J. H., Joe, C. O. & Park, T. G. Folate receptor mediated intracellular protein delivery using PLL-PEG-FOL conjugate. *J Control Release* **103**, 625-634, doi:10.1016/j.jconrel.2004.01.006 (2005).

132 Shu, S. J., Zhang, X. G., Wu, Z. M., Wang, Z. & Li, C. X. Gradient cross-linked biodegradable polyelectrolyte nanocapsules for intracellular protein drug delivery. *Biomaterials* **31**, 6039-6049, doi:10.1016/j.biomaterials.2010.04.016 (2010).

133 Brinegar, K. *et al.* The commercialization of genome-editing technologies. *Crit Rev Biotechnol* **37**, 924-932, doi:10.1080/07388551.2016.1271768 (2017).

134 Yin, H., Kauffman, K. J. & Anderson, D. G. Delivery technologies for genome editing. *Nat Rev Drug Discov* **16**, 387-399, doi:10.1038/nrd.2016.280 (2017).

135 Lee, K. *et al.* Nanoparticle delivery of Cas9 ribonucleoprotein and donor DNA in vivo induces homology-directed DNA repair. *Nat Biomed Eng* **1**, 889-901, doi:10.1038/s41551-017-0137-2 (2017).

136 Liu, J. & Shui, S. L. Delivery methods for site-specific nucleases: Achieving the full potential of therapeutic gene editing. *J Control Release* **244**, 83-97, doi:10.1016/j.jconrel.2016.11.014 (2016).

137 Joung, J. K. & Sander, J. D. INNOVATION TALENs: a widely applicable technology for targeted genome editing. *Nat Rev Mol Cell Bio* **14**, 49-55, doi:10.1038/nrm3486 (2013).

138 Urnov, F. D., Rebar, E. J., Holmes, M. C., Zhang, H. S. & Gregory, P. D. Genome editing with engineered zinc finger nucleases. *Nat Rev Genet* **11**, 636-646, doi:10.1038/nrg2842 (2010).

139 Yin, H. *et al.* Non-viral vectors for gene-based therapy. *Nature Reviews Genetics* **15**, 541-555, doi:10.1038/nrg3763 (2014).

140 Gaj, T., Guo, J., Kato, Y., Sirk, S. J. & Barbas, C. F. Targeted gene knockout by direct delivery of zinc-finger nuclease proteins. *Nat Methods* **9**, 805-+, doi:10.1038/Nmeth.2030 (2012).

141 Mali, P. *et al.* RNA-Guided Human Genome Engineering via Cas9. *Science* **339**, 823-826, doi:10.1126/science.1232033 (2013).

142 Cong, L. *et al.* Multiplex Genome Engineering Using CRISPR/Cas Systems. *Science* **339**, 819-823, doi:10.1126/science.1231143 (2013).

143 Wilson, G. S. & Gifford, R. Biosensors for real-time in vivo measurements. *Biosens Bioelectron* **20**, 2388-2403, doi:10.1016/j.bios.2004.12.003 (2005).

144 Ansari, S. A. & Husain, Q. Potential applications of enzymes immobilized on/in nano materials: A review. *Biotechnol Adv* **30**, 512-523, doi:10.1016/j.biotechadv.2011.09.005 (2012).

145 Wang, X. Y. & Uchiyama, S. Polymers for Biosensors Construction. *State of the Art in Biosensors - General Aspects*, 67-86, doi:10.5772/54428 (2013).

146 Sassolas, A., Blum, L. J. & Leca-Bouvier, B. D. Immobilization strategies to develop enzymatic biosensors. *Biotechnol Adv* **30**, 489-511, doi:10.1016/j.biotechadv.2011.09.003 (2012).

147 Wang, X. & Uchiyama, S. Amperometric glucose sensor fabricated by combining glucose oxidase micelle membrane and aminated glassy carbon electrode. *Anal Lett* **41**, 1173-1183, doi:10.1080/00032710802052429 (2008).

148 Hagiwara, T., Suzuki, I., Takeuchi, K., Hamana, H. & Narita, T. Synthesis and Polymerization of N-(4-Vinylphenyl)Maleimide. *Macromolecules* **24**, 6856-6858, doi:DOI 10.1021/ma00026a010 (1991).

149 Ren, X. L. *et al.* Amperometric glucose biosensor based on a gold nanorods/cellulose acetate composite film as immobilization matrix. *Colloid Surface B* **72**, 188-192, doi:10.1016/j.colsurfb.2009.04.003 (2009).

150 Gerhardt, G. A., Oke, A. F., Nagy, G., Moghaddam, B. & Adams, R. N. Nafion-Coated Electrodes with High Selectivity for Cns Electrochemistry. *Brain Res* **290**, 390-395, doi:Doi 10.1016/0006-8993(84)90963-6 (1984).

151 Krajewska, B. Application of chitin- and chitosan-based materials for enzyme immobilizations: a review. *Enzyme Microb Tech* **35**, 126-139, doi:10.1016/j.enzmictec.2003.12.013 (2004).

152 Kang, X. H. *et al.* Glucose Oxidase-graphene-chitosan modified electrode for direct electrochemistry and glucose sensing. *Biosens Bioelectron* **25**, 901-905, doi:10.1016/j.bios.2009.09.004 (2009).

153 Karaolanis, G., Lionaki, S., Moris, D., Palla, V. V. & Vernadakis, S. Secondary hyperoxaluria: a risk factor for kidney stone formation and renal failure in native kidneys and renal grafts. *Transplant Rev-Orlan* **28**, 182-187, doi:10.1016/j.trre.2014.05.004 (2014).

154 Hoppe, B., Beck, B. B. & Milliner, D. S. The primary hyperoxalurias. *Kidney international* **75**, 1264-1271, doi:10.1038/ki.2009.32 (2009).

155 Rumsby, G. Biochemical and genetic diagnosis of the primary hyperoxalurias: a review. *Molecular urology* **4**, 349-354 (2000).

156 Beck, B. B., Hoyer-Kuhn, H., Gobel, H., Habbig, S. & Hoppe, B. Hyperoxaluria and systemic oxalosis: an update on current therapy and future directions. *Expert Opin Investig Drugs* **22**, 117-129, doi:10.1517/13543784.2013.741587 (2013).

157 Bobrowski, A. E. & Langman, C. B. Hyperoxaluria and systemic oxalosis: current therapy and future directions. *Expert Opin Pharmacother* **7**, 1887-1896, doi:10.1517/14656566.7.14.1887 (2006).

158 Woo, E. J., Dunwell, J. M., Goodenough, P. W., Marvier, A. C. & Pickersgill, R. W. Germin is a manganese containing homohexamer with oxalate oxidase and superoxide dismutase activities. *Nature structural biology* **7**, 1036-1040, doi:10.1038/80954 (2000).

159 Whittaker, M. M., Pan, H. Y., Yukl, E. T. & Whittaker, J. W. Burst kinetics and redox transformations of the active site manganese ion in oxalate oxidase: implications for the catalytic mechanism. *The Journal of biological chemistry* **282**, 7011-7023, doi:10.1074/jbc.M609374200 (2007).

160 Whittaker, M. M. & Whittaker, J. W. Characterization of recombinant barley oxalate oxidase expressed by Pichia pastoris. *Journal of biological inorganic chemistry : JBIC : a publication of the Society of Biological Inorganic Chemistry* **7**, 136-145, doi:10.1007/s007750100281 (2002).

161 Zhang, H. *et al.* Antibodies elicited by yeast glycoproteins recognize HIV-1 virions and potently neutralize virions with high mannose N-glycans. *Vaccine* **33**, 5140-5147, doi:10.1016/j.vaccine.2015.08.012 (2015).

162 Gerngross, T. U. Advances in the production of human therapeutic proteins in yeasts and filamentous fungi (vol 22, pg 1409, 2004). *Nature biotechnology* **22**, 1589-1589, doi:DOI 10.1038/nbt1204-1589e (2004).

163 Dahiya, T. & Pundir, C. S. In vivo oxalate degradation by liposome encapsulated oxalate oxidase in rat model of hyperoxaluria. *The Indian journal of medical research* **137**, 136-141 (2013).

164 Raghavan, K. G. & Tarachand, U. Degradation of oxalate in rats implanted with immobilized oxalate oxidase. *FEBS Lett* **195**, 101-105 (1986).

165 Jin, Q., Chen, Y. J., Wang, Y. & Ji, J. Zwitterionic drug nanocarriers: A biomimetic strategy for drug delivery. *Colloid Surface B* **124**, 80-86, doi:10.1016/j.colsurfb.2014.07.013 (2014).

166 Keefe, A. J. & Jiang, S. Poly(zwitterionic)protein conjugates offer increased stability without sacrificing binding affinity or bioactivity. *Nat Chem* **4**, 59-63, doi:10.1038/nchem.1213 (2012).

167 Zhao, H. Effect of ions and other compatible solutes on enzyme activity, and its implication for biocatalysis using ionic liquids. *J Mol Catal B-Enzym* **37**, 16-25, doi:10.1016/j.molcatb.2005.08.007 (2005).

168 Li, J. *et al.* Robust enzyme-silica composites made from enzyme nanocapsules. *Chem Commun* **51**, 9628-9631, doi:10.1039/c5cc02053k (2015).

169 Moro, T. *et al.* Surface grafting of artificial joints with a biocompatible polymer for preventing periprosthetic osteolysis. *Nature Materials* **3**, 829-836, doi:10.1038/nmat1233 (2004).

170 Rodriguez, P. L. *et al.* Minimal "Self" Peptides That Inhibit Phagocytic Clearance and Enhance Delivery of Nanoparticles. *Science* **339**, 971-975, doi:10.1126/science.1229568 (2013).

171 Deeks, S. G., Lewin, S. R. & Havlir, D. V. The end of AIDS: HIV infection as a chronic disease. *Lancet* **382**, 1525-1533, doi:10.1016/S0140-6736(13)61809-7 (2013).

172 Maartens, G., Celum, C. & Lewin, S. R. HIV infection: epidemiology, pathogenesis, treatment, and prevention. *Lancet* **384**, 258-271, doi:10.1016/S0140-6736(14)60164-1 (2014).

173 Perelson, A. S. *et al.* Decay characteristics of HIV-1-infected compartments during combination therapy. *Nature* **387**, 188-191, doi:DOI 10.1038/387188a0 (1997).

174 Finzi, D. *et al.* Latent infection of CD4(+) T cells provides a mechanism for lifelong persistence of HIV-1, even in patients on effective combination therapy. *Nat Med* **5**, 512-517 (1999).

175 Chun, T. W., Moir, S. & Fauci, A. S. HIV reservoirs as obstacles and opportunities for an HIV cure. *Nat Immunol* **16**, 584-589, doi:10.1038/ni.3152 (2015).

176 Archin, N. M. *et al.* Administration of vorinostat disrupts HIV-1 latency in patients on antiretroviral therapy (vol 487, pg 482, 2012). *Nature* **489**, doi:10.1038/nature11455 (2012).

177 Sigal, A. *et al.* Cell-to-cell spread of HIV permits ongoing replication despite antiretroviral therapy. *Nature* **477**, 95-U100, doi:10.1038/nature10347 (2011).

178 Wen, J. *et al.* Specific Elimination of Latently HIV-1 Infected Cells Using HIV-1 Protease-Sensitive Toxin Nanocapsules. *Plos One* **11**, doi:ARTN e0151572
10.1371/journal.pone.0151572 (2016).

179 Shan, L. *et al.* Stimulation of HIV-1-Specific Cytolytic T Lymphocytes Facilitates Elimination of Latent Viral Reservoir after Virus Reactivation. *Immunity* **36**, 491-501, doi:10.1016/j.immuni.2012.01.014 (2012).

180Scerra, S., Melica, G. & Lelievre, J. D. CCR5 knockout strategies ... A way toward HIV cure? *J Anti-Infect* **13**, 184-190, doi:10.1016/j.antinf.2011.07.003 (2011).

181 Ebina, H., Misawa, N., Kanemura, Y. & Koyanagi, Y. Harnessing the CRISPR/Cas9 system to disrupt latent HIV-1 provirus. *Scientific Reports* **3**, 2510 (2013).

182 Mandal, P. *et al.* Efficient ablation of genes in human hematopoietic stem and effector cells using CRISPR/Cas9. *Cell Stem Cell* **15**, 643-652, doi:10.1016/j.stem.2014.10.004 (2014).

183 Fu, Y. F. *et al.* High-frequency off-target mutagenesis induced by CRISPR-Cas nucleases in human cells. *Nat Biotechnol* **31**, 822-+, doi:10.1038/nbt.2623 (2013).

184 Cradick, T. J., Fine, E. J., Antico, C. J. & Bao, G. CRISPR/Cas9 systems targeting beta-globin and CCR5 genes have substantial off-target activity. *Nucleic Acids Research* **41**, 9584-9592, doi:10.1093/nar/gkt714 (2013).

185 Mussolino, C. *et al.* A novel TALE nuclease scaffold enables high genome editing activity in combination with low toxicity. *Nucleic Acids Research* **39**, 9283-9293, doi:10.1093/nar/gkr597 (2011).

186 Sakuma, T. *et al.* Repeating pattern of non-RVD variations in DNA-binding modules enhances TALEN activity. *Sci Rep-Uk* **3**, doi:ARTN 3379

10.1038/srep03379 (2013).

187 Holkers, M. *et al.* Differential integrity of TALE nuclease genes following adenoviral and lentiviral vector gene transfer into human cells. *Nucleic Acids Res* **41**, doi:ARTN e63

10.1093/nar/gks1446 (2013).

188 Ebina, H. *et al.* A High Excision Potential of TALENs for Integrated DNA of HIV-Based Lentiviral Vector. *Plos One* **10**, doi:ARTN e0120047

10.1371/journal.pone.0120047 (2015).

189 Guo, J., Gaj, T. & Barbas, C. F. Directed Evolution of an Enhanced and Highly Efficient FokI Cleavage Domain for Zinc Finger Nucleases. *J Mol Biol* **400**, 96-107, doi:10.1016/j.jmb.2010.04.060 (2010).

190 Liu, J. *et al.* Efficient delivery of nuclease proteins for genome editing in human stem cells and primary cells. *Nat Protoc* **10**, 1842-1859, doi:10.1038/nprot.2015.117 (2015).

191 Mak, A. N., Bradley, P., Cernadas, R. A., Bogdanove, A. J. & Stoddard, B. L. The crystal structure of TAL effector PthXo1 bound to its DNA target. *Science* **335**, 716-719, doi:10.1126/science.1216211 (2012).

192 Ebina, H., Misawa, N., Kanemura, Y. & Koyanagi, Y. Harnessing the CRISPR/Cas9 system to disrupt latent HIV-1 provirus. *Sci Rep-Uk* **3**, doi:ARTN 2510

10.1038/srep02510 (2013).

193 Andre, V. M., Cepeda, C. & Levine, M. S. Dopamine and Glutamate in Huntington's Disease: A Balancing Act. *Cns Neurosci Ther* **16**, 163-178, doi:10.1111/j.1755-5949.2010.00134.x (2010).

194 Lapish, C. C., Seamans, J. K. & Chandler, L. J. Glutamate-dopamine cotransmission and reward processing in addiction. *Alcohol Clin Exp Res* **30**, 1451-1465, doi:10.1111/j.1530-0277.2006.00176.x (2006).

195 Chefer, V. I., Thompson, A. C., Zapata, A. & Shippenberg, T. S. Overview of brain microdialysis. *Curr Protoc Neurosci* **Chapter 7**, Unit7 1, doi:10.1002/0471142301.ns0701s47 (2009).

196 Danbolt, N. C. Glutamate uptake. *Prog Neurobiol* **65**, 1-105, doi:Doi 10.1016/S0301-0082(00)00067-8 (2001).

197 Ungerstedt, U. & Hallstrom, A. Invivo Microdialysis - a New Approach to the Analysis of Neurotransmitters in the Brain. *Life Sci* **41**, 861-864, doi:Doi 10.1016/0024-3205(87)90181-0 (1987).

198 Tolosa, V. M., Wassum, K. M., Maidment, N. T. & Monbouquette, H. G. Electrochemically deposited iridium oxide reference electrode integrated with an electroenzymatic glutamate sensor on a multielectrode array microprobe. *Biosens Bioelectron* **42**, 256-260, doi:10.1016/j.bios.2012.10.061 (2013).

199 Wassum, K. M. *et al.* Silicon wafer-based platinum microelectrode array biosensor for near real-time measurement of glutamate in vivo. *Sensors-Basel* **8**, 5023-5036, doi:10.3390/s8085023 (2008).

200 Tseng, T. T. C., Yao, J. & Chan, W. C. Selective enzyme immobilization on arrayed microelectrodes for the application of sensing neurotransmitters. *Biochem Eng J* **78**, 146-153, doi:10.1016/j.bej.2013.04.019 (2013).

201 Bernard, A., Renault, J. P., Michel, B., Bosshard, H. R. & Delamarche, E. Microcontact printing of proteins. *Adv Mater* **12**, 1067-1070, doi:Doi 10.1002/1521-4095(200007)12:14<1067::Aid-Adma1067>3.0.Co;2-M (2000).

202 Xia, Y. N. & Whitesides, G. M. Soft lithography. *Angew Chem Int Edit* **37**, 550-575, doi:Doi 10.1002/(Sici)1521-3773(19980316)37:5<550::Aid-Anie550>3.3.Co;2-7 (1998).

203 Kumar, A. & Whitesides, G. M. Features of Gold Having Micrometer to Centimeter Dimensions Can Be Formed through a Combination of Stamping with an Elastomeric Stamp and an Alkanethiol Ink Followed by Chemical Etching. *Appl Phys Lett* **63**, 2002-2004, doi:Doi 10.1063/1.110628 (1993).